- SELF-CONSISTENT DETERMINATION OF BINDING ENERGIES AND CHARGE TRANSFERS IN CHEMISORPTION SYSTEMS -

A thesis presented for the degree of Doctor of Philosophy of the University of London, and for the Diploma of Imperial College by Jean-Paul Muscat.

Department of Mathematics

Imperial College of Science and Technology

London S.W.7

-Acknowledgements-

It is a pleasure to thank my supervisor Dr D.M.Newns for his encouragement throughout this work, and for many helpful discussions.

It is also a pleasure to acknowledge the hospitality and kindness of the staff and students of the solid state physics group at Imperial College.

I would also like to acknowledge the financial support of the Science Research Council through a research studentship.

CONTENTS

Chapter 1: Introduction 1

Chapter 2: Alkali Adsorption on Transition Metals: a Simple Model

2.1 Introduction 12

2.2 The Model Hamiltonian 20

2.3 Solution in Hartree-Fock Approximation 28

Chapter 3: Linear Response Formalism

3.1 The Polarizability of the Free Alkali Atom 41

3.2 Dielectric Response of the Substrate 42

3.3 Determination of the Green Functions 46

Chapter 4: Alkali Adsorption on Transition Metals: The Importance of the s-p Hybridization

4.1 Introduction 51

4.2 The Model Hamiltonian 52

4.3 Formal Solution 56

4.4 The Low Coverage Problem 59

4.5 Results and Discussion 67

Chapter 5: The Chemisorption of Transition Atoms of the Third Series on Tungsten: Review of the Theory up till now

5.1 Introduction 82

5.2 The Tight Binding Approximation 83

5.3 The Virtual Level Description 86

5.4 Surface Molecules 90

Chapter 6: The Three Atom Model

6.1 The Model 103

6.2 Formal Solution 105

6.3 Results and Discussion 112

References 125

Abstract

This work is concerned with various aspects of chemisorption theory. In the first part of the thesis, we study the work function variation of transition metals on adsorption of alkali atoms. We introduce first a simple model which takes account of the transfer of charge on the adatom only. This model is used to estimate the position and width of the valence ns level of adsorbed alkali atoms. The important corrections arising from the intra-amic polarization are then estimated in linear response theory, and shown to be comparable to the neutralisation arising from the transfer of charge. A more complex model is then formulated in which both these effects are included implicitly. An analysis valid at low coverages, is used to estimate values for the widths of the ns and np levels (assumed equal) and their mean energy. A self-consistent numerical determination of work function/coverage curves is then given. From this treatment a more complete determination of the parameters from comparison with experimental results is achieved. Results for the system Cs/Re(0001) show that the widths of the levels are quite large, falling in the range (0.7eV, 2eV). An implication is that the adsorbate levels are strongly hybridized. The model was applied to the system Cs adsorbed on a layer of oxygen on tungsten. It was found in this case that the widths of the levels were considerably smaller.

In the second part of the thesis, we study the chemisorption of transition atoms of the third series on tungsten. The binding energy and charge transfer of an adatom are determined by use of a degenerate three atom Hubbard Hamiltonian. The Hamiltonian is solved by making an ansatz for the wavefunction. The observed experimental trend is reproduced for large values of the intra-atomic Coulomb interaction U, thus emphasizing the importance of correlation in this problem.

Chapter 1

Introduction

Great interest has been focused recently on the varied aspects of the theory of adsorption. This interest has been triggered off by the wealth of experimental techniques designed to probe the geometry and electronic spectra of clean and adsorbate covered surfaces.

The type of adsorption is generally divided into two classes , physisorption in which the bond strength is weak ($\leq$ .1eV) and chemisorption where it is strong ($\geq$ .5eV) (Hayward and Trapnell,1957). Qualitatively the physisorption bond relies on Van der Waals attractive forces, sometimes called dispersional forces, and does not include exchange of electrons between the adsorbate and the substrate (Young and Crowell,1962), in contrast to the chemisorption bond in which electrons may be shared (covalent bonding) or transferred (ionic bonding). From a theoretical point of view, the distinction between chemisorption and physisorption is not sharp, however we shall only consider here subjects related to chemisorption processes. A number of reviews giving up to date accounts of the research being carried out in the field, have appeared recently. (Grimley,1971a, Wojciechowski,1971,Schrieffer,1972,Gadzuk,1974,Gomer,1974).

Ideally, the information one seeks , includes (a) the geometry and (b) the electronic structure of clean and adsorbate covered sur-

faces. It also proves useful to know some general properties of the surface, preferably in the form of measurable physical quantities.

Many experimental techniques have been developed recently in order to provide us with this kind of information.

One of the quantities of interest which we might like to measure, is the work function ϕ of a metal , this is defined as the energy difference between an electron at the Fermi level and the vacuum level (i.e the minimum energy required to remove an electron from the metal). One of the methods used extensively to measure work functions is field emission microscopy (Müller,1973). In this technique the potential outside the surface is reduced with the application of an electric field, thus allowing electrons from the metal to be emitted. This method has also been used to determine work function changes due to adsorbed atoms, the change in work function being related to the electric dipole moment per adsorbate. Results of alkali adsorption on transition metals show a substantial decrease in work function ($\sim$3eV) indicating that alkalis are adsorbed as cations (Schmidt and Gomer, 1966). While O adsorption tends to increase the work function by as much as 2eV, so that O adsorbs in the anionic state. Finally we note that very little change in ϕ is registered as a result of H adsorption indicating that H adsorbs in its neutral state (Hayward and Trapnell, 1957).

Another quantity of interest is the binding energy ΔE of an atom to a surface, this being defined as the work required to remove the atom from the surface. This is an important quantity since the size of the binding energy determines whether we are dealing with chemisorption (large ΔE) or physisorption (small ΔE) bonds, and consequently determines which set of theoretical approximations can be applied to the problem in question.

Many structural techniques have been developed to determine the position of various atomic nuclei at or near the surface. The technique of low energy electron diffraction (LEED) is well suited for determining surface structure , because low energy electrons penetrate only a few layers into the solid , and because the wavelength of low energy electrons is of the order of atomic spacings (Duke, 1973). The method of reflection high energy electron diffraction (RHEED) is useful in detecting the existence of small islands on the surface which cannot be seen on LEED patterns . The angle of incidence of these beams is very small so that again the penetration does not exceed two or three atomic layers. (Dobson,1974)

These techniques have shown that the substrate surface periodicities of transition metals are generally those of the ideal planes of the bulk crystal. A conclusion which does not generally hold for non metals (Schmidt,1972). The adsorbate structures vary with the nature of the adsorbate, with the surface concentration and with the crystal plane on which adsorption occurs.

In addition a number of spectroscopic techniques have been developed to study the electronic structure of surfaces. These include field emission , photoemission, ion neutralisation and Auger electron spectroscopy. In these experiments , the emitted electrons are energy resolved , and the energy distribution of the beam of electrons is then related to the spectrum of elementary excitations of the solid.

The high resolution experiments of Plummer (Gadzuk and Plummer, 1973 and references therein) were the first to show structure in the field emission total energy distribution (TED) of different clean metals. Field emission studies of adsorbates have been made, and the virtual states of the adsorbate have been identified in the TED, when the structure of the enhancement emission of an adsorbate on a metal

can be related to the broadened and shifted energy levels of the adsorbate. One of the earliest studies of adsorption was Plummer and Young's investigation of alkaline earth metals adsorbed on W and Mo. (Plummer and Young,1970). Their results for Ba show a broad resonance and two small sharp peaks sligthly below the Fermi level. The position of these narrow peaks correspond to the ^3D and ^1D states of the free atom respectively, while the broad resonance can be associated with a broadened 6s level. A number of other adsorbates such as Zr (Plummer, Gadzuk and Young,1969) H_2 and O_2 (Gadzuk and Plummer,1971) and CO (Young and Gomer,1973) all on tungsten substrates show specific TED structures, but they are mostly either too diffuse or too strongly dependent on the degree of coverage to be associated with certainty to distinct free atomic levels.

In x-ray and u-v photoemission spectroscopy (XPS and UPS respectively) one studies electrons emitted from a sample which is being exposed to a flux of photons of known energy. In XPS, the photon energies are sufficient to eject core electrons, thus providing direct values for the core energy levels and a means of identification of the atoms. The advantage of UPS (in these experiments only valence electrons can be emitted) is the much higher resolution obtainable (Brundle,1974).UPS has been used extensively to determine the electronic energy levels of adsorbed gases on surfaces. Eastman and Cashion (1971) have observed that chemisorbed CO on Ni exhibits two well defined energy levels situated at 7.5eV and 10.7eV below the Fermi level with energy widths of about 2eV and 1eV respectively. These have been identified with the ($\sigma 2p$) and ($\pi 2p$) molecular orbitals of CO. Chemisorbed O shows a single level of width 2eV centered at 5.5eV below the Fermi level. This level has been identified as the broadened p-level of the adatom , which has been shifted upwards ap-

preciably(~3eV) from the p-orbital energy of the free O atom. As the oxygen exposure is increased this level broadens into a valence band with three distinct peaks (Eastman and Cashion,1971). A similar behaviour was observed for the system O/W (Baker and Eastman,1973).

The technique of ion neutralisation spectroscopy (INS) is based on an Auger type transition in which an ion is neutralised to its ground state by an electron from inside the metal, resulting in another electron being ejected from the solid (Hagstrum,1966). This technique has proved very useful in determining electronic spectra of clean and adsorbate covered surfaces . Hagstrum and Becker have reproduced quite accurately Eastman and Cashion's results for the systems O/Ni (Hagstrum and Becker,1969) and CO/Ni (Becker and Hagstrum, 1973) in the energy range in which this technique is restricted. The CO results were corroborated by their own UPS results. Hagstrum and Becker have also found structure appearing in the spectra of chemisorbed S and Se on Ni (Hagstrum and Becker,1969).

The technique of Auger electron spectroscopy (AES) is accomplished by irradiating the surface of the solid with a primary electron beam, while the energy analysis is performed on the resultant secondary electrons. AES is a valuable addition to any surface study for evaluating surface cleanliness and for determining the coverage and purity of adsorbed layers (Chang 1971, Palmberg 1972). The technique has been used extensively with LEED experiments for correlating observed patterns with surface chemistry.

All these techniques provide us with a wealth of information on chemisorption systems , and we shall refer to them as we develop the thesis.

The plan for the thesis is the following, in part 1 (chapters 2, 3,and 4) we propose a simple theoretical model designed to explain

and reproduce quantitatively work function variations of transition metals on adsorption of alkali atoms, in part 2 (chapters 5 and 6) we attempt a theoretical understanding of the experimental results on the adsorption energies of 5d transition atoms on W. But before we deal with either of these problems in particular , let us introduce some general concepts which are related to both of them.

In order to fix ideas , let us consider an atom with a single valence orbital $|ns\rangle$ (n denotes the shell number) far from a metal surface. The ionization potential I is defined as the energy required to take away the outer electron off the neutral atom. Except for alkali atoms , I is usually larger than the substrate work function ϕ. For example I = 13.6eV for H , while I is anomalously small for alkalis (being 3.9eV for Cs). Typically ϕ is about 4.5eV. The electron affinity A, defined as the binding energy of an extra electron making a negative ion, is generally small (e.g A = .75eV for H^-). Since the extra electron enters the same atomic orbital that is involved in determining I, the difference I - A = U is due to the Coulomb repulsion between the two electrons occupying $|ns\rangle$ in the negative ion. For an atom like H one finds U = 12.85eV, this value is considerably smaller than the energy one would calculate from the Coulomb repulsion between two electrons in the neutral $|1s\rangle$ orbital which is given by the integral

$$U = \int d^3x\, d^3y\, \varphi_{1s}(\underline{x}) \frac{e^2}{|\underline{x} - \underline{y}|} \varphi_{1s}(\underline{y}) \qquad (1.1)$$

and φ_{1s} represents the $|1s\rangle$ wavefunction . The values of U calculated from (1.1) are too large , one finds U =17eV which would make the ion H^- unstable.In reality, the electrons will attempt to stay apart so

that they see a weaker repulsion.

The energy of the valence orbital $|ns\rangle$ is denoted by E_{ns}, when the adatom-substrate separation is large , E_{ns} is given by the difference

$$E_{ns} = \phi - I \qquad (1.2)$$

As the adatom-metal separation d decreases, the interaction between the adatom and the substrate is switched on. The effect of this interaction is to introduce a lifetime broadening of the valence $|ns\rangle$ level of the adatom , we can thus say that the original discrete level at E_{ns} persists in the combined system as a virtual level of width Δ (Gurney,1935). For large enough d, the probability of finding the energy of $|ns\rangle$ at energy ϵ becomes a distribution peaked sharply at E_{ns}, but with a tail continuing below the Fermi level, which will be occupied. Accordingly there is a non zero expectation value $\langle n_s \rangle$ of the number of electrons on the adatom. The adatom thus becomes partly ionized and an image charge is induced in the substrate, the role of the image term which we shall discuss more thoroughly below, is to shift the valence level upwards. We also notice that the level is shifted downwards as a result of the interaction with the metal and upwards as a result of the intra-atomic Coulomb interaction(Gadzuk,1967).

This simple model first introduced by Gurney(1935) may be used to explain qualitatively some of the observed work function variations of transition metals on adsorption of alkali atoms. The experiments show that as alkali atoms are adsorbed onto the surface of a transition metal, the work function ϕ decreases rapidly from its initially high value. With continued adsorption , ϕ reaches a

minimum, before rising to the value characteristic of the saturated monolayer which is still much lower than the work function of the bare surface.

As we discussed above, when the adatoms come close to the surface, they become partly ionized, the charge on the adatoms being given by $q = e(1 - \langle n_s \rangle)$. This creates image charges in the substrate, which lower the work function by an amount

$$\Delta\phi = -4\pi qds \qquad (1.3)$$

where s is the surface concentration of adatoms.

Following Gurney , we note that at finite s, the proximity of other adatoms carrying a positive charge q will shift down the level E_{ns}, **thus increasing** the occupied portion of the density of states and thus $\langle n_s \rangle$. A progressive neutralisation of the adatoms occurs which will continually reduce the rate of decrease of ϕ with s (i.e the dipole moment $\mu = 2qd$) and may result in a minimum in ϕ.

A knowledge of the position and width of the adsorbate valence levels , as determined by one of the spectroscopic techniques which we described above, now assumes its full significance. Our aim here is to correlate as much as possible the electronic structure of adsorbed systems to the observed variations in work function.

Attempts to interpret decreases in the dipole moment μ with coverage s date back even further (Langmuir,1933). It is found that work function vs coverage curves can be fitted quite well , by a simple depolarization model based on the Topping formula (Topping, 1927). This is derived by putting the dipole moment μ associated with a single atom equal to the sum of its zero coverage moment μ_o plus the change in moment arising from the electric field due to

the other adsorbates, i.e

$$\mu = \mu_o + \alpha E_\perp \qquad (1.4)$$

where α is an effective polarizability, and $E_\perp$ is the electric field in the direction perpendicular to the surface. When s is small it can be shown that $E_\perp$ is proportional to $s^{3/2}$ (see below), which when replaced in (1.4) yields the so-called Topping formula

$$\mu = \mu_o/(1 + A\alpha s^{3/2}) \qquad (1.5)$$

A is a constant characteristic of the particular surface lattice considered, calculations of A in simple cases will be given below (also see Topping, 1927). This shows the importance of the s-p hybridization on which the polarizability α must depend.

In setting up a theoretical model, certain approximations must be made , and the validity of these approximations will of course depend on the physical nature of the system . For instance if the width Δ of the valence level is large compared with the intra-atomic interaction on the adatom U , then it turns out that the chemisorption problem can be treated as one of self-consistency within the Hartree-Fock approximation. If the metal-adatom system may be described by a model based on the Anderson Hamiltonian for magnetic impurities in metals(Anderson, 1961), then the criterion which Δ and U must satisfy is the inequality $\pi\Delta > U$. This turns out to be the case for the alkali/transition metal systems for which U is small (it must be remembered that U is further reduced by image effects as we shall discuss below), and for which Δ is expected to be large (we have no experimental results for alkalis,

but for Ba , the width of the 6s level is about 1eV (Plummer and Young,1970) and we expect comparable widths for the alkalis).

If on the contrary U is large, then the electron correlation effects become important. The Hartree-Fock approximation which amounts to no more than 1^{st} order perturbation theory in the perturbation U of course breaks down and more sophisticated techniques must be employed.

The adsorption of 5d transition atoms on W provides us with an example in which correlation effects play a predominant role. The general trend observed by Plummer and Rhodin (1968) for the binding energies ΔE of 5d atoms on W , was that ΔE varied linearly with the number of unpaired electrons in the 5d shell, increasing from Hf to a maximum for Re before decreasing linearly to Au. The size of the binding energies (e.g the binding energy of Re on W(100) is 9.3eV compared to the cohesive energy of W which is 8.7eV) indicates strongly that ΔE will be mainly due to the interaction of the d electrons of the free atom with the d-band of W .

We must of course remember that on adsorption, the atom is no longer free, but will be in a state which is nearly that of its metallic state. In other words it will have lost some of its s-electrons (let us recall for instance that the s-band of W contains 1.28 electrons per atom (Girvan et al, 1968) while of course the free W atom has two s-electrons).

If we assume that one of the s-electrons of the free atom is spread in the s-band of the W substrate, with an energy gain of the order of the s-d interaction, then the problem of the adsorption of a $5d^n6s^2$ atom will be treated as the interaction of a $5d^{n+1}$ level with the W d-band.

The difficulty with this problem is the importance played by

the Coulomb interaction U, both on the adsorbate and the substrate atoms. In order to include the correlation effects on the substrate atoms, the problem should be formulated in terms of the Hubbard(1963) Hamiltonian (Newns,1970b, Grimley and Thorpe 1971b). We note that in this formulation , there is no variation of ΔE with adatom if U is zero. The solution of the Hubbard Hamiltonian is rather complex and neither of these works go beyond the two-atom limit. It is our aim in part 2 of the thesis to introduce some bandwidth effects by looking at the problem of three atoms, one adsorbed atom , and two substrate atoms of which one lies on the surface and the other inside the metal.

Chapter 2

ALKALI ADSORPTION ON TRANSITION METALS: A SIMPLE MODEL

2.1 Introduction

On adsorption of alkali atoms , the work function ϕ of transition metals undergoes characteristic changes which we described in detail in chapter 1. The earliest observations of this behaviour were reported in the middle twenties (Ives,1924, Langmuir and Kingdon,1925, Becker,1926). Since those early observations there have been many other such measurements . We note in particular the works of Gomer and his co-workers who have studied the systems K/W (Schmidt and Gomer 1966) and Cs/W (Sidorski,Pelly and Gomer 1969) of Fehrs and Stickney(1971) who have obtained results for various alkalis on W and Ta, of Gavrilyuk et al(1966) who have studied adsorption of Li and Cs on W , of Gerlach and Rhodin(1968) who have studied the adsorption of various alkalis on Ni. We also note the excellent results of Fehrs and Mackrakis(1970) for the system Cs/Re(0001).

Finally let us recall that the experimental studies have not been confined to alkali/pure metal systems, in particular we note the results obtained for the system Cs adsorbed on a tungsten substrate covered by a layer of oxygen (Papageorgopoulos and Chen,1972, Desplat,1974).

The ideas most relevant to a theoretical understanding of alkali adsorption on transition metals were first introduced by Gurney (1935) and briefly discussed in chapter 1. These ideas have been developed further by a number of writers. Most of the studies have been of a single alkali atom on a metal surface (Bennett and Falicov 1966, Gadzuk 1967, Remy 1970, Gadzuk et al 1971, Grimley 1971a). Some work has been done in extending these treatments away from the single adatom case(Grimley 1967a,b,Bennett 1968). We shall discuss some of these models later on , let us first discuss the role of the image force in alkali adsorption on transition metals. How one should include the image effect in the model is however not quite obvious. In the adiabatic approximation, one can argue that when the electron is in the valence orbital it experiences the self-image energy $e^2/4d$ (this is defined as the energy required to remove the charge to $d = \infty$), thus giving us the renormalised energy level

$$E_{ns}' = E_{ns} + e^2/4d \qquad (2.1.1)$$

The distance d is an effective length which is approximately equal to the sum of the adatom-substrate spacing plus the screening length in the metal (Gomer and Swanson 1963, Newns 1969a,1970,Beck and Celli 1970, Lang 1972). This ensures that the potential has well defined limits for both large d going to the classical limit and small d going to a finite value.

This is not the only approximation which has been used in these kinds of studies, e.g if the image is assumed to be a completely static quantity, the valence level of the adatom is renormalised

to

$$E_{ns}' = E_{ns} + e^2(1 - \langle n_s \rangle)/2d \qquad (2.1.2)$$

where $\langle n_s \rangle$ is the expectation value for the number of electrons in the alkali valence orbital.

Both the results (2.1.1) and (2.1.2) tend to shift the adatom valence level upwards, but the quantitative difference is significant.

Hewson and Newns (1974) have discussed these approximations to the image term. In their model the interaction between the electron and its image is described by a model Hamiltonian in which the charge is assumed to interact with the surface plasmons in the substrate. The Hamiltonian was solved in limiting cases. In particular it was found that in cases such as those we will study here (Cs adsorbed on W or Re), the adiabatic approximation is reasonably well satisfied, and we shall use it from now on.

This leads us to define an effective ionization level

$$I' = I - e^2/4d \qquad (2.1.3)$$

similarly the electron affinity A may be renormalised to

$$A' = A + e^2/4d \qquad (2.1.4)$$

The effective value of U , thus becomes

$$U_{eff} = I' - A' = U - e^2/2d \qquad (2.1.5)$$

U can thus be considerably reduced by image effects as emphasized by Schrieffer (1973).

Amongst the earliest quantitative formulation of the Gurney

model, is Bennett and Falicov's treatment of alkali adsorption on transition metals.Whithin their model , the relevant parameters (the broadening and the shift of the adatom valence level) are estimated by use of 1^{st} order perturbation theory. In this approach the metal is assumed free-electron like, and a convenient wavefunction is assumed for the adatom. Bennett and Falicov assume that the wavefunction φ has the Slater form (Slater,1930)

$$\varphi(r) = \left[\frac{(2\gamma)^{2n^*+1}}{4\pi\,\Gamma(2n^*+1)}\right]^{1/2} r^{n^*-1} e^{-\gamma r} \qquad (2.1.6)$$

where γ is the coefficient of screening, and n^* is the effective quantum number. The static approximation for the image potential is used.

If χ are the metallic wavefunctions and φ the atomic wavefunction then the width Δ of the adatom valence level is given by

$$\Delta = \pi \int |\langle \chi | H | \varphi \rangle|^2 N_o(\mu, E)\, d\mu \qquad (2.1.7)$$

where μ is the radial linear momentum and N_o is the metallic density of states for a single spin.

The shift of the level E_φ depends on the matrix element

$$E_\varphi = \langle \varphi | H | \varphi \rangle \qquad (2.1.8)$$

If Δ is assumed not to vary with energy , then the adatom valence level is taken to have a Lorentzian density of states

$$\rho(E) = \frac{1}{\pi} \frac{\Delta}{(E - E_\varphi)^2 + \Delta^2} \qquad (2.1.9)$$

The effective charge is then given by

$$q = \frac{1}{\pi}\left[\arctan\left(\frac{E_F - E_\varphi}{\Delta}\right) + \frac{\pi}{2}\right] \qquad (2.1.10)$$

q depends on E_φ and Δ which are in turn functions of q. The problem is thus reduced to one of self-consistency.

The trend predicted by Gurney from purely qualitative considerations, is reproduced very clearly here. For example in the case of a caesium atom, the width of the virtual level increases from 0.11eV when the adatom-metal separation d is large (d=8Å), to 3.1eV when d = 2.85Å. The occupancy of the level was found to be generally quite small (in the absence of an external field) being practically zero at large d (d = 8Å), and less than 0.2 when d = 2.8Å.

In spite of the simplifying assumptions, the authors conclude that the alkali atom becomes ionized.

Bennett (1968) has generalised the above treatment in the low coverage limit to include two types of interaction between adsorbed atoms. The first type of interaction is the long range Coulomb potential at one adsorbate due to all the other adatoms. This lowers the net charge, its general effect is that of the parametrized depolarization function (1.5) discussed in chapter 1. Bennett has assumed that the electric field $E_\perp$ is proportional to s rather than $s^{3/2}$ as in (1.5), in contrast to most other workers (Topping 1927, Langmuir 1933, Schmidt and Gomer 1966).

The second type of interaction is that due to direct overlap of localised orbitals, which is of course most important between nearest neighbour adsorbed ions. Bennett considered the ion dimer (the simplest example of this interaction). The net charge per nucleus for isolated ions and ion dimers were found to be similar.

Bennett gives results obtained for the system K/W(100). He finds that the occupancy of the level increases from 0.33 at zero coverage to 0.40 at con-

centration 0.15, for a value of d = 2.85Å. This means that the virtual level is gradually shifted downwards with increasing coverage as emphasized by Gurney(1935). The fact that both sets of results for the two different species are so similar, was attributed to a number of combining effects.

Gadzuk (1967) has used a similar model to that of Bennett and Falicov with different approximations, the most drastic being the assumption that the interaction between the adatom and the metal can be replaced by the interaction between the adion and the valence electron and its image in the substrate as illustrated in fig.1. Thus the Hamiltonian has the following form

$$H = -\frac{\hbar^2}{2m}\nabla^2 - \frac{e^2}{r} - \frac{e^2}{4d} + \frac{e^2}{R} \qquad (2.1.11)$$

Gadzuk was unable to obtain any quantitative results with such approximations.

Remy (1970) used an approximation to the classical image potential

$$V(\zeta) = e^2(R^{-1} - (4d)^{-1}) \qquad (2.1.12)$$

which is valid at d = 0, this consisted in making the potential continuous, this was done by a translation of the origin by ζ_0 in such a way that $V(\zeta_0) = V_0$ (a constant equal to the potential of the electrons inside the metal). The total potential is then equal to the sum of $V(\zeta)$ plus the potential due to the interaction between the bond electron and ion core, which is switched on as soon as the electron leaves the metal surface. The bond being assured by periodic transitions from the $|ns\rangle$ valence level of the adatom to the conduction band of the substrate, Remy was able to calculate, using perturbation theory the frequency w of the transition, thus deducing the lifetime of the state $\tau = 1/w$ and the broadening $\Delta = \hbar w$.

Remy's results for the width of the level again show the expected variation with d. Although one could argue that the difference in values between the small d and large d regions is perhaps a little too great(e.g it was found that for the syatem Cs/W, at d = 2Å, the width Δ was very large($\simeq$10eV)

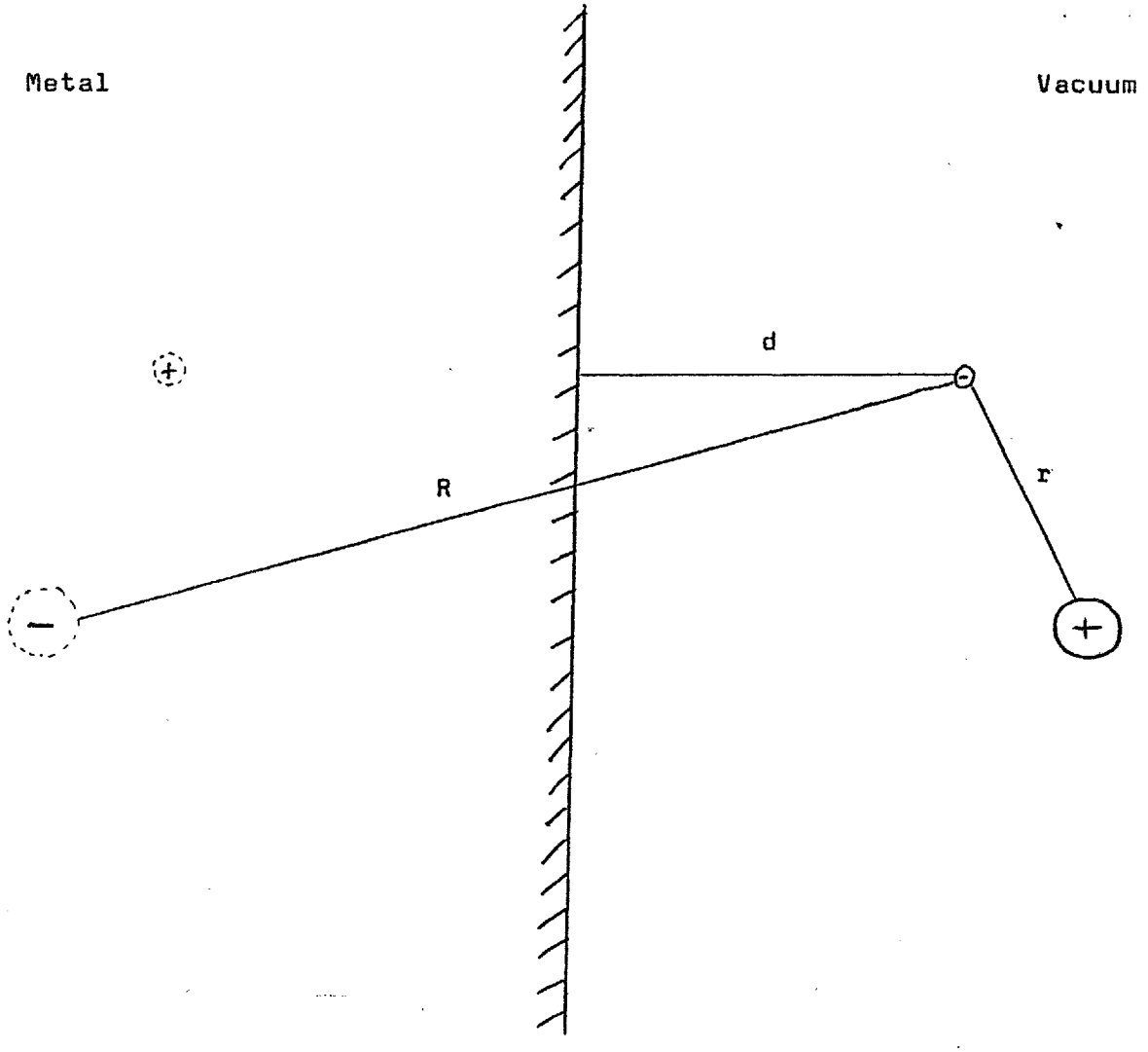


Fig.1 The model for the interaction between the atom and the metal surface adopted by Gadzuk (1967).

compared to other results (Bennett and Falicov 1966), while at d=10Å, Δ had decreased to 10^{-4}eV).

Lang has used a "jellium" model of the metallic substrate-adsorbate system to determine work function vs coverage curves in alkali/transition metal systems. In his model the substrate ionic lattice is replaced by a semi-infinite uniform positive background and the layer of adsorbate ions by an adjoining uniform positive slab . Using the techniques employed for the study of the inhomogeneous electron gas (Hohenberg and Kohn 1964, Kohn and Sham 1965), he obtained the electron density associated with this positive charge configuration, by solving self-consistently a set of one particle equations introduced by Kohn and Sham (1965). From this density, the work function for the model follows immediatly according to the relation

$$\phi = \Delta\Phi - \bar{\mu} \qquad (2.1.13)$$

where $\bar{\mu}$ is the bulk chemical potential of the electrons relative to the mean electrostatic potential in the metal interior, and $\Delta\Phi$ is the rise in mean electrostatic potential across the metal surface, i.e

$$\Delta\Phi = \Phi(\infty) - \Phi(-\infty) = 4\pi\int_{-\infty}^{\infty} dx\, x\left[n(x) - n_+(x)\right] \qquad (2.1.14)$$

where $n_+(x)$ is the density of the positive background configuration, and $n(x)$ is the electron density obtained from the self-consistent calculations.

The changes in coverage were treated as changes in the density of the adsorbate background slab.

This model is of course designed to treat the high coverages region, and achieves good agreement with the results of recent measurements in that region. Lang has attempted to extrapollate his model to the low coverage region thus neglecting the possibility of a Mott transition, further it seems unclear whether the adsorbate valence level has been renormalised correctly.

Phenomenological theories of work function changes have been formulated by Gyftopoulos and Levine (1962) and Steiner and Gyftopoulos (1967). In these the work function of the adatom-metal system is equated to its electronegativity. These theories are among the few which account for covalent bonding and the overlapping of alkali-metal atomic orbitals at high coverages, as well as for the classical depolarization effects.

In the first part of this work, we extend the Gurney approach up to the work function minimum, and hence try to estimate the width and the position of the valence $|ns\rangle$ level of the adsorbed alkali atoms from experimental work function measurements. A preliminary account of this work has been published (Muscat and Newns 1972).

2.2. The model Hamiltonian

Several chemisorption studies (Edwards and Newns 1967, Newns 1969b, Grimley 1967a,b,1970) have been based on a picture in which the metal-adatom system is describable within the Anderson model of localised magnetic states in metals (Anderson 1961).

For any adsorbate atom, the Hamiltonian we are using is a derivative of the Anderson model, to include for interactions between the adatom and the rest of the adlayer. The states of the interacting metal-adatom system are constructed from linear combinations of the unperturbed continuum of metal states $|\underline{k}\rangle$ and the ground state orbital of the adatom $|ns\rangle$. We note that the first excited states $|np_\alpha\rangle$ ($\alpha = x,y,z$) of the adatom are not included in this simple model. These must however be included to determine the intra-atomic polarization effects. A more realistic model in which both the transfer of charge to the adatom, and the intra-adatom polarization are implicitly in-

cluded is considered in chapter 4.

It must be remembered that the set of metal states ($|\underline{k}\rangle$) is complete, it then follows that the basis set comprising of the $|\underline{k}\rangle$'s and the adatom state $|ns\rangle$ must be overcomplete. A property which may be expressed mathematically by the condition that $|ns\rangle$ is orthogonal to the linear combination of metal states from which the states of the interacting system are constructed. Grimley has shown that the basis set ($|ns\rangle, |\underline{k}\rangle$) can be regarded as complete, if the Hamiltonian H is replaced by a pseudo-Hamiltonian H^{ps} defined by

$$H^{ps} = H - SH \ ,$$

where S is the overlap matrix, whose off diagonal elements $\langle ns|\underline{k}\rangle$ are non-zero. We shall assume here that our basis set forms a complete set.

The Hamiltonian H may be written in the form

$$H = H_o + H_I \qquad (2.2.1)$$

where H_o is the Hamiltonian corresponding to a single atom on the surface, and H_I represents the electrostatic interactions due to all the other atoms in the layer.

In the language of second quantization, H_o may be written in the form

$$H_o = \sum_{\underline{k},\sigma} \epsilon_{\underline{k}} n_{\underline{k}\sigma} + \sum_{\sigma} E_{ns'} n_{s\sigma} + U_{eff} n_{s\uparrow} n_{s\downarrow}$$

$$+ \sum_{\underline{k},\sigma} \left[V_{s\underline{k}} C^{+}_{k\sigma} C_{s\sigma} + h.c \right] \qquad (2.2.2)$$

The first term represents the semi-infinite substrate, $\epsilon_{\underline{k}}$ are the energies

corresponding to the states $\varphi_{\underline{k}}$. We must of course remember that the $\varphi_{\underline{k}}$'s are not the usual Bloch functions. Deep in the bulk $\varphi_{\underline{k}}$ behaves like a Bloch state while $\varphi_{\underline{k}}$ decreases exponentially into the vacuum. In addition some members of the set $(\varphi_{\underline{k}})$ might be surface states decaying to zero inside the metal too. $n_{\underline{k}\sigma}$ is the number operator $n_{\underline{k}\sigma} = c^{+}_{\underline{k}\sigma} c_{\underline{k}\sigma}$ where $c^{+}_{\underline{k}\sigma}, c_{\underline{k}\sigma}$ are Fermion creation and destruction operators obeying the anticommutation rules

$$\left\{ c^{+}_{\underline{k}\sigma}, c^{+}_{\underline{k}'\sigma} \right\} = \left\{ c_{\underline{k}\sigma}, c_{\underline{k}'\sigma} \right\} = 0$$

and

$$\left\{ c^{+}_{\underline{k}\sigma}, c^{+}_{\underline{K}'\sigma} \right\} = \delta_{\underline{k}\underline{k}'} \qquad (2.2.3)$$

The second term is the unperturbed energy of the $|ns\rangle$ level renormalised by image effects, the third term corresponds to the repulsive energy of the $|ns\rangle$ functions, also renormalised by image effects, and finally the last term represents the interaction between the atomic state and the continuum of metal states. $V_{s\underline{k}}$ is an adatom-metal transfer integral defined by

$$V_{s\underline{k}} = \langle ns | V | \underline{k} \rangle \ , \qquad (2.2.4)$$

where V is the perturbation in the Hamiltonian, associated with bringing the adatom up to the surface.

We have neglected the Coulomb repulsions between electrons on the same orbital $|\underline{k}\rangle$ in the metal. We mainly rely on the fact that the free electrons in the metal are delocalised and much better screened than in the atom.

H_I describes the effect of the potential $V(\underline{x})$ due to the adatoms other than that described by (2.2.2), which is taken to lie at the origin of the co-ordinate system. In general

$$H_I = \sum_{\sigma} \int \psi^{+}_{\sigma}(\underline{x}) V(\underline{x}) \psi_{\sigma}(\underline{x}) \, d^3x \qquad (2.2.5)$$

where $\psi_\sigma^+(\underline{x})$ is the creation operator for an electron of spin σ at $\underline{x}$

$$\psi_\sigma^+(\underline{x}) = \sum_\nu \varphi_\nu^*(\underline{x})\, c_{\nu\sigma}^+ \qquad (2.2.6)$$

and ν runs over the orbitals of the metal and the adatom. Due to screening, $V(\underline{x})$ is assumed to be small where the substrate wavefunctions are non-zero, so that we may expand $\psi_\sigma(\underline{x})$ in terms of the eigenstates of the adatom alone. So that if we keep only the one belonging to the valence shell, we find

$$\psi_\sigma(\underline{x}) = c_{s\sigma}\, \varphi_{ns}(\underline{x}) \qquad (2.2.7)$$

Since $\underline{x}$ is small, we may expand $V(\underline{x})$ to first order in $\underline{x}$, this gives

$$V(\underline{x}) = V(\underline{0}) + \underline{x}\cdot\nabla V(\underline{x})\Big|_0 \qquad (2.2.8)$$

Substituting for $V(\underline{x})$ and $\psi_\sigma(\underline{x})$ in (2.2.5), we find

$$H_I = \sum_\sigma \Phi\, n_{s\sigma} \qquad (2.2.9)$$

and $\Phi = V(\underline{0})$.

In order to calculate Φ, some assumption about the distribution of atoms on the surface is necessary. We assume that on account of electrostatic repulsion, the adatoms do not cluster but are spread uniformly on the surface. It is possible that at low coverages the distribution is randomised, with ordered structures appearing at higher coverages. However the assumption of a particular structure at low coverages leads to results only weakly structure dependent (see below) so that in this region the results can be considered known despite probable randomisation. At about the work function minimum a square lattice arrangement is observed for caesium on tungsten (Gavrilyuk et al 1966, MacRae et al 1969).

If the adlayer is assumed to form a square lattice, the position vectors of the adatoms are given by $\underline{r}_a = s^{-\frac{1}{2}}(l,m,0)$ and that of their images by $\underline{r}_i = \underline{r}_a - 2d\underline{k}$, where l and m are integers and $\underline{k}$ is a unit vector in the direction perpendicular to the surface. Φ is obtained by summing $qe(\frac{1}{r_a} - \frac{1}{r_i})$ over all the adatom sites i.e

$$\Phi(s) = qes^{\frac{1}{2}} \sum_{l=-\infty}^{\infty} \sum_{m=-\infty}^{\infty} \left[(l^2 + m^2)^{-\frac{1}{2}} - (l^2 + m^2 + 4d^2 s)^{-\frac{1}{2}}\right] \qquad (2.2.10)$$

the summation excluding the term l = 0, m = 0 simultaneously.

$\Phi(s)$ may be expanded in an infinite power series in s given by

$$\Phi(s) = qes^{1/2} \sum_{k=1}^{\infty} \frac{(-1)^{k+1}}{k!} \frac{1}{2}\cdot\frac{3}{2}\cdots\left(k-\frac{1}{2}\right) \sum_{l=-\infty}^{\infty} \sum_{m=-\infty}^{\infty} \frac{(4d^2 s)^k}{(l^2+m^2)^{k+1/2}} \qquad (2.2.11)$$

A reasonable approximation to $\Phi(s)$ for small s, would be to neglect all but the k = 1 term in the summation, i.e

$$\Phi = 2e^2 d^2 s^{3/2} A \qquad (2.2.12)$$

and $$A = \sum_{l=-\infty}^{\infty} \sum_{m=-\infty}^{\infty} (l^2 + m^2)^{-3/2}$$

A is the constant which appeared in eq(1.5). It was first tabulated by Topping (1927), its numerical value being 9.033.

The physical interpretation of this approximation is that each charge-image system is replaced by a dipole of length 2d, an approximation which is valid for small values of the ratio d/a (a is the nearest neighbour distance in the adlayer, $a = s^{-\frac{1}{2}}$ for a square lattice), i.e for small s.

Let us now consider the case of an equitriangular adlayer (fig.2). The position vectors of the atoms are $\underline{r}_a = \frac{a}{2}\left\{m + l, \sqrt{3}(m - l), 0\right\}$, where m and l are integers defined in fig.2. The potential $\Phi(s)$ is given in this case by

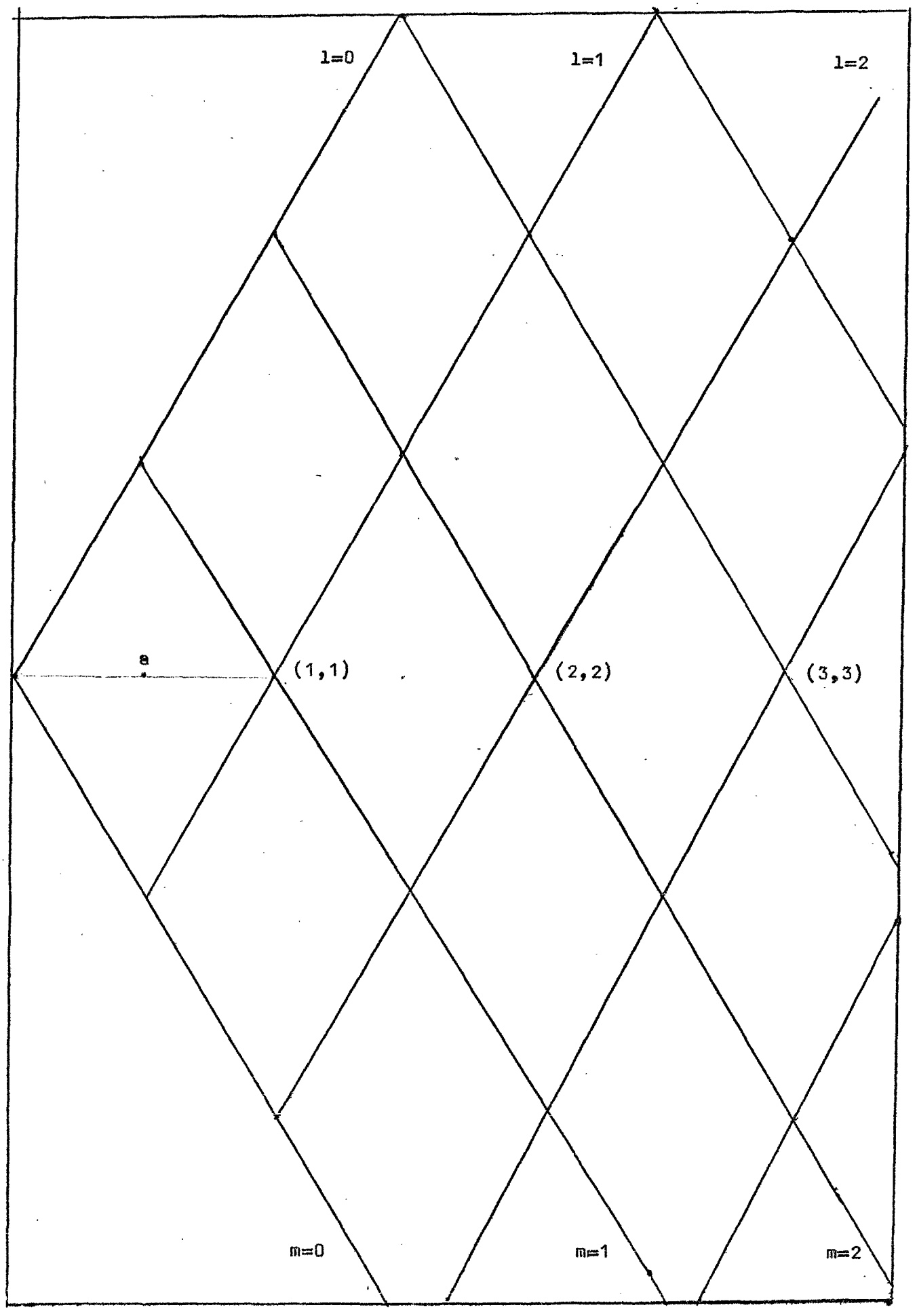


Fig.2 Equitriangular lattice arrangement for the adlayer

$$\Phi(s) = \frac{qe}{a} \sum_{l=-\infty}^{\infty} \sum_{m=-\infty}^{\infty} \left[(l^2+m^2-lm)^{-\frac{1}{2}} - (l^2-lm+m^2-4d^2/a^2)^{-\frac{1}{2}} \right] \qquad (2.2.13)$$

and a is related to the surface concentration by the simple rule $a = (2/\sqrt{3}s)^{\frac{1}{2}}$. In the dipole approximation $\Phi(s)$ becomes

$$\Phi(s) = 2e^2d^2s^{3/2}A^* \qquad (2.2.14)$$

where

$$A^* = (2/\sqrt{3})^{-3/2} \sum_{l=-\infty}^{\infty} \sum_{m=-\infty}^{\infty} (l^2 - lm + m^2)^{-3/2}$$

calculations (Topping 1927) give $A^* = 8.893$.

It thus appears that $\Phi(s)$ in the dipole approximation is practically equal for both square and equitriangular networks. We shall assume from now on that the adlayer is a square lattice. Plots of $\Psi(s) = \Phi(s)/q$ as a function of s are given in fig.3 for different values of d.

The various infinite double series may be calculated, by summing over a finite number of terms, and estimating the error made by neglecting the other terms. e.g for A we have

$$A = 4S_{n^*} + 8E_{n^*} \qquad (2.2.15)$$

where

$$S_{n^*} = \sum_{l=1}^{n^*} \sum_{m=0}^{n^*} (l^2 + m^2)^{-3/2} \qquad (2.2.16)$$

and E_{n^*} is the correction needed to balance the neglect of terms $l,m > n^*$ in the series

$$E_{n^*} = \int_{n^*+\frac{1}{2}}^{\infty} dx \int_0^x dy (x^2 + y^2)^{-3/2} = \frac{1}{\sqrt{2}} \frac{1}{n^* + \frac{1}{2}} \qquad (2.2.17)$$

with the inclusion of this correction term A(n*) is found to be a rapidly

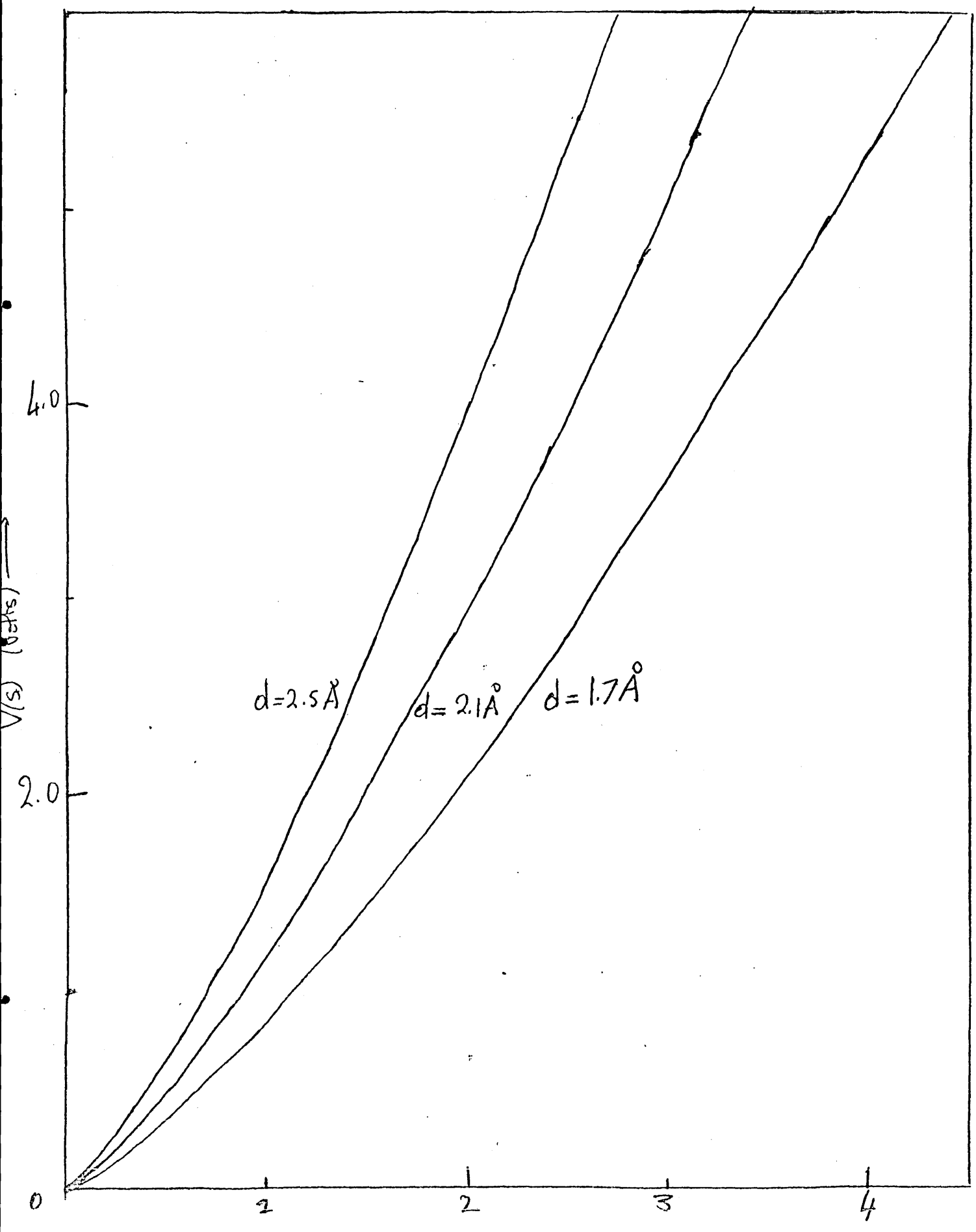


Fig. 3

converging function of n*, and it is found that a value of n* = 20 is quite sufficient to obtain results with the accuracy of Topping(1927).

2.3. Solution in Hartree-Fock approximation

The Hamiltonian (2.2.1) was solved in the Hartree-Fock approximation. This approximation has been criticised when applied to the calculation of localised magnetic moments in metals (Schrieffer and Mattis 1965, Hewson 1966, Blandin 1968), because it overemphasizes the tendency towards magnetic solutions. The Hartree-Fock approximation includes the perturbation U_{eff} only to first order, and should be valid for sufficiently small U_{eff}. For the alkalis U is expected to be small, it is further reduced by the renormalisation from image effects as discussed above. The small values of the occupancies of the levels in alkali/transition metal systems (Wojciechowski 1966, 1968, Bennett and Falicov 1966, Bennett 1968) strongly indicate that no magnetic solutions exist (Grimley 1970b). Some workers have gone beyond the Hartree-Fock approximation, in their solution of the Anderson Hamiltonian as applied to the chemisorption of a single alkali atom on a metal surface. We note in particular the work of Gadzuk, Hartman and Rhodin (1971), who use the low density approximation (LDA) of Schrieffer and Mattis (1965), in which the Coulomb integral U is replaced by an effective potential; to determine binding energies for alkali atoms on metal surfaces. This approximation should be suited to describe the chemisorption of a single alkali, since the occupation of the adatom level is small compared with unity (Bennett and Falicov 1966). This approximation may not be used in our case. In fact the occupations of the levels will increase with the number of adatoms on the surface (Gurney 1935), and may reach values which are outside the range of validity of the L.D.A.

The Fock Hamiltonian for any spin σ may then be written

$$H^{\sigma} = \sum_{\underline{k}} \epsilon_{\underline{k}} n_{\underline{k}\sigma} + E_{\sigma} n_{s\sigma} + \sum_{\underline{k}} (V_{s\underline{k}} c_{\underline{k}\sigma}^{+} c_{s\sigma} + h.c) \qquad (2.3.1)$$

where

$$E_{\sigma} = E_{ns}^{\prime} + U_{eff} n + \Phi \qquad (2.3.2)$$

and $n = \langle n_{s\uparrow} \rangle = \langle n_{s\downarrow} \rangle$.

We follow here the method employed by Anderson to solve (2.3.1), an equivalent method for determining the Green functions exists (Zubarev 1960).

Let us denote our basis set of eigenstates by $|\nu\rangle$, then the one-electron state creation operator $c_{\nu\sigma}^{+}$ and the energies ϵ_{ν} satisfy the equation of motion

$$\left[H^{\sigma}, c_{\nu\sigma}^{+}\right] = \epsilon_{\nu} c_{\nu\sigma}^{+} \qquad (2.3.3)$$

and

$$c_{\nu\sigma}^{+} = \sum_{\underline{k}} \langle \nu | \underline{k} \rangle c_{\underline{k}\sigma}^{+} + \langle \nu | s \rangle c_{s\sigma}^{+} \qquad (2.3.4)$$

The equations for the various unperturbed operators, are

$$\left.\begin{aligned} \left[H^{\sigma}, c_{\underline{k}\sigma}^{+}\right] &= \epsilon_{\underline{k}} c_{\underline{k}\sigma}^{+} + V_{\underline{k}s} c_{s\sigma}^{+} \\ \text{and} \\ \left[H^{\sigma}, c_{s\sigma}^{+}\right] &= E_{\sigma} c_{s\sigma}^{+} + \sum_{\underline{k}} V_{s\underline{k}} c_{\underline{k}\sigma}^{+} \end{aligned}\right\} \qquad (2.3.5)$$

If we now substitute these commutators in the equation of motion (2.3.3) then equating the coefficients of each operator, we find

$$\left.\begin{aligned} \epsilon_{\nu} \langle \nu | \underline{k} \rangle &= \epsilon_{\underline{k}} \langle \nu | \underline{k} \rangle + V_{\underline{k}s} \langle \nu | s \rangle \\ \text{and} \\ \epsilon_{\nu} \langle \nu | s \rangle &= E_{\sigma} \langle \nu | s \rangle + \sum_{\underline{k}} V_{s\underline{k}} \langle \nu | \underline{k} \rangle \end{aligned}\right\} \qquad (2.3.6)$$

These equations can be solved exactly by Green function methods. The most interesting quantity is the mean density of admixture of the adatom valence level into the continuum levels of energy ϵ.

$$\rho_{s\sigma}(\epsilon) = \sum_{\nu} \delta(\epsilon_\nu - \epsilon) \, |\langle \nu | s \rangle|^2 \qquad (2.3.7)$$

since it determines the fractional occupation of the level

$$n = \langle n_{s\sigma} \rangle = \int_{-\infty}^{\epsilon_F} \rho_{s\sigma}(\epsilon) \, d\epsilon \qquad (2.3.8)$$

This and other quantities of interest may be obtained by studying the Green operator (e.g see Messiah 1965)

$$\hat{G}(\epsilon) = \lim_{\delta \to 0+} (\epsilon + i\delta - H)^{-1} \qquad (2.3.9)$$

We may now derive the Green functions

$$G^{\sigma}_{\alpha\beta}(\epsilon) = \sum_{\nu} \frac{\langle \alpha | \nu \rangle \langle \nu | \beta \rangle}{(\epsilon + i\delta - \epsilon_\nu)} \qquad (2.3.10)$$

where $|\alpha\rangle$ and $|\beta\rangle$ are members of the basis set of $|\nu\rangle$. The density $\rho_{s\sigma}(\epsilon)$ as given by (2.3.7) may be rewritten

$$\rho_{s\sigma}(\epsilon) = \frac{1}{\pi} \sum_{\nu} |\langle \nu | s \rangle|^2 \lim_{\delta \to 0} \frac{\delta}{(\epsilon - \epsilon_\nu)^2 + \delta^2} \qquad (2.3.11)$$

Finally using (2.3.10) it is easily shown that

$$\rho_{s\sigma}(\epsilon) = -\frac{1}{\pi} \operatorname{Im} G^{\sigma}_{ss}(\epsilon) \qquad (2.3.12)$$

If we now multiply both of equations (2.3.6) by $\langle\nu|s\rangle(\epsilon + i\delta - \epsilon_\nu)^{-1}$ and sum over all ν, we find

$$\left.\begin{aligned}(\mathcal{E} - E_\sigma)\, G^\sigma_{ss} - \sum_{\underline{k}} V_{s\underline{k}}\, G^\sigma_{\underline{k}s} &= 1 \\ (\mathcal{E} - \epsilon_{\underline{k}})\, G^\sigma_{\underline{k}s} - V_{\underline{k}s}\, G^\sigma_{ss} &= 0\end{aligned}\right\} \qquad (2.3.13)$$

and $\mathcal{E} = \epsilon + i\delta$.

We may then solve for G^σ_{ss}, and we find

$$G^\sigma_{ss}(\epsilon) = \left[\mathcal{E} - E_\sigma - \sum_{\underline{k}} |V_{s\underline{k}}|^2 (\mathcal{E} - \epsilon_{\underline{k}})^{-1}\right]^{-1} \qquad (2.3.14)$$

the sum in (2.3.14) may be evaluated; we find

$$\lim_{\delta \to 0+} \sum_{\underline{k}} |V_{s\underline{k}}|^2 (\mathcal{E} - \epsilon_{\underline{k}})^{-1} \equiv \Lambda - i\Delta \qquad (2.3.15)$$

where

$$\Lambda = P\left\{\sum_{\underline{k}} \frac{|V_{s\underline{k}}|^2}{\epsilon - \epsilon_{\underline{k}}}\right\} \qquad (2.3.16)$$

is an effective energy shift of the adatom level, and P denotes the Cauchy principal value. The Hilbert transform of Λ, Δ given by

$$\Delta = \pi \sum_{\underline{k}} |V_{s\underline{k}}|^2 \delta(\epsilon - \epsilon_{\underline{k}}) \qquad (2.3.17)$$

represents the width of the level.

If the surface density of states of the substrate is assumed constant, (this is not too serious an approximation for a metal like tungsten, whose density of states exhibits a broad maximum at the centre of the band), then Λ and Δ become energy independent, and it is easily shown from

(2.3.14) that $G_{ss}^{\sigma}(\epsilon)$ behaves exactly as if there were a "virtual state" at

$$\epsilon = E_{\sigma} + \Lambda + i\Delta .$$

The density distribution of the s-state is thus given by the Lorentzian

$$\rho_{s\sigma}(\epsilon) = \frac{1}{\pi} \frac{\Delta}{(\epsilon - E(s))^2 + \Delta^2} \qquad (2.3.18)$$

and

$$E(s) = E_{\sigma} + \Lambda \qquad (2.3.19)$$

in analogy to the Bennett-Falicov model which we reviewed in section 2.1.

Taking the zero of energy at the Fermi level n is now easily shown to be given by

$$n = \tfrac{1}{2} - \frac{1}{\pi} \arctan(E(s)/\Delta) \qquad (2.3.20)$$

E(s) is itself dependent on n through (2.3.2) and (2.3.19), so that we have a self-consistent problem in n and E(s), this can be solved numerically for different values of the surface coverage s. The results will further depend on the additional parameters $E_o = E_{ns}' + \Lambda$ and U_{eff}. The graphical solution of the self-consistent problem is illustrated in fig.4. Let us introduce the parameters $\alpha = (E_o - \mathcal{F})/\Delta$, $\beta = (U_{eff} + 2\mathcal{F})/\Delta$, the straight lines in the diagram correspond to (a) $\alpha = 2$, $\beta = 1$, (b) $\alpha = 1$, $\beta = 3$ and (c) $\alpha = 0$, $\beta = 5$. The passage from (a) to (c) corresponds to an increase in s. We thus see from this simple plot that as we increase the coverage s, the valence energy level of the adatom is gradually pushed downwards relative to ϵ_F, thus increasing the occupation n of the level.

Our aim in developing this simple model is to estimate the width Δ and position of the $|6s\rangle$ level of adsorbed caesium atoms, using experimental results for Cs/W systems. We develop expressions which are valid either in the low coverage region, or at the work-function minimum, and compare them

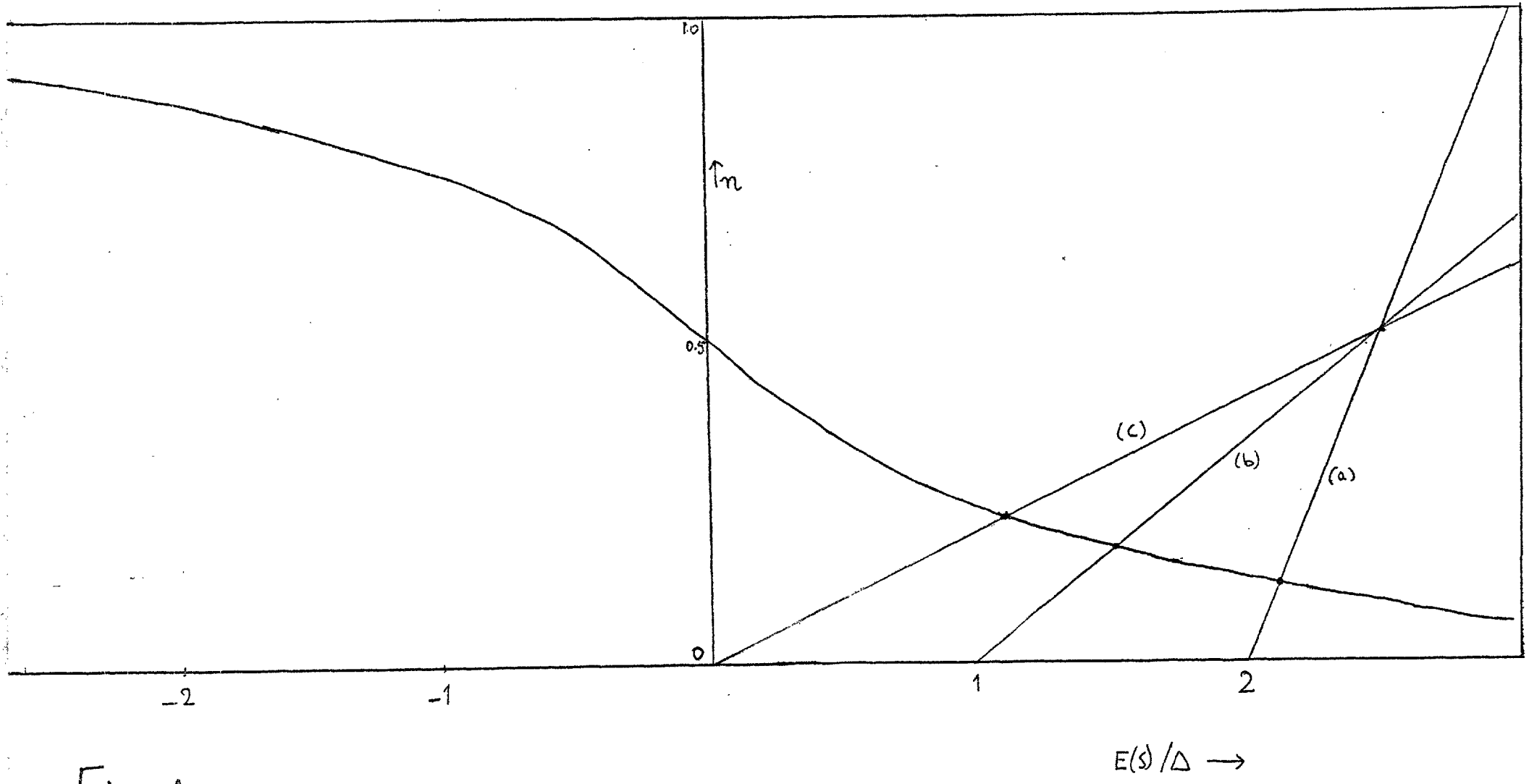


Fig. 4

to the experimental measurements.

(a) The low coverage region

Treating $\Phi(s)$ in the dipole approximation (2.2.12), it is easily shown that the self-consistent equation (2.3.20) may be rewritten

$$E_o + U_{eff}n + 2e^2d^2As^{3/2}(2n - 1) = \Delta \cot \pi n , \qquad (2.3.21)$$

while at zero coverage, this becomes

$$E_o + U_{eff}n_o = \Delta \cot \pi n_o \qquad (2.3.22)$$

and $n_o = n(0)$. Elimination of E_o from (2.3.21) and (2.3.22) gives

$$2e^2d^2As^{3/2}(2n_o - 1) = (n_o - n)(U_{eff} + \pi\Delta \operatorname{cosec}^2 \pi n_o) \qquad (2.3.23)$$

where we have used the approximation

$$\cot \pi n - \cot \pi n_o \simeq -\pi (n - n_o)\operatorname{cosec}^2 \pi n_o ,$$

which is valid for small $n_o - n$.

Using the relation

$$\Delta\phi = -4\pi eds(1 - 2n) \qquad (2.3.24)$$

(this is obtained from (1.3) by using the relation $q = e(1 - 2n)$), it is easily shown that

$$n - n_o = \tfrac{1}{2}(2n_o - 1)\left[\frac{\Delta\phi}{s\left(\frac{d\phi}{ds}\right)_o} - 1\right] , \qquad (2.3.25)$$

if we now replace this in (2.3.23) we find

$$\frac{\Delta\phi}{s\left(\frac{d\phi}{ds}\right)_o} = 1 - \frac{4e^2d^2As^{3/2}}{U_{eff} + \pi\Delta\,\mathrm{cosec}^2\pi n_o} \qquad (2.3.26)$$

This relation is equivalent to the depolarization functions which we introduced in chapter 1, and which have been used by several authors to fit experimental data (Langmuir 1932, Schmidt and Gomer 1966). The quantity

$$\alpha = \frac{4e^2d^2}{U_{eff} + \pi\Delta\,\mathrm{cosec}^2\pi n_o} \qquad (2.3.27)$$

has the dimension of volume, and represents the effective polarizability of the system.

The results of this subsection have been compared with work function vs coverage measurements for the system Cs/W. We have used the results of Fehrs and Stickney (1971) whose low coverage results are particularly good. Following equation (2.3.26) a plot of $\Delta\phi(s)/s$ vs $s^{3/2}$ at low coverages is given in fig.5. This plot tends to magnify the errors at small s but the results of Fehrs and Stickney are accurate enough for the slope and intercept to be determined. The experimental polarizability is then equated to our theoretical expression (2.3.27). If we assume for simplicity that U_{eff} may be neglected, and express d in the form

$$d = \frac{1}{4\pi e(2n_o - 1)}\left(\frac{d\phi}{ds}\right)_o, \qquad (2.3.28)$$

we can obtain a relation between the parameters Δ and n_o. Use of equation (2.3.22) gives us the relation between E_o and Δ which is plotted in fig.6 (the full curve).

(b) The work function minimum

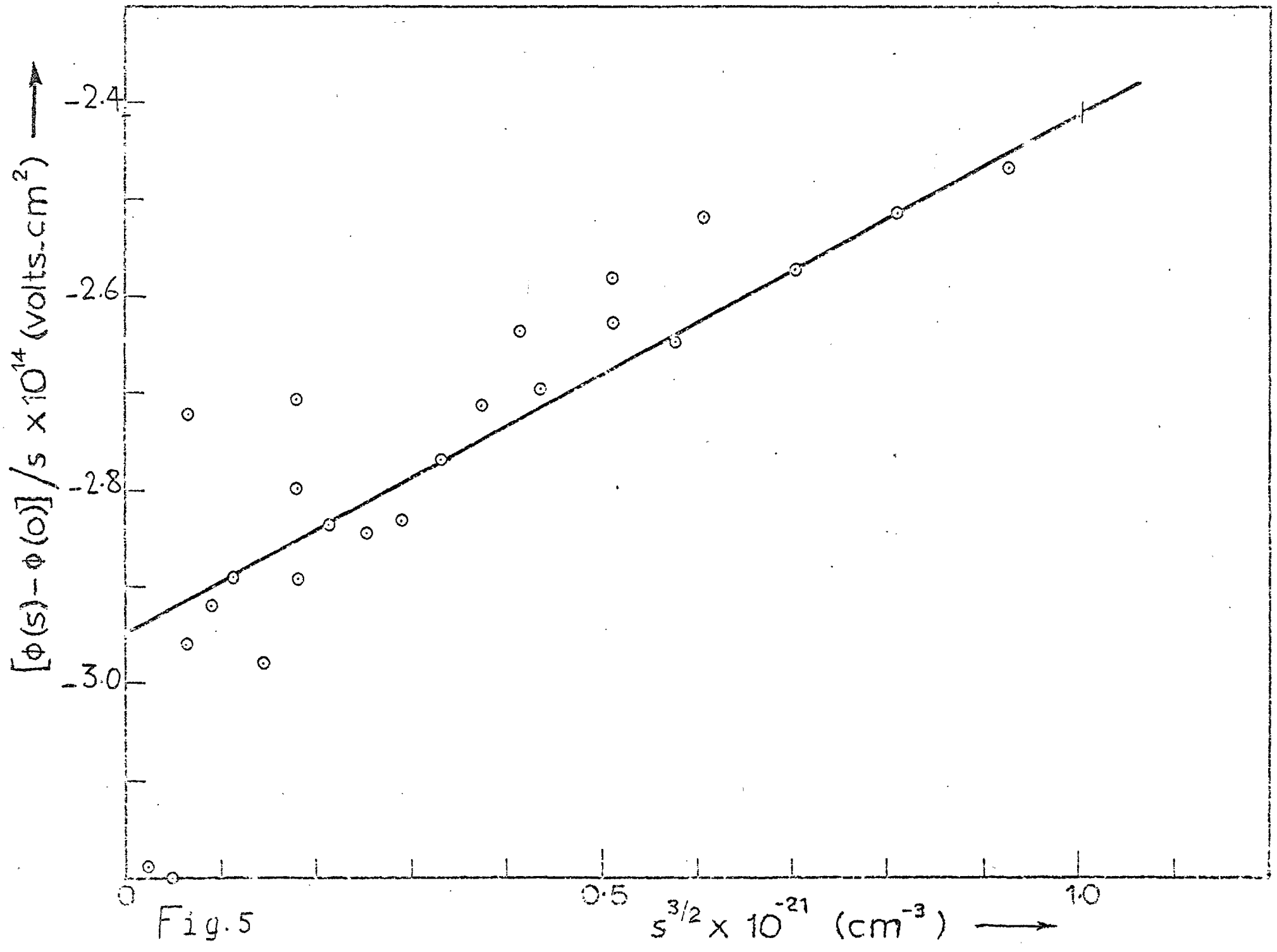

-2.4
-2.6
-2.8
-3.0
$[\phi(s)-\phi(0)]/s \times 10^{14}$ (volts-cm^2) ⟶
0
0.5
1.0
$s^{3/2} \times 10^{-21}$ (cm^{-3}) ⟶

Fig. 5

The condition for the minimum may be written

$$\frac{d}{ds}(\Delta\phi) = 0 \qquad (2.3.29)$$

assuming d to be independent of coverage, we find from (2.3.24)

$$2s\frac{dn}{ds} + (2n - 1) = 0 \qquad (2.3.30)$$

If we differentiate both the self-consistent equations (2.3.19) and (2.3.20) with respect to s it is easily shown that equation (2.3.30) reduces to

$$2s^2\frac{d}{ds}\left(\frac{\Psi(s)}{s}\right) = U_{eff} + \pi\Delta\,\mathrm{cosec}^2\pi n \qquad (2.3.31)$$

Elimination of n between equations (2.3.20) and (2.3.31) gives us a relationship between E_o and Δ at fixed s and U_{eff} similar to the existence curve for magnetic solutions in the Anderson model (Anderson 1961). If U_{eff} is taken to be zero, the relation between E_o and Δ may be written

$$E_o = \pm\left\{\frac{2\Psi}{\pi}\arccos\left(\frac{\pi\Delta}{2\beta}\right)^{\frac{1}{2}} + \Delta\left(\frac{2\beta}{\pi\Delta} - 1\right)^{\frac{1}{2}}\right\} \qquad (2.3.32)$$

and $\beta = s^2\frac{d}{ds}\left(\frac{\Psi(s)}{s}\right)$.

We now fix s at the coverage at the minimum $s_{min} = 2.5\times10^{14}$ cm^{-2} (Fehrs and Stickney 1971, Gavrilyuk et al 1966, Sidorski et al 1969), and plot the curves (2.3.32) for various values of d, also in fig.6.

(c) Determination of the parameters

Elimination of s between (2.3.20) and (2.3.31) gives us yet another

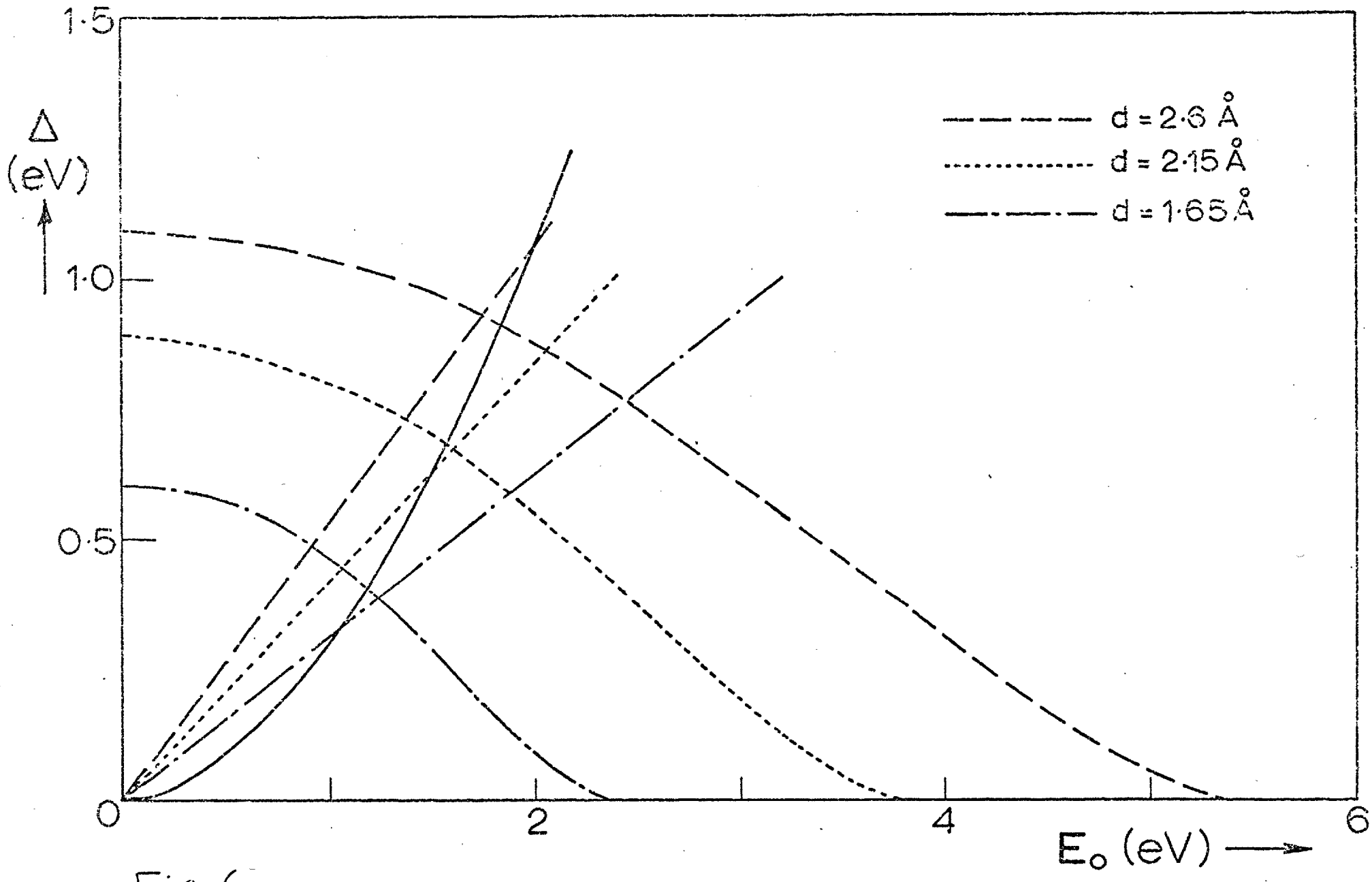


Fig. 6

useful relation between Δ and E_o. If despite rather inadequate accuracy near the minimum, the low coverage approximation for $\mathcal{F}(s)$ is used i.e $\mathcal{F}(s) = 2e^2d^2As^{3/2}$, we can eliminate the s dependence of (2.3.20) and (2.3.31) by remarking that

$$2s^2\frac{d}{ds}\left(\frac{\mathcal{I}(s)}{s}\right) = \mathcal{F}(s)$$

The resulting expression is

$$E_{ns} + \Lambda + \frac{U}{2} = \Delta\left[\tan\frac{\pi}{2}Z + \pi Z\sec^2\frac{\pi}{2}Z\right] + \frac{3}{2}U_{eff}Z \qquad (2.3.33)$$

and

$$Z = 1 - 2n .$$

This is a reasonable approximation to the empirical linear relationship found by Swanson and Strayer (1968) between Z and the adatom ionization potential at the work function minimum, provided that V_{sk} and U are assumed not to vary with adatom. If we assume that U_{eff} may be neglected compared to $\pi\Delta$, it is found from Swanson and Strayer's results that $\Delta = 1.83eV$.

An extension of equation (2.3.33) valid at higher coverages may be obtained for a given value of s_{min}, Z being now derived from the experimental values of s_{min}, and the work function minimum. The resulting linear relationship between E_o and Δ is also plotted for a few values of d in fig.6. The intersections between the two sets of curves corresponding to the high coverage region for a given value of d in the range between the ionic and the atomic radii of Cs, are seen to be in fair agreement with the low coverage data.

Taking an intermediate value of d ($d = 2.15\text{Å}$) at s_{min} gives $\Delta \simeq .65eV$, $E_o \simeq 1.55eV$. For comparison we note that E_{ns}' given by (2.1.1) gives a value $E_{ns}' = 2.3eV$ at $d = 2.15\text{Å}$.

The discrepancy between this result and the value of Δ obtained from the Swanson-Strayer relationship may be largely due to the low coverage approximation on which the latter is based. Attempts to calculate Δ from first principles seem to give widely divergent results (Bennett 1968, Remy 1970), but Bennett found that the experimental polarizability for the K/W system was compatible with his value $\Delta = 2.3$eV which is much larger than ours.

A contribution to the dipole moment variation of the adlayer is also to be expected from the intra-atomic polarizability which is large for free alkali atoms, and this is the subject of the next chapter.

Chapter 3

LINEAR RESPONSE FORMALISM

3.1. The polarizability of the free alkali atom

It is well known from atomic spectra that the f-sum rule is almost entirely satisfied by the ns-np transitions (Condon and Shortley 1935) so that a calculation of the polarizability of an atom may be formulated in terms of the ns and np levels of the atom alone.

The polarizability of the free alkali atom with one electron may be calculated in 2^{nd} order perturbation theory.

If E is the applied uniform electric field, then the potential arising from E is given by

$$V = eEx \qquad (3.1.1)$$

The induced dipole moment $\langle \mu \rangle$ is proportional to the electric field and in the same direction, the ratio α of the dipole moment to field strength is called the polarizability

$$\alpha = \frac{\langle \mu \rangle}{E} \qquad (3.1.2)$$

The dipole moment $\langle \mu \rangle$ is given by

$$\langle \mu \rangle = \langle \psi | ex | \psi \rangle \qquad (3.1.3)$$

where $|\Psi\rangle$ are the eigenstates of the system. If only the $|ns\rangle$ and $|np\rangle$ levels of the atom are included then $|\Psi\rangle$ is given by

$$|\Psi\rangle = |s\rangle + \frac{|p\rangle\langle p|V|s\rangle}{E_p - E_s} \qquad (3.1.4)$$

From which it follows that

$$\alpha = 2e^2 \frac{|\langle s|x|p\rangle|^2}{E_p - E_s} \qquad (3.1.5)$$

Finally we may eliminate the matrix element $\lambda = \langle s|x|p\rangle$. Indeed according to the f-sum rule (Schiff 1955) we have

$$(E_p - E_s)|\langle s|x|p\rangle|^2 \simeq \frac{\hbar^2}{2m} \qquad (3.1.6)$$

For cassium , the energy separation between the s and p levels is equal to $2E = 1.44eV$ (Atomic Energy Levels, Circular of the National Bureau of Standards 467, Volume III), and from (3.1.5) and (3.1.6) we find

$$\lambda = -1.62\mathring{A} \quad , \quad \alpha = 52.5\mathring{A}^3 \ .$$

These values are of course unlikely to remain exact in the case of an adsorbed atom with valence orbitals as extended as those of Cs. We think it possible that the effect of the surface in intersecting the region of space where these orbitals are large would be to reduce the matrix element λ considerably. We have thus employed a range of λ values in this work.

3.2 Dielectric response of the substrate

The linear dipole polarizability of the adatom-substrate system may be formulated in terms of the $|ns\rangle$ and $|np_z\rangle$ levels of the adatom alone (z is the direction perpendicular to the surface). The neglect of the states

$|np_x\rangle$ and $|np_y\rangle$ is based on the assumptions that

(i) the matrix elements $\langle np_x|V|\underline{k}\rangle$ and $\langle np_y|V|\underline{k}\rangle$ will be small compared to $\langle np_z|V|\underline{k}\rangle$ (this is due to the large size of the Cs atom, and the relative flatness of the surfaces we are considering), so that the $|np_z\rangle$ orbital will couple much more strongly with the metal states than the $|np_x\rangle$ and $|np_y\rangle$ orbitals, if the matrix elements $\langle np_x|V|\underline{k}\rangle$ and $\langle np_y|V|\underline{k}\rangle$ are small, the lifetime broadening of $|np_x\rangle$ and $|np_y\rangle$ will be small, so that these states will be kept almost empty;

(ii) the electric fields parallel to the surface will be small, so that there is only weak coupling between $|np_x\rangle$, $|np_y\rangle$ and $|ns\rangle$.

Neglecting U_{eff}, the Hamiltonian (2.3.1) is conveniently generalised to its present form

$$H^{\sigma} = \epsilon_s n_{s\sigma} + \epsilon_p n_{p\sigma} + \sum_{\underline{k}} \epsilon_{\underline{k}} n_{\underline{k}\sigma} + \sum_{\underline{k}} (V_{s\underline{k}} c^{+}_{\underline{k}\sigma} c_{s\sigma} + V_{p\underline{k}} c^{+}_{\underline{k}\sigma} c_{p\sigma} + h.c) \qquad (3.2.1)$$

where

$$\epsilon_s = E'_{ns} + \Phi \quad \text{and} \quad \epsilon_p = \epsilon_s + 2E \qquad (3.2.2)$$

We now calculate the linear response of the system to a perturbing potential $V(\underline{x},t)$ in the Hamiltonian. We use here the formalism introduced by Newns (1970).

The response $\delta\rho$ of the system to V may be obtained from the expression (Kubo 1957)

$$\delta\rho(\underline{x},t) = \int_0^t dt' \int d^3x' \, R(\underline{x},t,\underline{x}',t')V(\underline{x}',t') \qquad (3.2.3)$$

where the response function R is defined by

$$R(\underline{x},t,\underline{x}',t') = ie^2 \sum_{\sigma,\sigma'} \langle \phi_0 | [\rho_{\sigma}(\underline{x}',t'), f_{\sigma'}(\underline{x},t)] | \phi_0 \rangle \qquad (3.2.4)$$

with

$$\rho_\sigma(\underline{x},t) = \sum_{i,j} c^{+}_{i\sigma}(t)c_{j\sigma}(t)\varphi^{*}_{i}(\underline{x})\varphi_j(\underline{x}) \qquad (3.2.5)$$

The perturbation is assumed to be switched on at $t = 0$. φ_i are the one-particle wavefunctions of the unperturbed system. $|\phi_o\rangle$ is the time independent Heisenberg ground state of the unperturbed system. The creation and destruction operators are given by

$$c_{i\sigma}(t) = e^{-iw_i t}c_{i\sigma} \qquad (3.2.6)$$

where $\hbar w_i = \epsilon_i$ is the energy eigenvalue of φ_i. The time dependence may then be factored out of the commutator in (3.2.4). So that we have

$$\langle\phi_o|[c^{+}_{i\sigma}c_{j\sigma},\ c^{+}_{l\sigma'},c_{m\sigma'}]|\phi_o\rangle = (n_i-n_j)\delta_{im}\delta_{jl}\delta_{\sigma\sigma'} \qquad (3.2.7)$$

where at zero temperature

$$\left.\begin{aligned} n_i &= 1\ ;\quad \epsilon_i < \epsilon_F \\ n_i &= 0\ ;\quad \epsilon_i > \epsilon_F \end{aligned}\right\} \qquad (3.2.8)$$

substituting back in (3.2.3) we find

$$R(\underline{x},\underline{x}',t-t') = 2ie^2 \sum_{i,j} (n_i - n_j)e^{i(t'-t)(w_i-w_j)}$$

$$\varphi_i^{*}(\underline{x}')\varphi_j(\underline{x}')\varphi_j^{*}(\underline{x})\varphi_i(\underline{x}) \qquad (3.2.9)$$

While in Fourier representation equations (3.2,3) and (3.2.9) become

$$\delta\rho(\underline{x},w) = \int d^3x R(\underline{x},\underline{x}',w)V(\underline{x}',w) \qquad (3.2.10)$$

$$R(\underline{x},\underline{x}',w) = 2e^2 \sum_{i,j} \frac{n_i - n_j}{w_i - w_j + w - i\delta} \varphi_i^*(\underline{x}')\varphi_j(\underline{x}') \times \varphi_j^*(\underline{x})\varphi_i(\underline{x}) \qquad (3.2.11)$$

Equations (3.2.10) and (3.2.11) give the linear response of any large system of non interacting fermions.

The dipole moment in any given direction η is related to the static response function $\rho(\underline{x},0)$ of the system as follows

$$\mu_\eta = \int x_\eta \rho(\underline{x},0) d^3x = \int x_\eta d^3x \int d^3x' R(\underline{x},\underline{x}',0) V(\underline{x}',0) \qquad (3.2.12)$$

The perturbing potential $V(\underline{x})$ is given by equation (2.2.8), and may be rewritten in the form

$$V(\underline{x}) = V(\underline{0}) + \sum_{\nu=1}^{3} x_\nu E_\nu \qquad (3.2.13)$$

where E_ν is the electric field in the ν direction. (3.2.12) may be rewritten

$$\mu_\eta = \mu_0 + \sum_{\nu=1}^{3} \alpha_{\eta\nu} E_\nu \qquad (3.2.14)$$

where $\alpha_{\eta\nu}$ represents the polarizability in the η direction due to a field in the ν direction, and is given by the relation

$$\alpha_{\eta\nu} = -\frac{2e^2}{\pi} \sum_{\substack{m_1,m_2 \\ m_3,m_4}} \langle m_1|x_\eta|m_2\rangle\langle m_3|x_\nu|m_4\rangle \times \mathrm{Im} \int_{-\infty}^{\epsilon_F} dw \sum_{i,j} \frac{\langle j|m_1\rangle\langle m_2|i\rangle\langle i|m_3\rangle\langle m_4|j\rangle}{(w - w_i + i\delta)(w - w_j + i\delta)} \qquad (3.2.15)$$

where we have used the identity

$$\frac{n_i - n_j}{w_i - w_j} = -\frac{1}{\pi} \mathrm{Im} \int_{-\infty}^{\epsilon_F} \frac{dw}{(w - w_i + i\delta)(w - w_j + i\delta)} \quad ,\delta = 0^+ \qquad (3.2.16)$$

and summed over the dummy variables m_1, m_2, m_3, m_4. The expression (3.2.15) for $\alpha_{\eta\nu}$ may be rewritten in terms of the Green functions $G_{m_i m_j}$ defined in the usual way (i.e see eq (2.3.10)), i.e

$$\alpha_{\eta\nu} = -\frac{2e^2}{\pi} \mathrm{Im} \sum_{\substack{m_1, m_2 \\ m_3, m_4}} \int_{-\infty}^{\epsilon_F} dw \; G_{m_2 m_3}(w) G_{m_1 m_4}(w)$$

$$\times \langle m_1 | x_\eta | m_2 \rangle \langle m_3 | x_\nu | m_4 \rangle \qquad (3.2.17)$$

Equation (3.2.17) represents the intra-atomic polarizability in any direction η due to an electric field in any direction ν. In our case the most important contribution to α will come from the component α_{zz}. Further the only matrix elements in (3.2.17) which are not negligible according to the f-sum rule are those with m_i = s, or p, hence (3.2.17) becomes

$$\alpha_{zz} = -\frac{2e^2\lambda^2}{\pi} \mathrm{Im} \int_{-\infty}^{\epsilon_F} dw \left[2G_{ss}(w) G_{pp}(w) + 2G_{sp}(w) G_{ps}(w) \right] \qquad (3.2.18)$$

3.3. Determination of the Green functions.

We use here the method introduced by Anderson (Anderson 1961, Alexander and Anderson 1964, Moriya 1966), and already employed in chapter 2. Let us define the one electron creation operator $c^+_{\nu\sigma}$

$$c_{\nu\sigma}^{+} = \sum_{\underline{k}} \langle \nu | \underline{k} \rangle c_{\underline{k}\sigma}^{+} + \langle \nu | s \rangle c_{s\sigma}^{+} + \langle \nu | p \rangle c_{p\sigma}^{+} \qquad (3.3.1)$$

then $c_{\nu\sigma}^{+}$ and the corresponding energies ϵ_ν must satisfy the equation of motion

$$\left[H^{\sigma},\ c_{\nu\sigma}^{+}\right] = \epsilon_\nu c_{\nu\sigma}^{+} \qquad (3.3.2)$$

The various commutators are

$$\left.\begin{aligned} \left[H^{\sigma},\ c_{i\sigma}^{+}\right] &= \epsilon_i c_{i\sigma}^{+} + \sum_{\underline{k}} V_{i\underline{k}} c_{\underline{k}\sigma}^{+} \qquad i=s,p \\ \left[H^{\sigma},\ c_{\underline{k}\sigma}^{+}\right] &= \epsilon_{\underline{k}} c_{\underline{k}\sigma}^{+} + V_{\underline{k}s} c_{s\sigma}^{+} + V_{\underline{k}p} c_{p\sigma}^{+} \end{aligned}\right\} \qquad (3.3.3)$$

The equations for the various Green functions are

$$\left.\begin{aligned} (\epsilon - \epsilon_s) G_{ss}^{\sigma} - \sum_{\underline{k}} V_{s\underline{k}} G_{\underline{k}s}^{\sigma} &= 1 \\ (\epsilon - \epsilon_p) G_{ps}^{\sigma} - \sum_{\underline{k}} V_{p\underline{k}} G_{\underline{k}s}^{\sigma} &= 0 \\ (\epsilon - \epsilon_{\underline{k}}) G_{\underline{k}s}^{\sigma} - V_{\underline{k}s} G_{ss}^{\sigma} - V_{\underline{k}p} G_{ps}^{\sigma} &= 0 \end{aligned}\right\} \qquad (3.3.4)$$

with three analogous equations involving G_{pp}^{σ}, G_{sp}^{σ}, and $G_{\underline{k}p}^{\sigma}$. The solution of the set of equations (3.3.14) is straightforward though rather lengthy The result for G_{ss}^{σ} in its most general form is given by

$$G_{ss}^{\sigma}(\epsilon) = \left[(\epsilon - \epsilon_s) - \sum_{\underline{k}} \frac{|V_{sk}|^2}{\epsilon - \epsilon_{\underline{k}} + i\delta} \sum_{\underline{k}} \frac{V_{p\underline{k}} V_{\underline{k}s}}{\epsilon - \epsilon_{\underline{k}} + i\delta} \right.$$

$$\left. \times \left(\epsilon - \epsilon_p - \sum_{\underline{k}} \frac{|V_{p\underline{k}}|^2}{\epsilon - \epsilon_{\underline{k}} + i\delta}\right)^{-1} \right]^{-1} \qquad (3.3.5)$$

If we assume that the transfer integrals V_{sk} and V_{pk} are equal (an immediate consequence of this assumption is that the widths of the $|ns\rangle$ and $|np_z\rangle$ levels are equal), the expression for G^{σ}_{ss} and the corresponding expressions for G^{σ}_{ps} and G^{σ}_{pp} are considerably simplified. If this is done, and after use of the substitution

$$\Lambda - i\Delta = \lim_{\delta \to 0} \sum_{k} \frac{|V_{sk}|^2}{\epsilon - \epsilon_k + i\delta} \qquad (3.3.6)$$

we find

$$G^{\sigma}_{ss}(\omega) = \frac{\omega - E + i\Delta}{(\omega + E + i\Delta)(\omega - E + i\Delta) - (\Lambda - i\Delta)^2} \qquad (3.3.7)$$

where we have introduced the new variable

$$\omega = \epsilon - E_m$$

and

$$E_m = \epsilon_s + E + \Lambda = \epsilon_p - E + \Lambda \qquad (3.3.8)$$

i.e apart from the energy shift Λ, E_m represents the mean energy between the unperturbed energies of the s and p levels. Similarly we find

$$G^{\sigma}_{ps}(\omega) = \frac{\Lambda - i\Delta}{(\omega + E + i\Delta)(\omega - E + i\Delta) - (\Lambda - i\Delta)^2} \qquad (3.3.9)$$

and

$$G_{pp}(\omega) = \frac{\omega + E + i\Delta}{(\omega + E + i\Delta)(\omega - E + i\Delta) - (\Lambda - i\Delta)^2} \qquad (3.3.10)$$

These various Green functions must be substituted in the expression for α_{zz}. The integral proves to be tractable analytically only if Λ is neglected. Our neglect of Λ is rather intuitive. For a reasonably constant density of states, Λ will not change very much as ϵ changes. Usually the Λ effects do not domi-

- nate the Δ effects, and we hope to get a fair description by neglecting Λ. α_{zz} is then given by the relation

$$\alpha_{zz} = \frac{4e^2\lambda^2}{\pi} \int_{-\infty}^{-E_m} \frac{2\Delta w\left[(w^2-E^2)^2 + 4\Delta^2E^2\right]}{\left[(w^2 - E^2)^2 + 4\Delta^2E^2\right]^2}\, dw \,, \qquad (3.3.11)$$

the integral is straightforward, though rather lengthy, we only state the results here

$$\alpha_{zz} = \frac{4e^2\lambda^2}{\pi} \frac{1}{E^2-\Delta^2}\left[-\frac{1}{2}\frac{E^2}{(E^2-\Delta^2)^{\frac{1}{2}}}\arctan\left(\frac{2\Delta(E^2-\Delta^2)^{\frac{1}{2}}}{E_m^2 - E^2 + 2\Delta^2}\right)\right.$$

$$\left. + \frac{(E_m^2 + E^2)\Delta^3}{(E_m^2 - E^2)^2 + 4\Delta^2E_m^2}\right] \,, \quad E > \Delta \qquad (3.3.12)$$

$$\alpha_{zz} = \frac{4e^2\lambda^2}{\pi} \frac{1}{E^2-\Delta^2}\left[-\frac{1}{4}\frac{E^2}{(\Delta^2-E^2)^{\frac{1}{2}}}\ln\left(\frac{E_m^2 - E^2 + 2\Delta^2 + 2\Delta(\Delta^2-E^2)^{\frac{1}{2}}}{E_m^2 - E^2 + 2\Delta^2 - 2\Delta(\Delta^2-E^2)^{\frac{1}{2}}}\right)\right.$$

$$\left. + \frac{(E_m^2 + E^2)\Delta^3}{(E_m^2 - E^2)^2 + 4\Delta^2E_m^2}\right] \,, \quad E < \Delta \qquad (3.3.13)$$

$$\alpha_{zz} = -\frac{4e^2\lambda^2}{\pi} \frac{\Delta}{E_m^2 + \Delta^2} \,, \quad E = \Delta \qquad (3.3.14)$$

The effective polarizability arising from the transfer of charge to the adatom (the Gurney effect) is easily shown to be given by the relation

$$\alpha_{zz}^{G} = -\frac{2e^2d^2}{\pi} \frac{\Delta}{E(s)^2 + \Delta^2} \qquad (3.3.15)$$

It is now useful to consider two important limits. If $E(s) \gg \Delta$ (this corresponds roughly to the low coverage limit) then it is found that $\alpha_{zz}^{G}/\alpha_{zz} = d^2/2\lambda^2$. In the special case $E(s) = 0$, $\Delta = E$ which is not far from the realistic high coverage situation, then $\alpha_{zz}^{G}/\alpha_{zz} = d^2/\lambda^2$.

For Cs we have estimated $\lambda = -1.62\text{Å}$ from the f-sum rule, although perhaps in our problem λ should in fact be reduced. Even then it appears that the contribution from the intra-atomic polarizability is comparable to the Gurney polarizability. The inclusion of the intra-atomic polarizability should increase the values of Δ and E_o, derived in chapter 2 from experimental data.

The inclusion of the intra-atomic term should not however be restricted to the linear approximation, and calculations within a non linear framework are the subject of the next chapter.

Chapter 4

ALKALI ADSORPTION ON TRANSITION METALS : THE IMPORTANCE OF THE s-p HYBRIDIZATION

4.1. Introduction

So far the possibility of an induced adatom dipole moment μ normal to the surface has been neglected. Neglecting the polarizability of the ion core any polarization must come from the occupied part of the adatom density of states. Estimates of this effect which tends to depolarise the surface in the same sense as the Gurney neutralisation show it to be comparable to the latter (see chapter 3).

We note that, in the presence of a fixed electric field, a change in the local potential of an atom will change the occupancy n of the valence levels, and thus both the polarizability and the dipole moment μ, the two effects are thus coupled together. Our aim here is to calculate both the contributions to $\Delta\phi$ coming from μ and n, while allowing as far as possible for strong lifetime broadening effects which couple the $|ns\rangle$ and $|np\rangle$ levels themselves together. A preliminary account of this, has already been published (Muscat and Newns 1974).

The change in work function is given by

$$\Delta\phi = -4\pi(qd - \mu)s \qquad (4.1.1)$$

where

$$q = o(1 - n), \qquad (4.1.2)$$

$$n = \sum_{\sigma} (\langle n_{s\sigma} \rangle + \langle n_{p\sigma} \rangle) \qquad (4.1.3)$$

and

$$\mu = \sum_{\sigma} \langle c^{+}_{s\sigma} c_{p\sigma} + c^{+}_{p\sigma} c_{s\sigma} \rangle \qquad (4.1.4)$$

4.2. The model Hamiltonian

The Hamiltonian is a generalisation of that used in chapter 2. A single adatom is considered, the other adatoms being taken into account only through their electrostatic field. Interatomic correlations in the wavefunction are thus neglected from the start.

We write H in the form

$$H = H_0 + H_I \qquad (4.2.1)$$

where H_0 is the Hamiltonian for the adsorption of a single adatom at zero coverage, i.e

$$H_0 = \sum_{\underline{k}\sigma} \epsilon_{\underline{k}} n_{\underline{k}\sigma} + \sum_{\underline{k}\sigma} \left[V_{s\underline{k}} c^{+}_{\underline{k}\sigma} c_{s\sigma} + V_{p\underline{k}} c^{+}_{\underline{k}\sigma} c_{p\sigma} + h.c \right]$$

$$+ E_i \sum_{\sigma} (n_{s\sigma} + n_{p\sigma}) + E \sum_{\sigma} (n_{p\sigma} - n_{s\sigma}) \qquad (4.2.2)$$

where the first term represents the substrate, the second the coupling between the substrate and the adatom, and the last two, the unperturbed energy levels of the adatom renormalised by image effects

$$E'_{ns} = E_i - E \ , \quad E'_{np} = E_i + E \qquad (4.2.3)$$

respectively, and 2E = 1.44eV for Cs (Atomic Energy Levels, Circular of the N.B.S 467, vol III).

The Hamiltonian (4.2.2) is similar to (2.2.2) generalised to two adatom levels, except for the neglect of the Anderson Coulomb interaction U. As we have shown in chapter 2,U is considerably reduced by image effects from the adsorbed atom; we showed that a renormalisation of U exists which reduces U to $U - e^2/2d$. (Hewson and Newns 1974, Schrieffer 1973). This reduction amounts to 3.7eV when $d = 2\overset{o}{A}$.

H_I describes the effect of the potential due to the adatoms other than that described by (4.2.2), this is given by (see chapter 2)

$$H_I = \sum_\sigma \int \psi_\sigma^+(\underline{x}) V(\underline{x}) \psi_\sigma(\underline{x}) \, d^3x \qquad (4.2.4)$$

where ψ_σ is now given by

$$\psi_\sigma(\underline{x}) = c_{p\sigma} \varphi_p(\underline{x}) + c_{s\sigma} \varphi_s(\underline{x}) \qquad (4.2.5)$$

where φ_p and φ_s are the Schrodinger representatives of $|np_z\rangle$ and $|ns\rangle$. Keeping only the 1st two terms in the expansion of $V(\underline{x})$ (equation (2.2.8)), we find

$$H_I = \bar{\Phi} \sum_\sigma (n_{s\sigma} + n_{p\sigma}) + W \sum_\sigma (c_{s\sigma}^+ c_{p\sigma} + h.c) \qquad (4.2.6)$$

where $\bar{\Phi} = V(\underline{0})$, $W = e\lambda E_\perp$, $\nabla V(\underline{x})\Big|_0 = E_\perp = (0,0,E_\perp)$ and

$$\lambda = \langle ns|z|np_z\rangle \qquad (4.2.7)$$

In order to calculate $\bar{\Phi}$ and $E_\perp$, we shall assume that the adlayer is a square lattice. The position vectors of the adatoms are then given by $\underline{r}_a = s^{-\frac{1}{2}}(l,m,0)$ and that of their images by $\underline{r}_i = s^{-\frac{1}{2}}(l,m,-2ds^{\frac{1}{2}})$, where l and m are integers and s is the surface coverage of adatoms.

The electrostatic potential at the origin due to charges +q and -q at $\underline{r}_a$ and $\underline{r}_i$ respectively is given by

$$q\left(\frac{1}{r_a} - \frac{1}{r_i}\right) \tag{4.2.8}$$

further the electrostatic potential due to dipoles $\underline{\mu}$ at $\underline{r}_a$ and $\underline{r}_i$ is equal to

$$\frac{\underline{\mu}\cdot\underline{r}_a}{r_a^3} + \frac{\underline{\mu}\cdot\underline{r}_i}{r_i^3} \tag{4.2.9}$$

Now since the dipole is normal to the surface, and $\underline{r}_a$ is in the plane of the surface, the first term in (4.2.9) gives zero contribution.

The electric field at the origin due to charges +q and -q at $\underline{r}_a$ and $\underline{r}_i$ may be obtained by differentiating (4.2.8) with respect to z, which gives $2qd/r_i^3$. Finally the field due to dipoles $\underline{\mu}$ is given by

$$\frac{\mu}{r_a^3} + \frac{\mu}{r_i^3} - \frac{3\mu(4d^2)}{r_i^5} \tag{4.2.10}$$

Φ and $E_\perp$ may now be obtained by summing over all the lattice sites, and we find

$$\Phi = e^2(n-1)s^{\frac{1}{2}}\left[U_{\frac{1}{2}}(0) - U_{\frac{1}{2}}(4d^2s)\right] + 2e\mu ds^{3/2}U_{\frac{3}{2}}(4d^2s) \tag{4.2.11}$$

$$E_\perp = 2e(n-1)ds^{3/2}U_{3/2}(4d^2s) + \mu s^{3/2}\left[U_{3/2}(0) + U_{3/2}(4d^2s) - 12d^2sU_{5/2}(4d^2s)\right] \tag{4.2.12}$$

where

$$U_r(x) = \sum_{l=-\infty}^{\infty}\sum_{m=-\infty}^{\infty}(l^2 + m^2 + x)^{-r} \tag{4.2.13}$$

the summation excluding $l = 0$, $m = 0$ simultaneously.

In the region of small s, these expressions may be considerably simplified. If we take the first term in the expansion in powers of s, we find

$$\Phi = 2edAs^{3/2}\left[\mu + ed(n-1)\right] \qquad (4.2.14)$$

and

$$E_{\perp} = 2As^{3/2}\left[\mu + ed(n-1)\right] \qquad (4.2.15)$$

where $A = U_{3/2}(0) = 9.033$ (see chapter 2).

In this approximation, all the quantities may be expressed in terms of the total induced dipole moment μ_t of the adatom and its image.

$$\mu_t = 2\mu + 2ed(n-1) \qquad (4.2.16)$$

then we have

$$\Phi = ed\mu_t As^{3/2} \qquad (4.2.17)$$

and

$$E_{\perp} = \mu_t As^{3/2} \qquad (4.2.18)$$

From (4.2.18), an analogous expression to the depolarization formula encountered in chapter 2 in the case of the Gurney neutralisation, is obtained

$$\mu_t(s) = \mu_t(0) - \alpha As^{3/2} \qquad (4.2.19)$$

where α is an effective polarizability which will be derived later in the text. The expression (4.2.19) is essentially different to Bennett's depolarization function (Bennett 1968) in that he assumes that the electric field $E_{\perp}$ is proportional to s rather $s^{3/2}$.

4.3. Formal solution

We begin by solving the Hamiltonian H. This is done exactly by the Green function method already employed in previous chapters.

The important quantities are the Green functions, G^{σ}_{ss}, G^{σ}_{pp} and G^{σ}_{sp}, since they are directly related to the charge n, and the intra-atomic dipole moment μ, as follows

$$n = \sum_{\sigma}\left\{-\frac{1}{\pi}\,\mathrm{Im}\int_{-\infty}^{\epsilon_F}\left[G^{\sigma}_{ss}(\epsilon) + G^{\sigma}_{pp}(\epsilon)\right] d\epsilon\right\} \tag{4.3.1}$$

$$\mu = 2e\lambda\sum_{\sigma}\left\{-\frac{1}{\pi}\,\mathrm{Im}\int_{-\infty}^{\epsilon_F} G^{\sigma}_{sp}(\epsilon)\, d\epsilon\right\} \tag{4.3.2}$$

The equations for the Green functions are

$$\left.\begin{aligned}
&\left[\mathcal{E} - (E_i+\Phi-E)\right] G^{\sigma}_{ss} - WG^{\sigma}_{ps} - \sum_{\underline{k}} V_{s\underline{k}} G^{\sigma}_{\underline{k}s} = 1\\
&\left[\mathcal{E} - (E_i+\Phi+E)\right] G^{\sigma}_{ps} - WG^{\sigma}_{ss} - \sum_{\underline{k}} V_{p\underline{k}} G^{\sigma}_{\underline{k}s} = 0\\
&\left[\mathcal{E} - \epsilon_{\underline{k}}\right] G^{\sigma}_{\underline{k}s} - V_{\underline{k}p} G^{\sigma}_{ps} - V_{\underline{k}s} G^{\sigma}_{ss} = 0
\end{aligned}\right\} \tag{4.3.3}$$

with three analogous equations involving G^{σ}_{pp}, G^{σ}_{sp} and $G^{\sigma}_{\underline{k}p}$. We have used the substitution $\mathcal{E} = \epsilon + i\delta$. If we now put $\epsilon_s = E_i + \Phi - E$, $\epsilon_p = E_i + \Phi + E$, and eliminate $G^{\sigma}_{\underline{k}s}$ we find

$$\left.\begin{aligned}
&\left[\mathcal{E} - \epsilon_s - \sum_{\underline{k}} \frac{|V_{s\underline{k}}|^2}{\mathcal{E}-\epsilon_{\underline{k}}}\right] G^{\sigma}_{ss} - \left[W + \sum_{\underline{k}} \frac{V_{s\underline{k}}V_{\underline{k}p}}{\mathcal{E}-\epsilon_{\underline{k}}}\right] G^{\sigma}_{sp} = 1\\
&\left[\mathcal{E} - \epsilon_p - \sum_{\underline{k}} \frac{|V_{p\underline{k}}|^2}{\mathcal{E}-\epsilon_{\underline{k}}}\right] G^{\sigma}_{sp} - \left[W + \sum_{\underline{k}} \frac{V_{p\underline{k}}V_{\underline{k}s}}{\mathcal{E}-\epsilon_{\underline{k}}}\right] G^{\sigma}_{ss} = 0
\end{aligned}\right\} \tag{4.3.4}$$

Hence the results

$$G_{ss}^{\sigma}(\epsilon) = \left\{\mathcal{E} - \epsilon_s - \sum_{\underline{k}} \frac{|V_{s\underline{k}}|^2}{\mathcal{E}-\epsilon_{\underline{k}}} - \left(W + \sum_{\underline{k}} \frac{V_{s\underline{k}}V_{\underline{k}p}}{\mathcal{E}-\epsilon_{\underline{k}}}\right)^2 \times \left(\mathcal{E} - \epsilon_p - \sum_{\underline{k}} \frac{|V_{p\underline{k}}|^2}{\mathcal{E}-\epsilon_{\underline{k}}}\right)^{-1}\right\}^{-1} \tag{4.3.5}$$

$$G_{sp}^{\sigma}(\epsilon) = \left\{\left(\mathcal{E}-\epsilon_s - \sum_{\underline{k}} \frac{V_{s\underline{k}}^2}{\mathcal{E}-\epsilon_{\underline{k}}}\right)\left(\mathcal{E} - \epsilon_p - \sum_{\underline{k}} \frac{|V_{p\underline{k}}|^2}{\mathcal{E}-\epsilon_{\underline{k}}}\right) \times \left(W + \sum_{\underline{k}} \frac{V_{s\underline{k}}V_{\underline{k}p}}{\mathcal{E}-\epsilon_{\underline{k}}}\right)^{-1} - \left(W + \sum_{\underline{k}} \frac{V_{s\underline{k}}V_{\underline{k}p}}{\mathcal{E}-\epsilon_{\underline{k}}}\right)\right\}^{-1} \tag{4.3.6}$$

While by solving the three equations analogous to (4.3.3), we find

$$G_{pp}^{\sigma}(\epsilon) = \left\{\mathcal{E} - \epsilon_p - \sum_{\underline{k}} \frac{|V_{p\underline{k}}|^2}{\mathcal{E}-\epsilon_{\underline{k}}} - \left(W + \sum_{\underline{k}} \frac{V_{s\underline{k}}V_{p\underline{k}}}{\mathcal{E}-\epsilon_{\underline{k}}}\right)^2 \times \left(\mathcal{E} - \epsilon_s + \sum_{\underline{k}} \frac{V_{s\underline{k}}V_{\underline{k}p}}{\mathcal{E}-\epsilon_{\underline{k}}}\right)^{-1}\right\}^{-1} \tag{4.3.7}$$

These results are considerably simplified if we assume that the transfer integrals $V_{s\underline{k}}$ and $V_{p\underline{k}}$ are equal, this assumption implies that the two energy levels E_s and E_p have the same widths . Then by means of the substitution (3.3.6) , we find

$$G_{ss}^{\sigma}(\epsilon) = \frac{\epsilon - \epsilon_p + i\Delta}{(\epsilon - \epsilon_s + i\Delta)(\epsilon - \epsilon_p + i\Delta) - (W - i\Delta)^2} \tag{4.3.8}$$

$$G_{sp}^{\sigma}(\epsilon) = \frac{W - i\Delta}{(\epsilon - \epsilon_s + i\Delta)(\epsilon - \epsilon_p + i\Delta) - (W - i\Delta)^2} \tag{4.3.9}$$

$$G_{pp}^{\sigma}(\epsilon) = \frac{\epsilon - \epsilon_s + i\Delta}{(\epsilon - \epsilon_s + i\Delta)(\epsilon - \epsilon_p + i\Delta) - (W - i\Delta)^2} \tag{4.3.10}$$

We have assumed rather arbitrarily that the shift in energy Λ may be neglected. Inserting these results in (4.3.1) and (4.3.2) we find that

$$n = \frac{4\Delta}{\pi}\int_{-\infty}^{-E_i-\Phi} \frac{(W+w)^2 + E^2}{(w^2 - E^2 - W^2)^2 + 4\Delta^2(W+w)^2}\,dw = I_+ \qquad (4.3.11)$$

$$\mu = \frac{4e\lambda\Delta}{\pi}\int_{-\infty}^{-E_i-\Phi} \frac{(W+w)^2 - E^2}{(w^2 - E^2 - W^2)^2 + 4\Delta^2(W+w)^2}\,dw = e\lambda I_- \qquad (4.3.12)$$

where we have used the substitution $w = \epsilon - E_i - \Phi$ and taken $\epsilon_F = 0$. We note from (4.3.11) and (4.3.12) that $n = n(\Phi, W)$, $\mu = \mu(\Phi, W)$, now since Φ and $W = e\lambda E_\perp$ are themselves functions of n and μ through (4.2.11) and (4.2.12), we see that the equations (4.3.11) and (4.3.12) are a pair of coupled self-consistent equations which must be solved for n and μ before $\Delta\phi$ can be calculated. The calculation of the integrals I_+ and I_- is straightforward but rather lengthy, and we merely state the results.

$$I_\pm = \frac{4\Delta}{\pi}\left\{\frac{A_\pm}{2}\left[G(c,d) - G(-c,-d)\right] + (B_\pm + cA_\pm)F(c,d) + (D_\pm + A_\pm c)F(-c,-d)\right\} \qquad (4.3.13)$$

where

$$F(c,d) = \left[\frac{\pi}{2} - \arctan\left(\frac{E_i + \Phi + c}{\Delta + d}\right)\right]\Big/(\Delta + d) \qquad (4.3.14)$$

$$G(c,d) = \ln\left[(E_i + \Phi + c)^2 + (\Delta + d)^2\right] \qquad (4.3.15)$$

$$A_\pm = \frac{1}{4c}\left\{1 - \frac{\Delta d(2Wc + \Delta d) - (\Delta d + 2c^2)(W^2 \pm E^2)}{r^2(\Delta^2 + c^2)}\right\}$$

$$B_{\pm} = \frac{[(\Delta + d)^2 + c^2](2Wc + \Delta d) - (\Delta d + 2c^2)(W^2 \pm E^2)}{4r^2(\Delta^2 + c^2)}$$

$$D_{\pm} = \frac{(\Delta d + 2c^2)(W^2 \pm E^2) - [(\Delta - d)^2 + c^2](2Wc + \Delta d)}{4r^2(\Delta^2 + c^2)} \qquad (4.3.16)$$

$$r^2 = [(E^2 - W^2 - \Delta^2)^2 + 4\Delta^2 W^2]^{\frac{1}{2}}$$

$$c = \frac{1}{\sqrt{2}}(r^2 + E^2 - W^2 - \Delta^2)^{\frac{1}{2}} \qquad (4.3.17)$$

and

$$d = \frac{1}{\sqrt{2}}[r^2 - (E^2 - W^2 - \Delta^2)]^{\frac{1}{2}}$$

The procedure now is to compare our results with the experimental data available. This is done in two stages.

1. Equations (4.3.11) and (4.3.12) being soluble analytically in the low coverage limit, the results are fitted to experimental data in this region, and hence for given assumed values of d and λ, a relationship between E_i and Δ is obtained.

2. Making use of these values of E_i and Δ we solve (4.3.11) and (4.3.12) numerically for μ and n and thus obtain a value for $\Delta\phi$ as a function of s through (4.1.1). By varying d, λ, and Δ the best fit to the experimental results is then achieved.

4.4. The low coverage problem

In the low coverage limit, both Φ and W are small, so we can linearise equations (4.3.11) and (4.3.12) as follows

$$n = I^{+}(0) + \Phi I_{\Phi}^{+}(0) + WI_{W}^{+}(0) \qquad (4.4.1)$$

$$\frac{\mu}{2e\lambda} = I^{-}(0) + \Phi I_{\Phi}^{-}(0) + WI_{W}^{-}(0) \qquad (4.4.2)$$

and the subscripts Φ and W denote the partial derivatives with respect to Φ and W .

We have also shown that in this region $\mu_t(s)$ may be expanded as follows

$$\mu_t(s) = \mu_t(0) + PE_{\perp} \qquad (4.4.3)$$

where $E_{\perp} = As^{3/2}\mu_t(0)$, and P is the polarization given by

$$P = 2e^2\left[d^2 I_{\Phi}^{+}(0) + \lambda d(I_{\Phi}^{-}(0) + I_{W}^{+}(0)) + \lambda^2 I_{W}^{-}(0)\right] \qquad (4.4.4)$$

At zero coverage, both Φ and W are zero, so that the integrals $I^{\pm}$ are considerably simplified, The results are

$$I^{+}(0) = \frac{2}{\pi}\left[\pi - \arctan\left(\frac{E_i + (E^2 - \Delta^2)^{\frac{1}{2}}}{\Delta}\right) - \arctan\left(\frac{E_i - (E^2 - \Delta^2)^{\frac{1}{2}}}{\Delta}\right)\right] \qquad (4.4.5)$$

$$I^{-}(0) = \frac{\Delta}{\pi(E^2 - \Delta^2)^{\frac{1}{2}}} \ln\left(\frac{\left[E_i + (E^2 - \Delta^2)^{\frac{1}{2}}\right]^2 + \Delta^2}{\left[E_i - (E^2 - \Delta^2)^{\frac{1}{2}}\right]^2 + \Delta^2}\right) \qquad (4.4.6)$$

when $\Delta < E$.

In the special case $\Delta = E$ we have

$$I^{+}(0) = \frac{2}{\pi}\left[\pi - 2\arctan(E_i/E)\right] \qquad (4.4.7)$$

$$I^{-}(0) = \frac{4E_i E}{\pi(E_i^2 + E^2)} \qquad (4.4.8)$$

While in the region $\Delta > E$, we have

$$I^{+}(0) = \frac{2}{\pi}\left[\pi - \arctan\left(\frac{E_i}{\Delta + (\Delta^2 - E^2)^{\frac{1}{2}}}\right) - \arctan\left(\frac{E_i}{\Delta - (\Delta^2 - E^2)^{\frac{1}{2}}}\right)\right] \quad (4.4.9)$$

$$I^{-}(0) = \frac{2}{\pi}\,\frac{\Delta}{(\Delta^2 - E^2)^{\frac{1}{2}}}\left[\arctan\left(\frac{E_i}{\Delta - (\Delta^2 - E^2)^{\frac{1}{2}}}\right) - \arctan\left(\frac{E_i}{\Delta + (\Delta^2 - E^2)^{\frac{1}{2}}}\right)\right] \quad (4.4.10)$$

Both $I^{+}(0)$ and $I^{-}(0)$ are plotted as functions of the dimensionless ratio E_i/E in fig.1, for different values of Δ/E, and we see from this sketch that the contribution to the dipole moment μ_t from the intra-atomic term $I^{-}(0)$, which was neglected in the simple Gurney model, described in chapter 2, is far from negligible, being in fact a maximum at $E_i = E$.

The total induced dipole moment at zero coverage $\mu_t(0)$, may be written as a function of E_i and Δ, through the relation

$$\mu_t(0) = 2e\left[\lambda I^{-}(0) + d(I^{+}(0) - 1)\right] \quad (4.4.11)$$

together with the various expressions for $I^{+}(0)$ and $I^{-}(0)$ which we have just derived.

Let us now look at some simple limits, when $\Delta \to 0$ the situation is straightforward, the contribution from the intra-atomic term $I^{-}(0)$ is zero as expected, while three possibilities exist for the charge term $I^{+}(0)$. (i) if $E_i > E$ then $I^{+}(0) \to 0$ as $\Delta \to 0$, (ii) if $-E < E_i < E$ then $I^{+}(0) \to 2$ as $\Delta \to 0$, (iii) if $E_i < -E$ then $I^{+}(0) \to 4$. Each of these possibilities of course corresponds to both, one or none of the levels being above the Fermi level respectively.

Taking $E_i = E$ and $\Delta = E$, it is found that $I^{+}(0) = 1$, $I^{-}(0) = 2/\pi$, we see that in this case, the contribution to $\mu_t(0)$ arising from the charge term is zero, while the intra-atomic term gives quite a sizeable contribution.

For any Δ, it is found that as $E_i \to \infty$ both $I^{+}(0)$ and $I^{-}(0)$ tend to zero while if $E_i \to -\infty$, then $I^{+}(0) \to 4$ and $I^{-}(0) \to 0$.

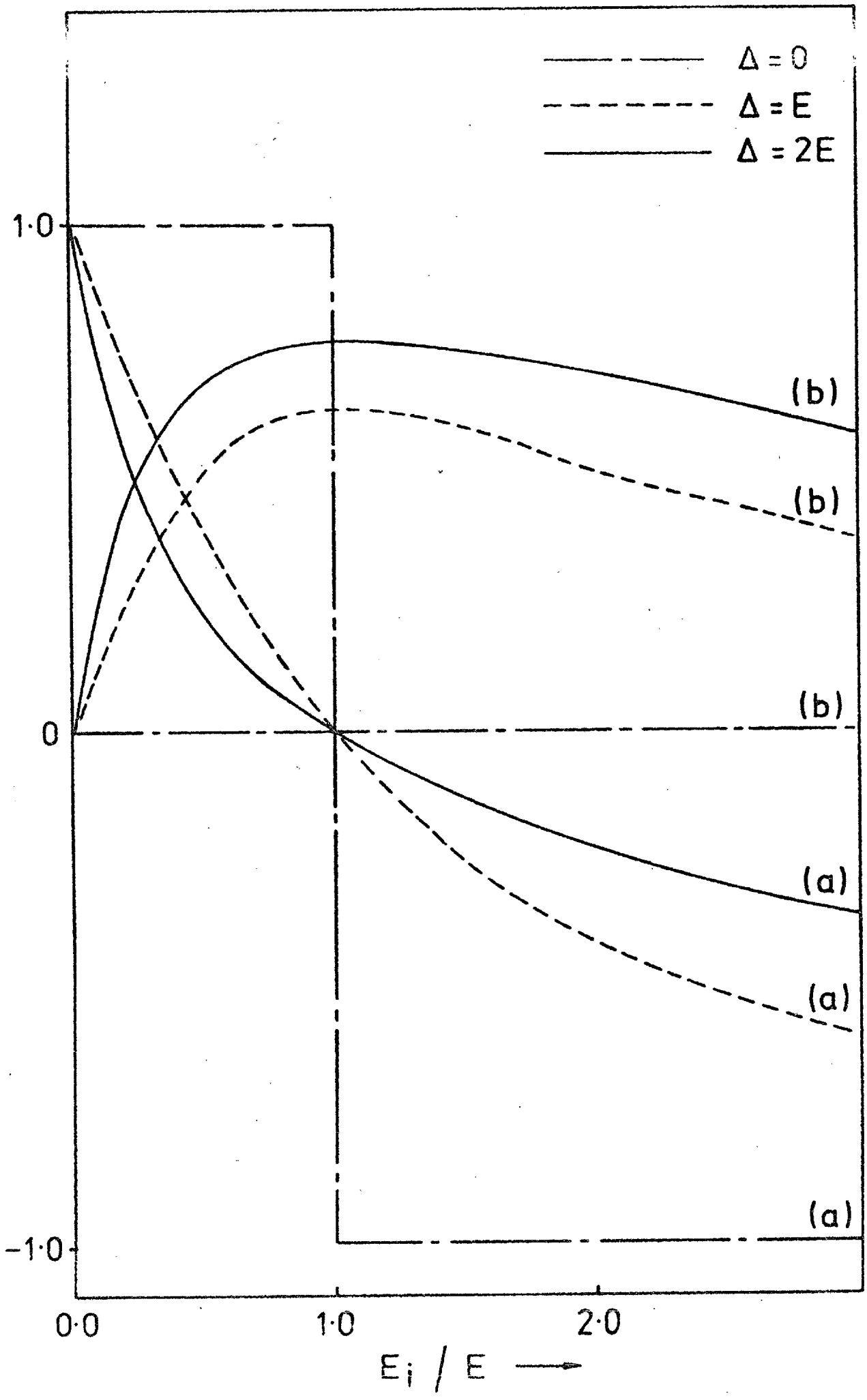


Fig.1 Curves (a) represent $I_+(0) - 1$, curves (b) represent $I_-(0)$

We can now match $\mu_t(0)$ to experimental results for zero coverage dipole moments, which apart from a constant of proportionality represent the initial slopes $(d\phi/ds)_o$ of the work function vs coverage curves.

We chose to study the system Cs/Re(0001) (Fehrs and Mackrakis 1970). Cs was chosen in the belief that the large size of the Cs atom would make the discreteness of its valence $|np\rangle$ and $|ns\rangle$ orbitals a reasonable assumption and Re because the experimental points of Fehrs and Mackrakis are particularly well distributed over all coverages.

The matching of our theoretical expression to the experimental value of $\mu_t(0)$ leads us to a relation between Δ and E_i, which we have plotted in fig.2 for different values of d and λ.

If d is kept fixed at some value, and λ is allowed to vary in the range $-1.6\text{Å} < \lambda < -1.0\text{Å}$, we see that for $\lambda = -1.6\text{Å}$ the values of the mean energy E_i are confined to a narrow strip around a value of E_i which is less than $2E = 1.44\text{eV}$, this value of E_i is very much smaller than the estimated value of $E_i \simeq 3\text{eV}$ at $d = 2.15\text{Å}$ from the formulae, $E_i = E_{ns}' - E$, $E_{ns}' = \phi - I + e^2/4\phi$, discussed in chapter 2. For a smaller value of $|\lambda|$, it is found that a much wider range of values of E_i is available. This is the first indication that the value of λ predicted by the f-sum rule ($\lambda = -1.6\text{Å}$) gives us rather poor agreement with estimates from other sources.

The polarization P depends on the partial derivatives $I_\Phi^\pm$ and $I_W^\pm$ evaluated at s = 0, through (4.4.4). The differentiation with respect to Φ is the reverse operation to the integration carried out in equations (4.3.11) and (4.3.12). The results are

$$I_\Phi^\pm(0) = -\frac{4\Delta}{\pi} \frac{E_i^2 \pm E^2}{(E_i^2 - E^2)^2 + 4\Delta^2 E_i^2} \qquad (4.4.12)$$

The other partial derivatives involve more work, the results are

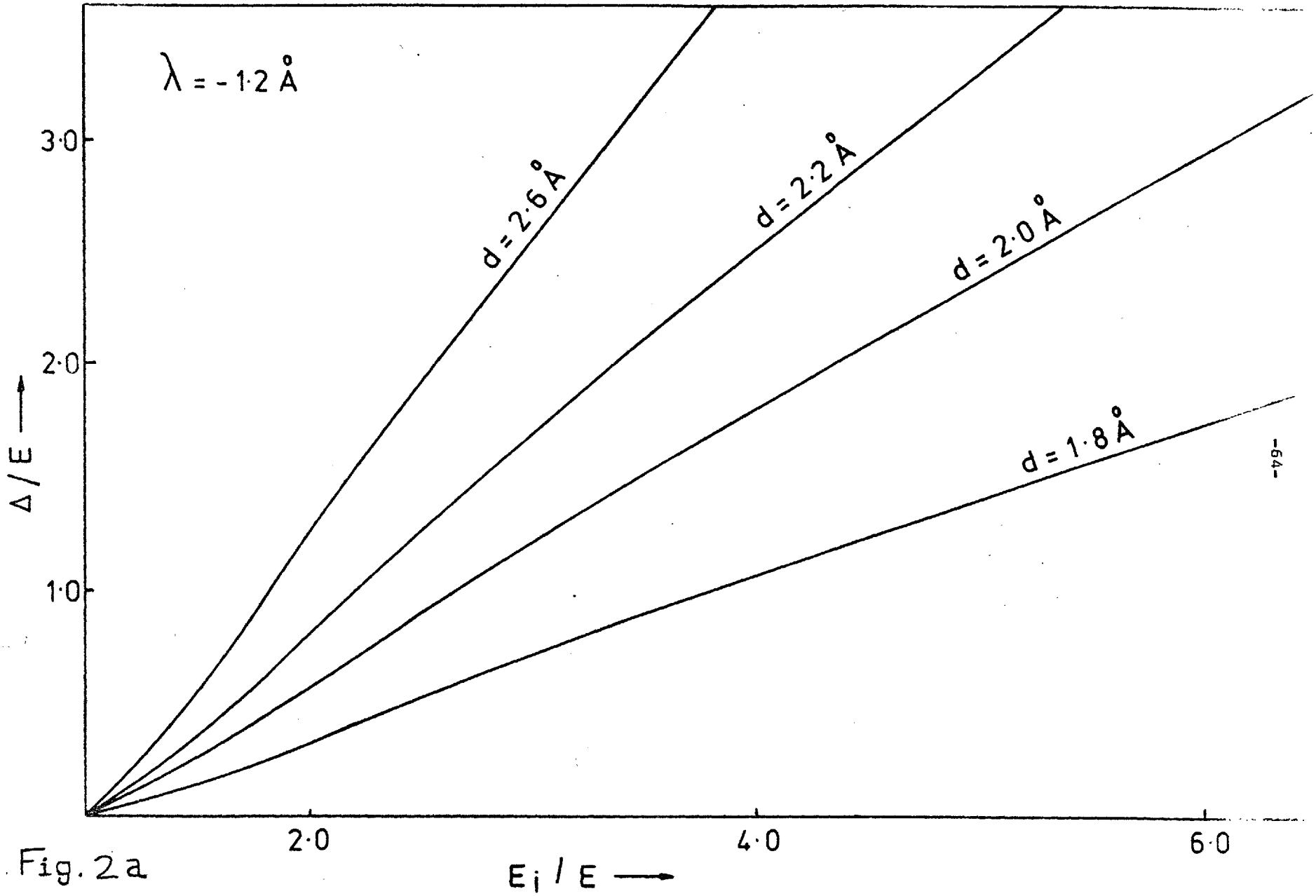


Fig. 2a

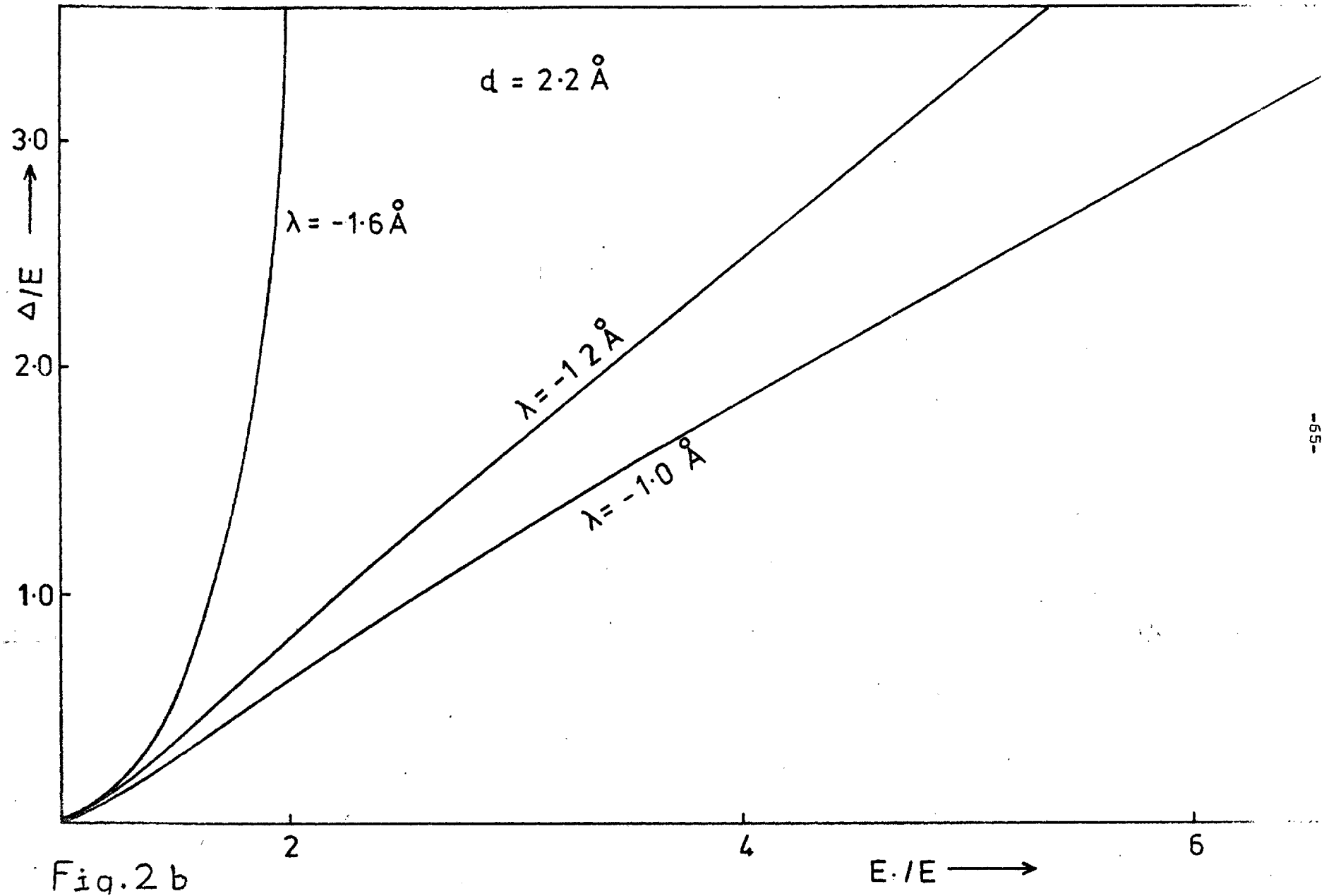


Fig. 2 b

$$I_W^+(0) = -\frac{4\Delta}{\pi}\frac{E_i^2 - E^2}{(E_i^2 - E^2)^2 + 4\Delta^2 E_i^2} \qquad (4.4.13)$$

$$I_W^-(0) = \frac{4}{\pi}\left[\frac{\Delta^3}{E^2 - \Delta^2}\left(\frac{E^2 + E^2}{(E_i^2 - E^2)^2 + 4\Delta^2 E_i^2}\right)\right.$$

$$\left. - \frac{E^2}{2(E^2 - \Delta^2)^{3/2}} \arctan\left(\frac{2\Delta(E^2 - \Delta^2)^{\frac{1}{2}}}{E_i^2 - E^2 + 2\Delta^2}\right)\right] \qquad (4.4.14)$$

with $\Delta < E$.

In the case $\Delta > E$, the result for $I_W^+(0)$ still holds, but $I_W^-(0)$ now becomes

$$I_W^-(0) = \frac{4}{\pi}\left[\frac{\Delta^3}{E^2 - \Delta^2}\left(\frac{E_i^2 + E^2}{(E_i^2 - E^2)^2 + 4\Delta^2 E_i^2}\right)\right.$$

$$\left. + \frac{E^2}{4(\Delta^2 - E^2)^{3/2}} \ln\left(\frac{E_i^2 + [\Delta + (\Delta^2 - E^2)^{\frac{1}{2}}]^2}{E_i^2 + [\Delta - (\Delta^2 - E^2)^{\frac{1}{2}}]^2}\right)\right] \qquad (4.4.15)$$

We recognise $I_W^-(0)$, it represents the intra-atomic polarizability α_{zz} as given by equations (3.3.13) and (3.3.14) at zero coverage.

In the limit $\Delta \to 0$, the polarization P goes to zero as expected. While if we assume that the Fermi level is at E_s (or equivalently $E_i = E$) we find that the cross term involving the product λd vanishes, and we are left with the pure charge term $I_{\underline{p}}^+(0) = -2/\pi\Delta$ and the intra-atomic polarizability term

$$I_W^-(0) = \frac{2}{\pi}\left[\frac{\Delta}{E^2 - \Delta^2} - \frac{E^2}{(E^2 - \Delta^2)^{3/2}} \arctan\left(\frac{(E^2 - \Delta^2)^{\frac{1}{2}}}{\Delta}\right)\right] \qquad (4.4.16)$$

if we further let $\Delta \to E$ we find that P is given by

$$P = -\frac{4e^2}{\pi\Delta}(\lambda^2 + d^2) \qquad (4.4.17)$$

The derivative of P exhibits a discontinuity at $\Delta = E$, we find in fact that

$$\frac{\partial P}{\partial E_i} \sim (E^2 - \Delta^2)^{-1} \qquad \text{as} \quad \Delta \to E$$

$$\frac{\partial P}{\partial \Delta} \sim (E^2 - \Delta^2)^{-2} \qquad \text{as} \quad \Delta \to E$$

Now in addition to the curves of fig.2, we may estimate $P\mu_t(0)$ from the experimental points and derive a further constraint on Δ and E_i, from (4.4.3) and (4.4.4).

For given values of d and λ, we are thus able to estimate Δ and E_i as indicated above, Picking a point on the E_i vs Δ curve characteristic of these values of d and λ, we then feed these values of Δ and E_i into the two variable self-consistent problem in n and μ, which we can now solve numerically for many values of s. We can thus by varying s and keeping all the other parameters constant, obtain a curve for $\mu_t(s)$ as a function of $s^{3/2}$ (figs.3) We then pick other points on the same E_i, Δ curve to find the best fit to the experimental results. The process is then repeated for different values of d and λ .

We have chosen to plot $\mu_t(s)$ as a function of $s^{3/2}$ in contrast to other workers (Schmidt and Gomer 1966, Gerlach and Rhodin 1969) who have plotted $\mu_t(s)$ vs s. We have done this to show the linear dependence of $\mu_t(s)$ on $s^{3/2}$ at low coverages, which our model of course implies.

4.5. Results and discussion.

The curves (fig.3) show no irregularity at the work function minimum, nor

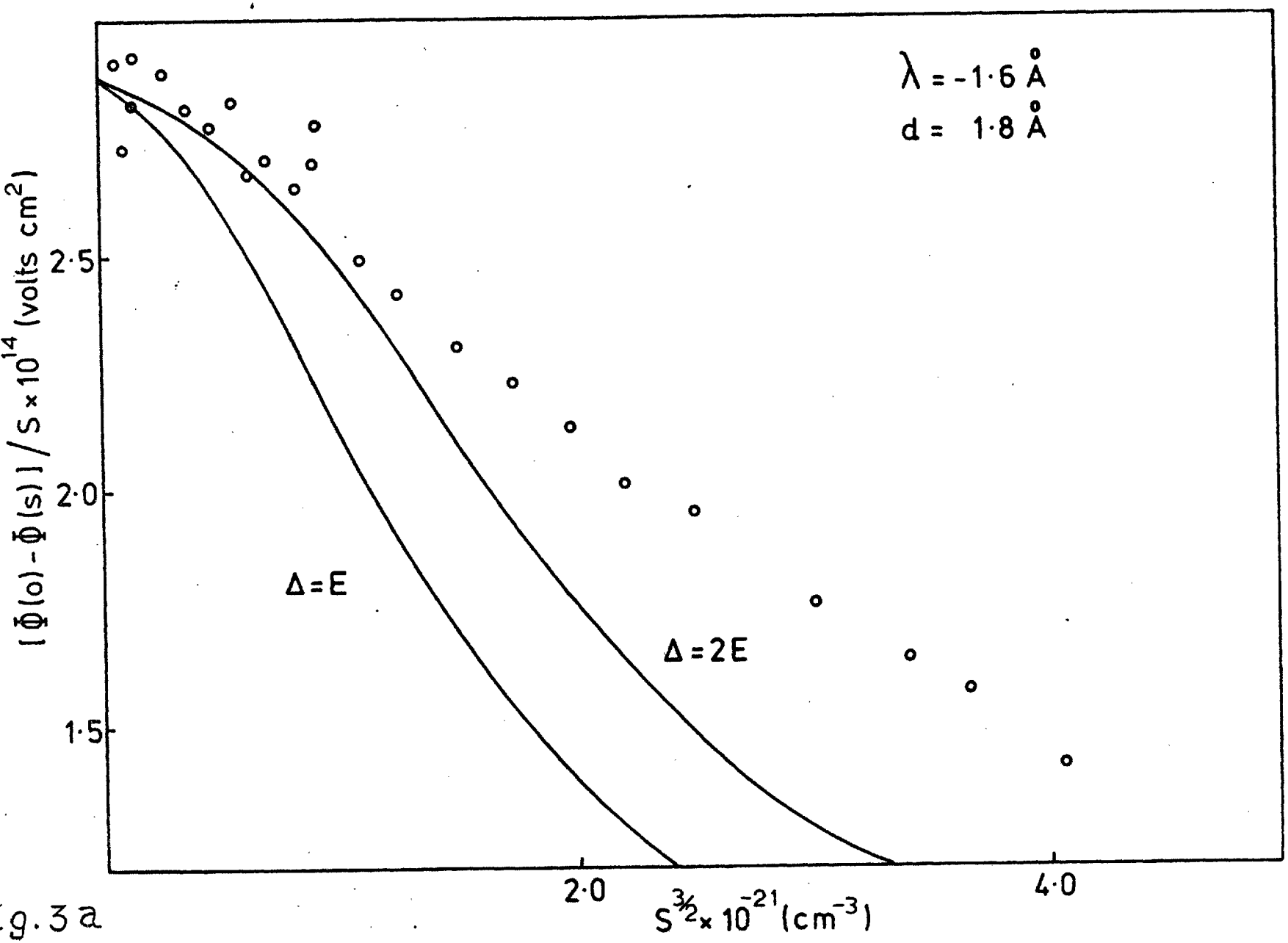

λ = -1·6 Å
d = 1·8 Å
Δ=E
Δ=2E
2·5
2·0
1·5
2·0
4·0
$|\Phi(o)-\Phi(s)|/S\times10^{14}$ (volts cm^2)
$S^{3/2}\times10^{-21}$ (cm^{-3})

Fig. 3a

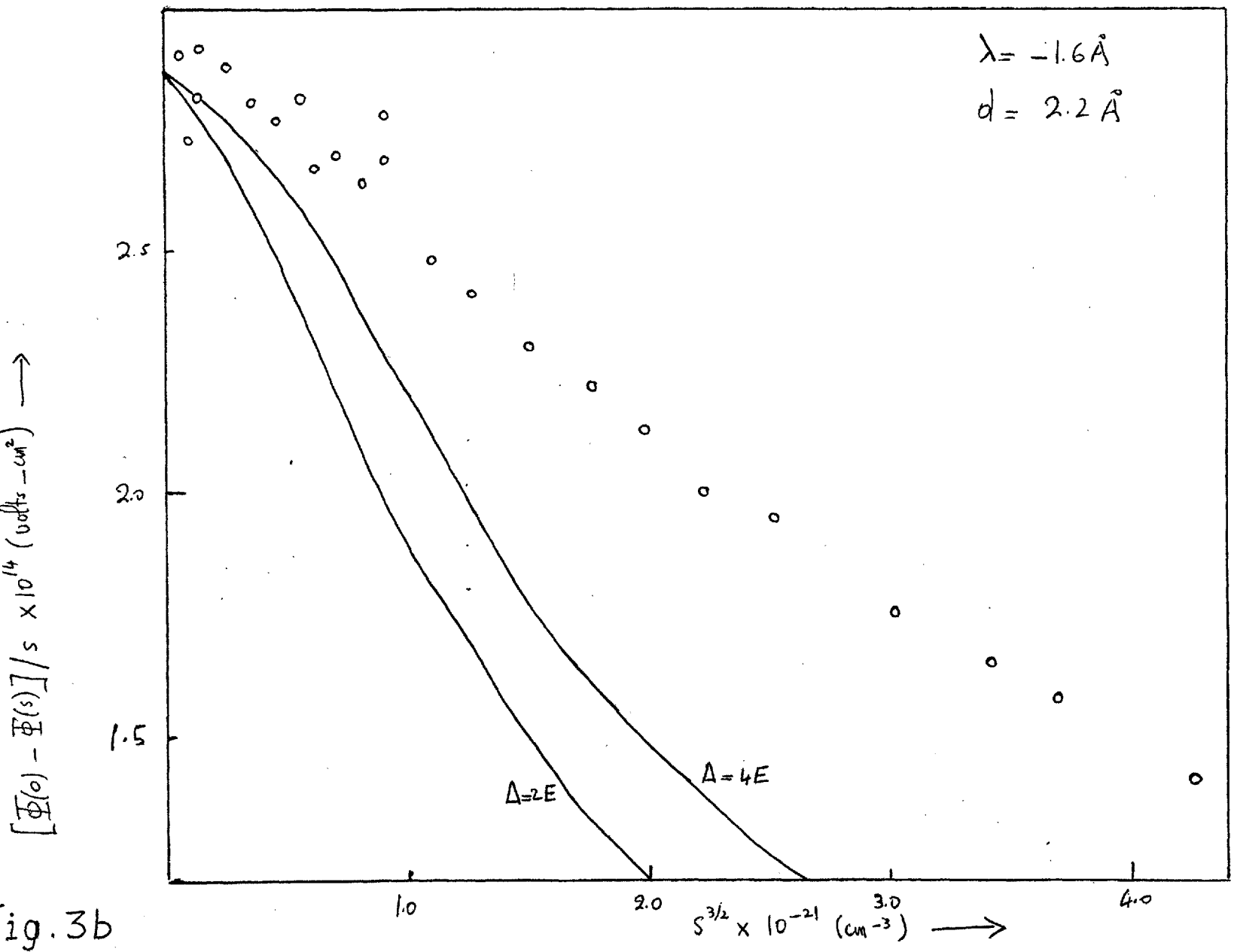

λ = −1.6 Å
d = 2.2 Å
Δ=2E
Δ=4E
2.5
2.0
1.5
1.0
2.0
3.0
4.0
[Φ(0) − Φ(s)]/s × 10^14 (watts − cm^2) ⟶
S^3/2 × 10^−21 (cm^−3) ⟶

Fig. 3b

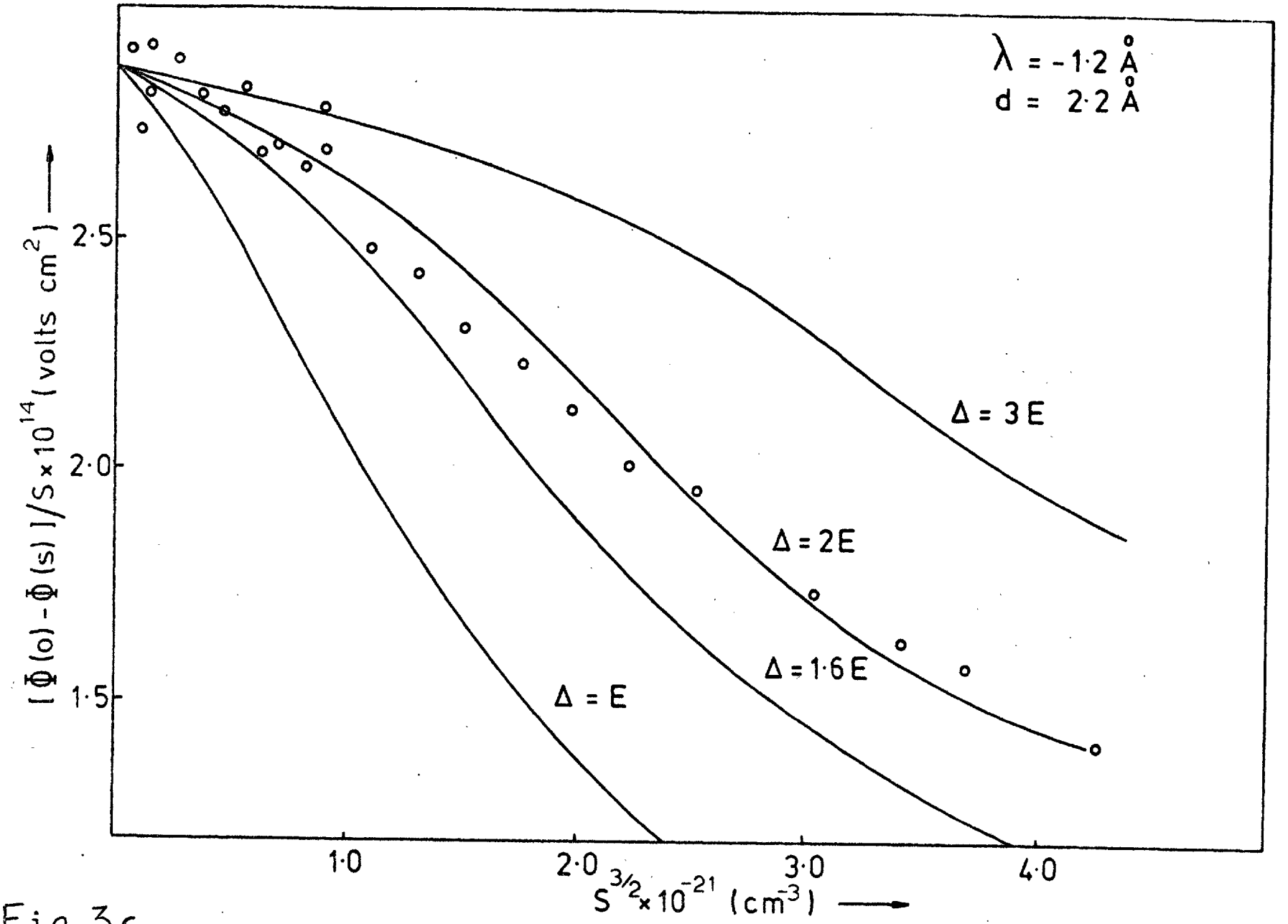

λ = -1·2 Å
d = 2·2 Å
Δ = 3E
Δ = 2E
Δ = 1·6E
Δ = E
[Φ(o) - Φ(s)]/S × 10^14 (volts cm^2)
2·5
2·0
1·5
1·0
2·0
3·0
4·0
S^3/2 × 10^-21 (cm^-3)

Fig. 3c

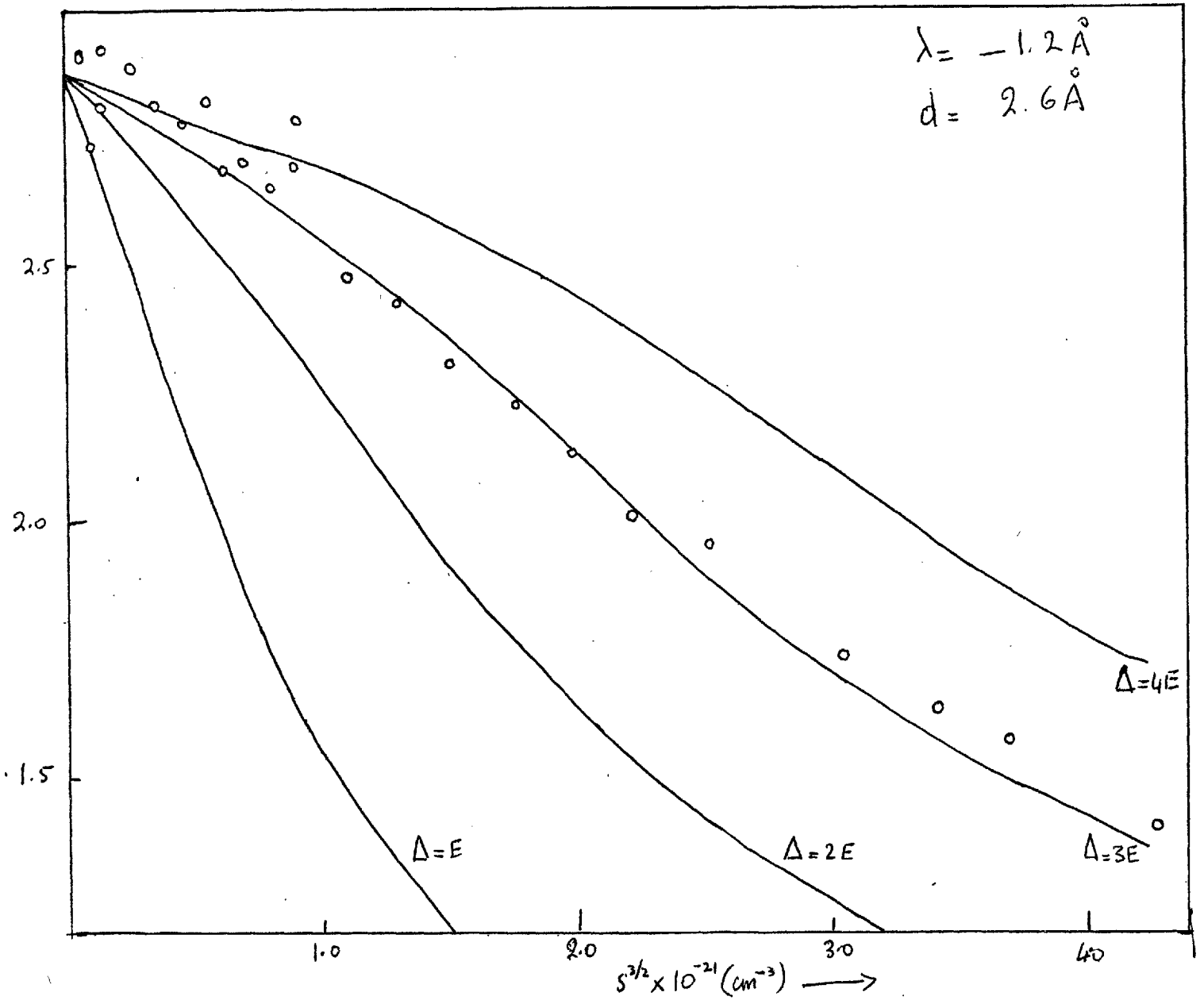

λ = −1.2 Å
d = 2.6 Å
Δ=4E
Δ=3E
Δ=2E
Δ=E
2.5
2.0
1.5
1.0
2.0
3.0
4.0
$[\Phi(0) - \Phi(s)]/s \times 10^{14}$ (volts-cm^2) ⟶
$s^{3/2} \times 10^{-21}$ (cm^{-3}) ⟶

Fig. 3d

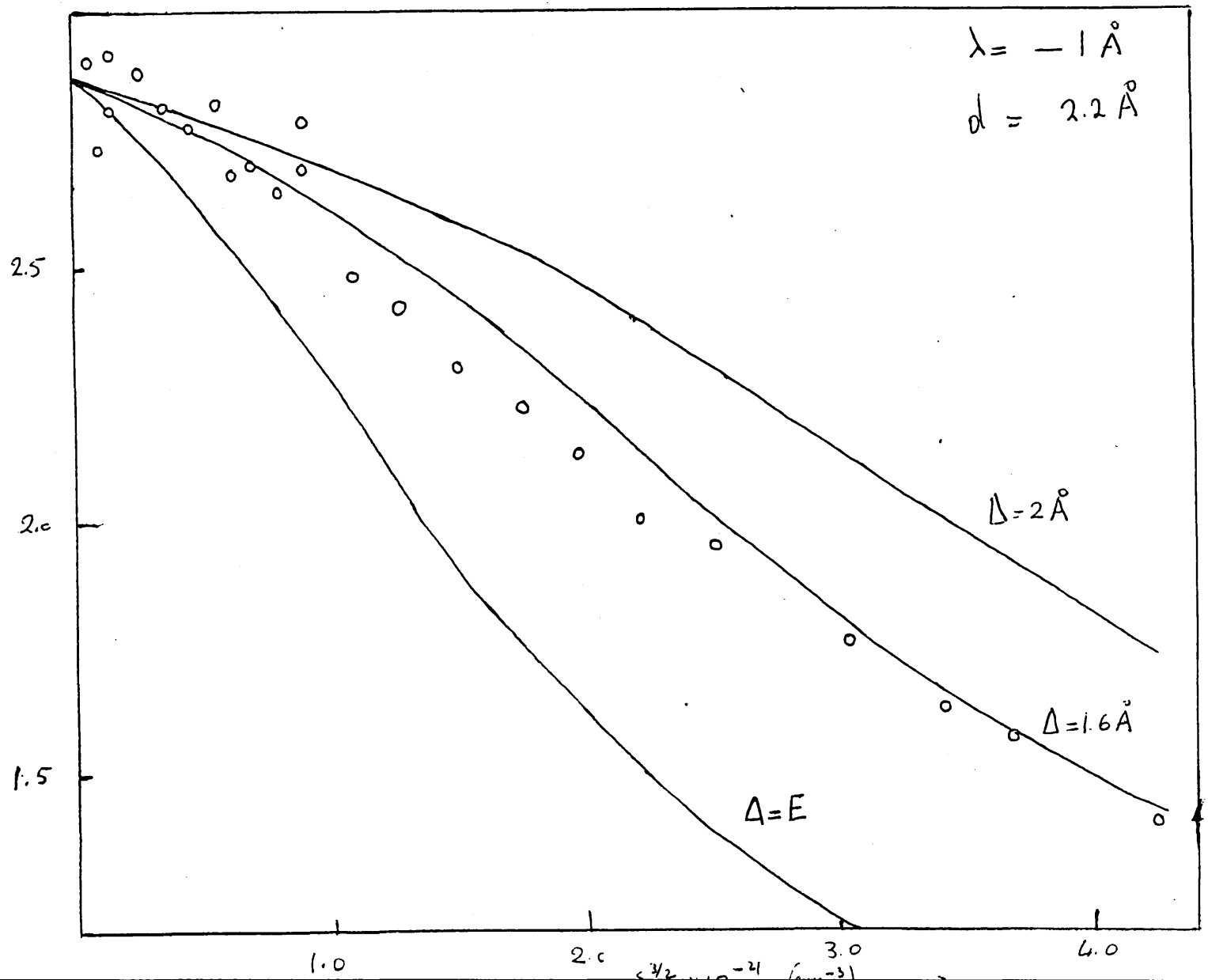

λ = −1 Å
d = 2.2 Å
Δ=2 Å
Δ=1.6 Å
Δ=E
2.5
2.0
1.5
1.0
2.0
3.0
4.0
$[\bar{I}_{(0)} - \bar{I}(s)]/s \times 10^{14}$ (volts-cm²) ⟶

Fig.3e

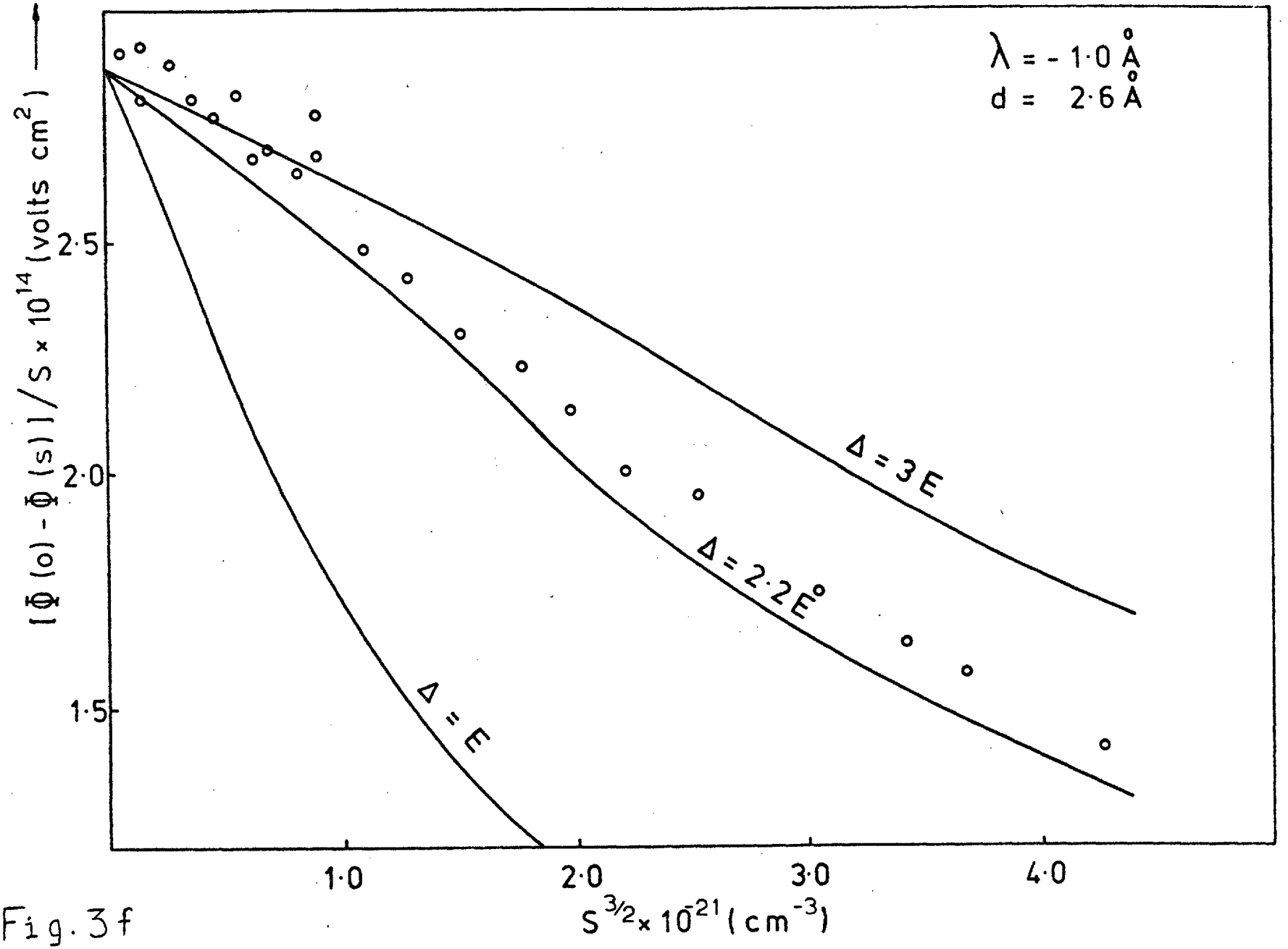

λ = - 1·0 Å
d = 2·6 Å
Δ = 3E
Δ = 2·2E°
Δ = E
2·5
2·0
1·5
1·0
2·0
3·0
4·0
|Φ (o) - Φ (s)| / S × 10^14 (volts cm^2)
S^3/2 × 10^-21 (cm^-3)

Fig. 3f

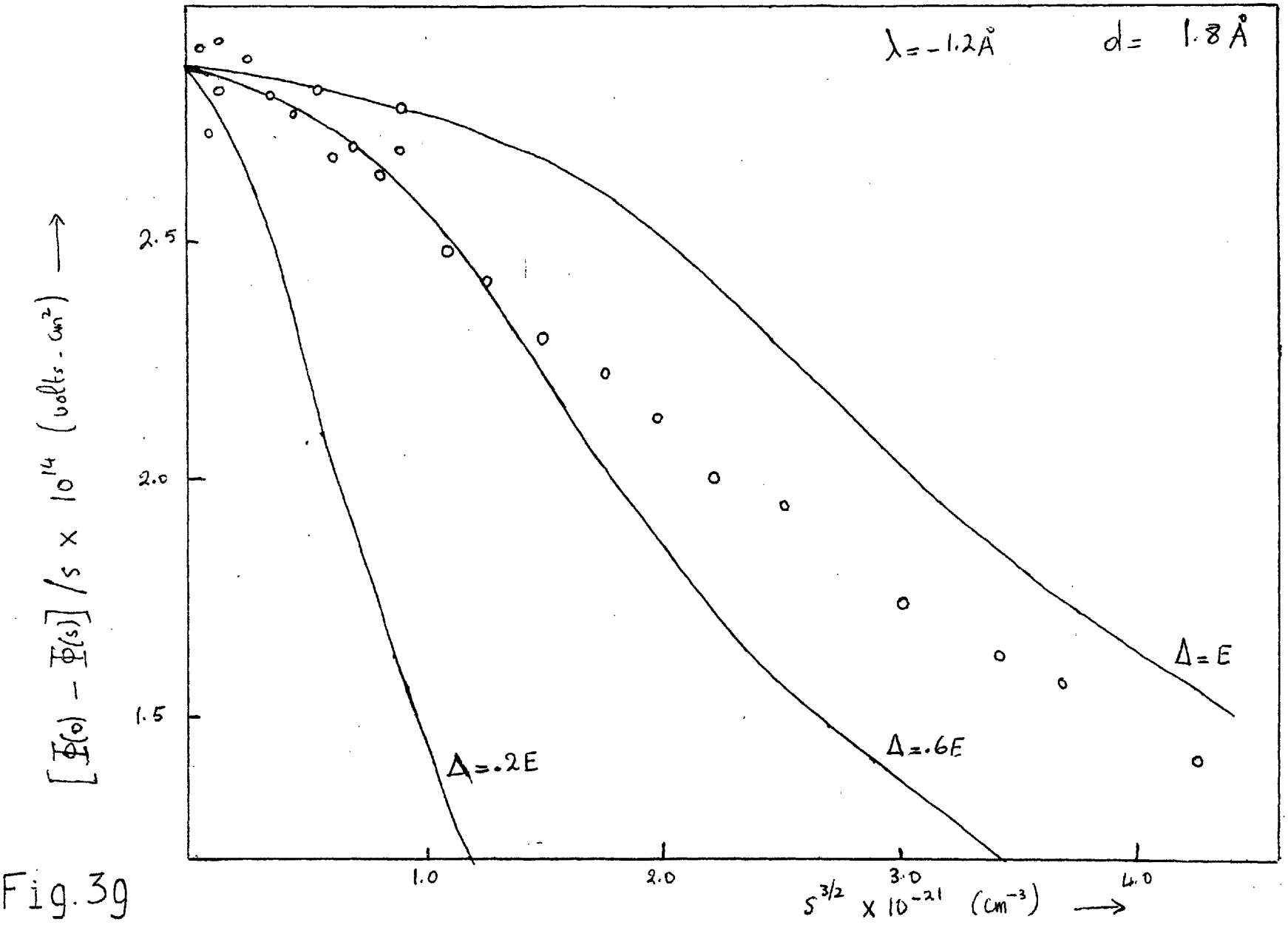

λ = -1.2Å
d = 1.8Å
Δ = E
Δ = .6E
Δ = .2E
2.5
2.0
1.5
1.0
2.0
3.0
4.0
[Φ(0) − Φ(s)] / s × 10^14 (volts · cm^2) ⟶
s^3/2 × 10^-21 (cm^-3) ⟶

Fig. 3g

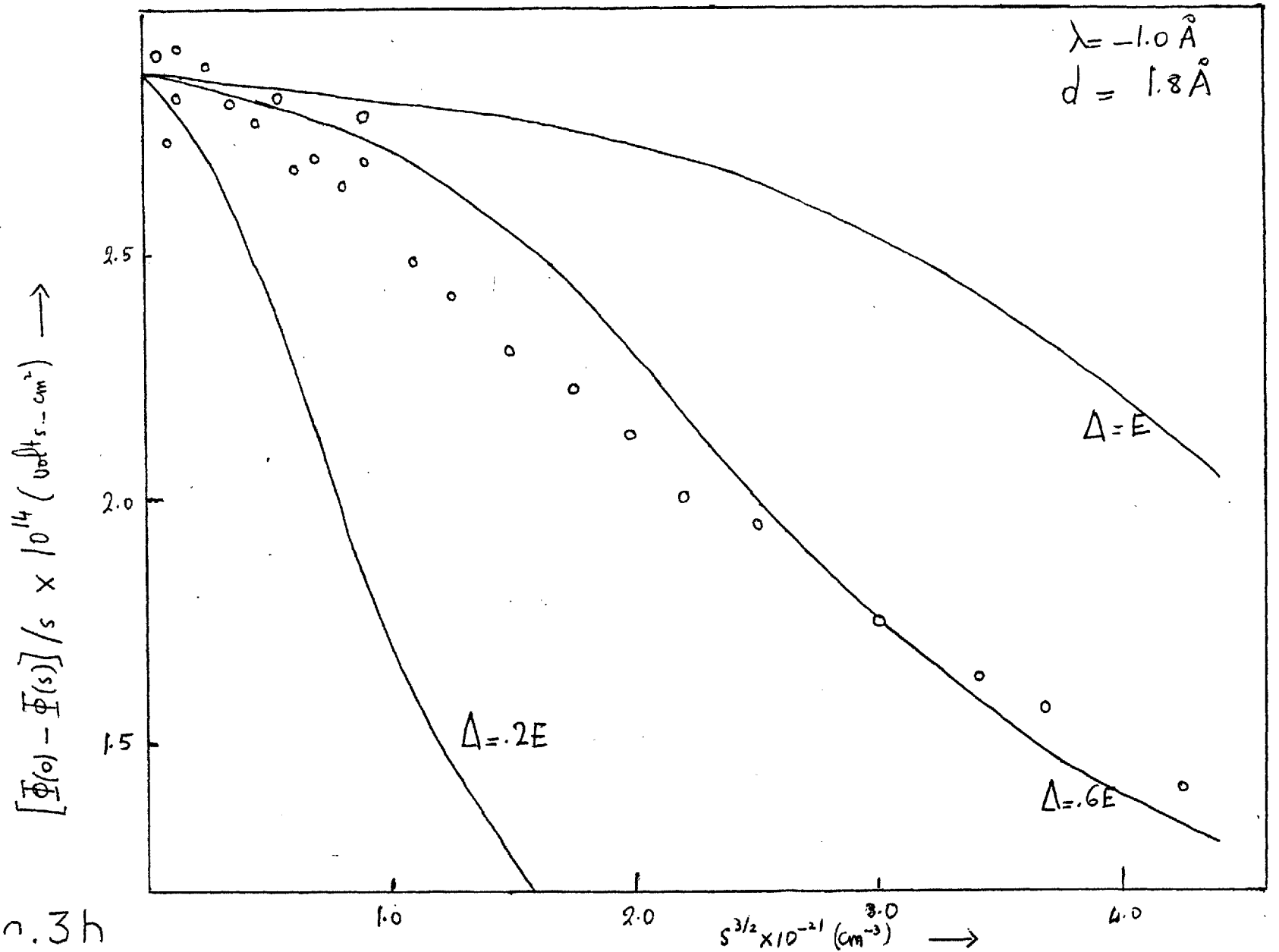

λ = −1.0 Å
d = 1.8 Å
Δ = E
Δ = .2E
Δ = .6E
2.5
2.0
1.5
1.0
2.0
3.0
4.0
$[\Phi(0) - \Phi(s)]/s \times 10^{14}$ (units $s - cm^2$) ⟶
$s^{3/2} \times 10^{-21}$ (cm^{-3}) ⟶

Fig. 3h

is there any reason to expect this. The minimum does not relate to any significant change in surface structure, and this is illustrated in the results.

For a value of λ predicted by the f-sum rule ($\lambda = -1.6\text{Å}$), the results are in very poor agreement with the experimental measurements available (figs. 3a and 3b), the pronounced curvature in the region $0 \leq s \leq 10^{14}$ cm^{-2} may be explained by the small value of the ratio $d/|\lambda|$ for which the use of the approximation (4.2.19) is inadequate.

For smaller values of $|\lambda|$ ($\lambda = -1.2\text{Å}$, $\lambda = -1.0\text{Å}$) we find quite good fits to the experimental results for values of $d \geq 2\text{Å}$ and values of Δ which increase with d. The curves (figs 3c,d,e,f) are linear in the regime $0 \leq s \leq 10^{14}$ which indicates that the low coverage approximation (4.2.19) is fairly good in this region.

If d is taken too small (e.g $d = 1.8\text{Å}$) (figs 3g,h), then the results again show very poor agreement with experiments.

It is also of interest to plot $\mu_t(s) \times s$ as a function of s, which with the appropriate constant of proportionality gives a work function/coverage curve (fig.4). These curves certainly exhibit the qualitative features of the experimental curves (initial sharp decrease in ϕ, minimum in ϕ, small increase in ϕ after the minimum) for most values of the parameters, although good quantitative agreement is obtained for the relatively narrow range of parameters found in fig.2 to be in agreement with experiment.

Table 1 gives estimates for Δ and E_i, which give the best fit to the experimental results, for different values of λ and d. Where a range for the parameters is given the agreement with experimental results is generally poor for a wide range of coverages, the lower and upper bounds of the interval (Δ_1, Δ_2) correspond to the values of the parameters giving the best results at low and high coverages respectively.

When the results are in good agreement with the experimental points over the whole range of coverages considered ($0 \leq s \leq 3\times10^{14}$ cm^{-2}), the appropriate values of Δ are fairly large ($.72\text{eV} = E \leq \Delta \leq 3E = 2.16\text{eV}$). These large va-

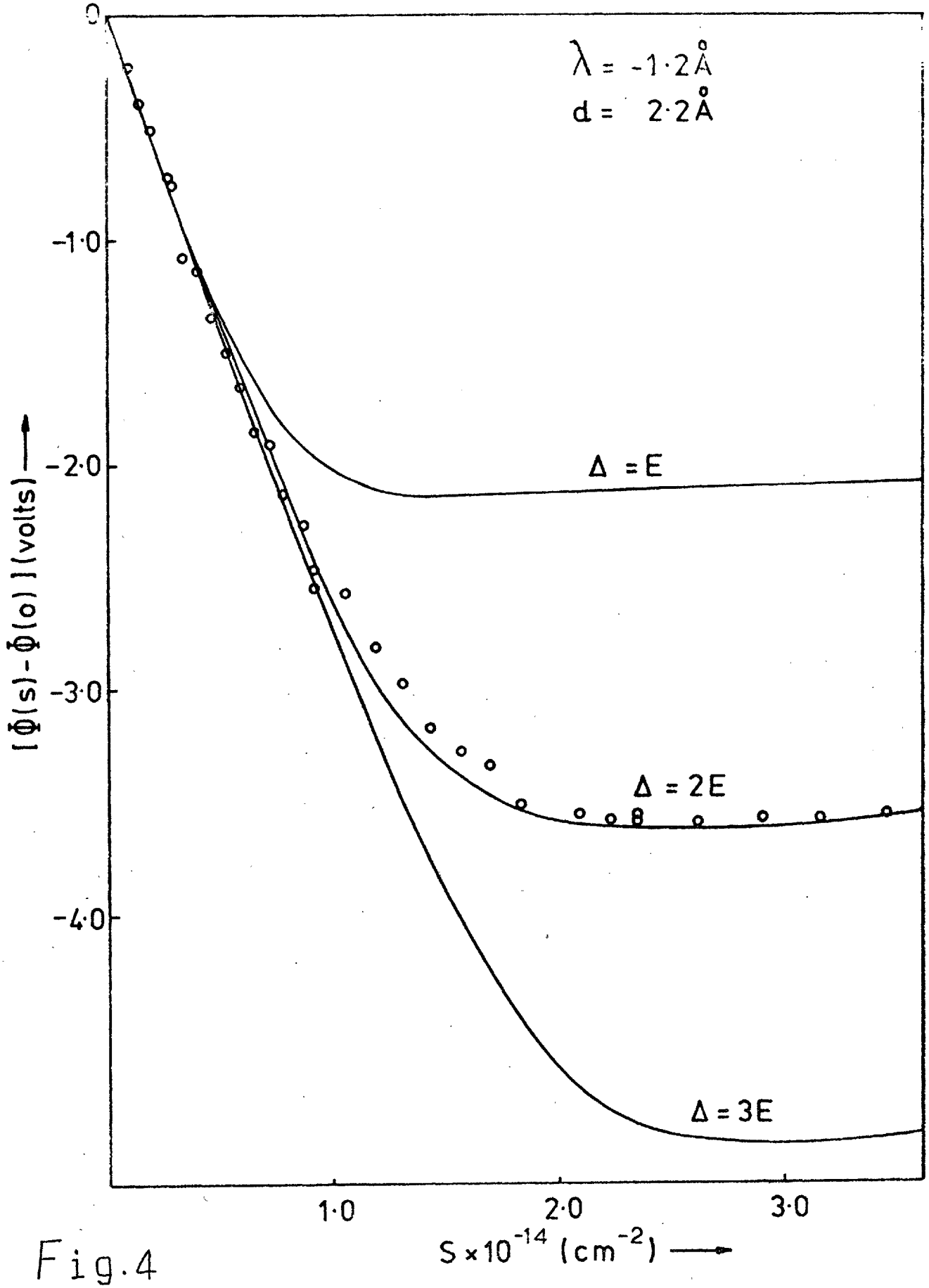


Fig.4

Table 1

Estimated width and position of adatom levels

λ (Å)	-1.0			-1.2		
d(Å)	1.8	2.2	2.6	1.8	2.2	2.6
Δ/E	[.4, .6]	$1.6 \pm .1$	$2.4 \pm .1$	[.6, .9]	$2.0 \pm .1$	$3.0 \pm .1$
E_i/E	[2.5, 3.2]	$3.5 \pm .1$	$3.3 \pm .1$	[2.7, 3.3]	$3.4 \pm .1$	$3.3 \pm .1$

lues of Δ indicate that the s and p adatom energy levels are strongly hybridized as illustrated in fig.5a. The corresponding energy range of E_i is a narrow strip aroubd $E_i = 3.4E = 2.5eV$. Correspondingly, we find $E_{ns}' = 1.3eV$ which is somewhat smaller than the estimated value of $E_{ns}' = 2.3eV$ at $d=2.15\mathring{A}$ which we discussed earlier. The present model may be used to describe other alkali-transition metal systems, although some of the approximations which we have used are more suited to describe Cs than smaller alkali adsorbates such as K or Na.

However we do not wish to extend this model to other alkali-pure metal systems, instead we have made calculations for the system Cs adsorbed on W covered by a layer of O (Papageorgopoulos and Chen 1972, Desplat 1974). The complexity of this system evidently renders it hard to characterise and we cannot expect the accuracy of the work function coverage curves to be comparable with that on a pure metal surface. But the results available do show a substantially different behaviour from those characteristic of Cs/ pure metals systems. The work function coverage curve for this system differs from that considered earlier , in that the initial drop in ϕ is much steeper and consequently the work function at the minimum is much lower. The results in this case (fig.6) indicate that the value of d must be much greater than in the previous example ($d \gtrsim 4.2\mathring{A}$) while the values of Δ are much smaller ($\Delta \simeq .4E = .29eV$ when $d = 4.2\mathring{A}$, $\Delta \simeq .6E = .43eV$ when $d = 4.5\mathring{A}$), so that for this system the two adsorbate energy levels are well defined Lorentzians with narrow widths (fig.5b) in contrast to the situation found for the Cs/ Re(0001) system.

The difference in these sets of results are explained by the presence of the oxygen layer, which naturally increases d, and is also responsible for the large decrease in level width Δ. The oxygen layer plays the role of a potential barrier at the surface, which renders the tunnelling of the Cs valence electrons more difficult, this increases the lifetime of the valence states on the adatom and consequently decreases the widths Δ .

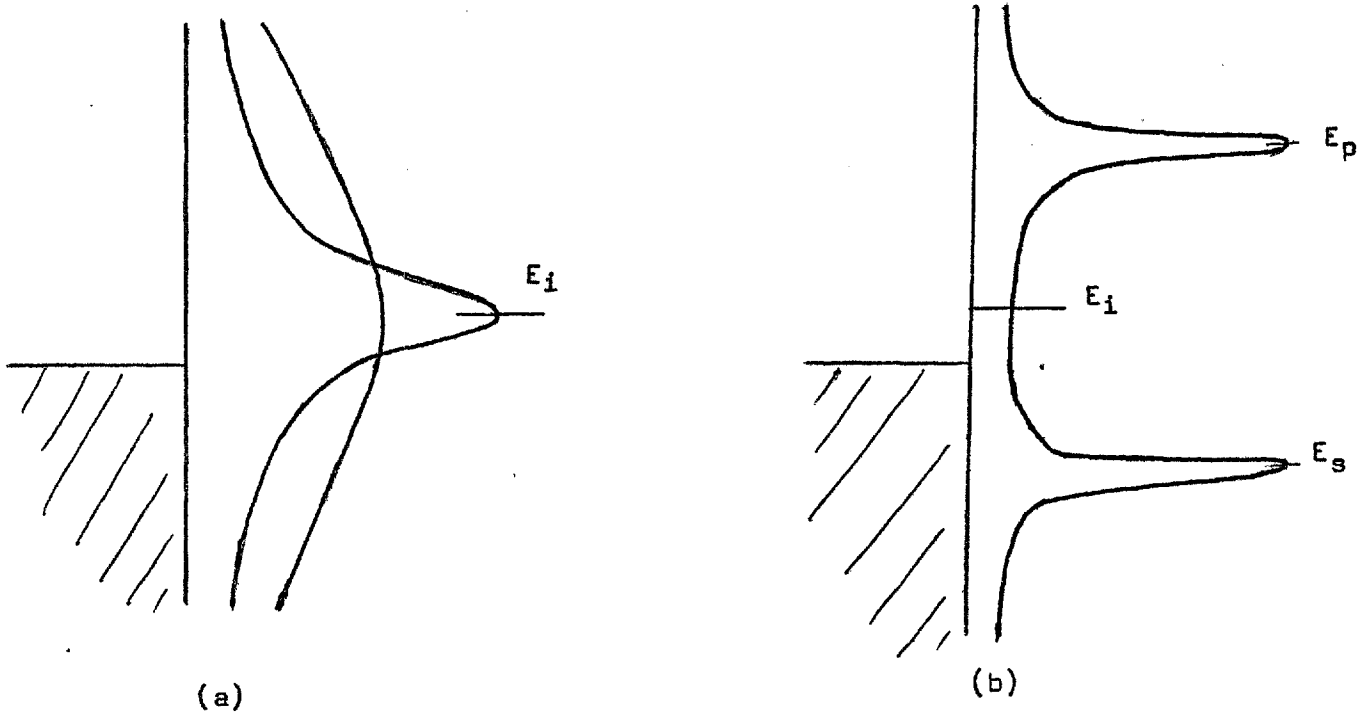


Fig.5 Energy levels for (a) Cs/Re(0001), (b) Cs/ W + layer of O

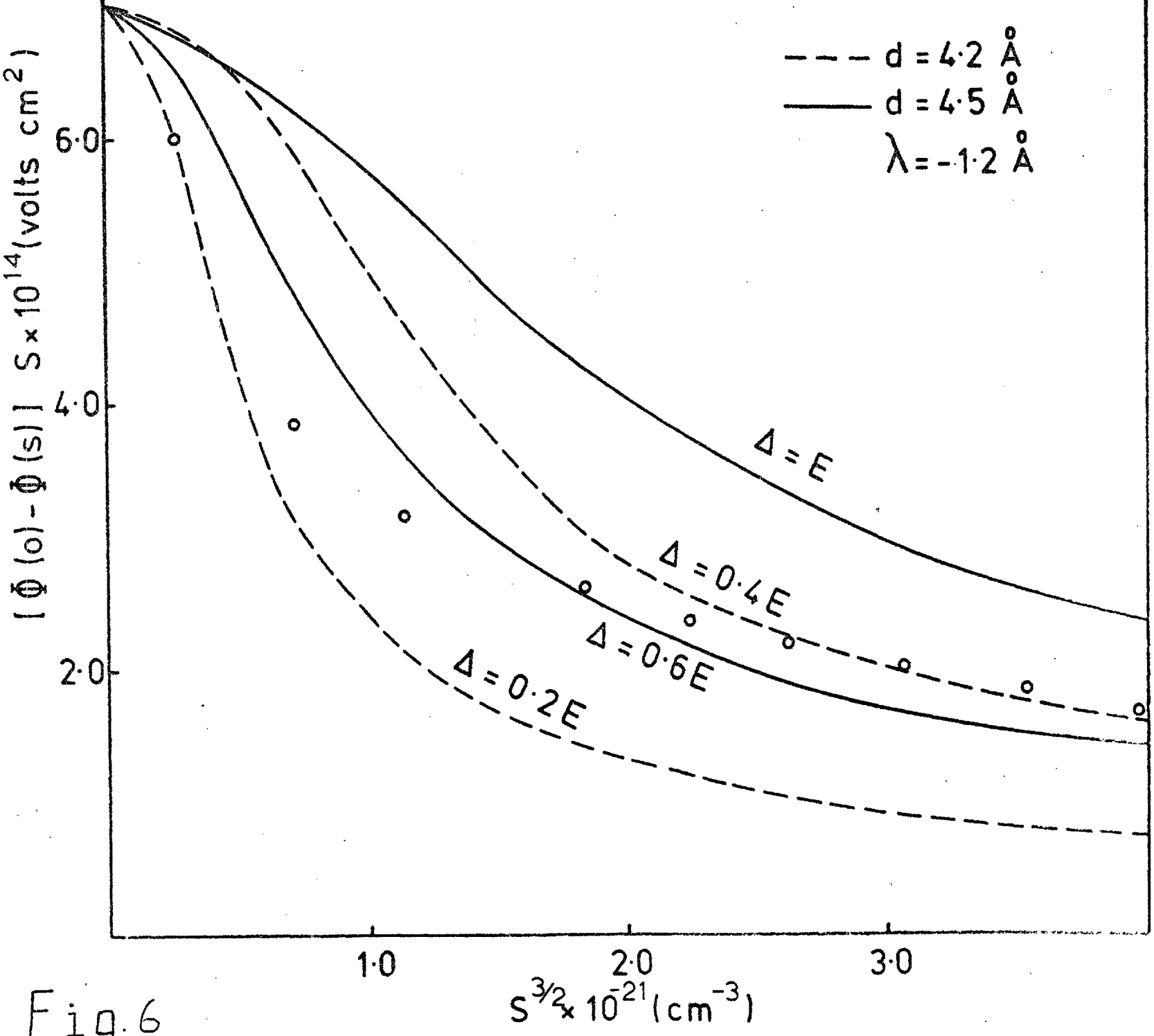

- - - d = 4·2 Å
—— d = 4·5 Å
λ = -1·2 Å
Δ = E
Δ = 0·4E
Δ = 0·6E
Δ = 0·2E
6·0
4·0
2·0
1·0
2·0
3·0
[Φ(o) - Φ(s)] S × 10^14 (volts cm^2)
S^3/2 × 10^-21 (cm^-3)

Fig. 6

We conclude part 1 of the thesis, by remarking that our attempt at a correlation of experimental results in the form of macroscopic properties (e.g the work function) of a given chemisorption system, to its microscopic properties (the electronic levels) has met with some success in understanding the physics of the particular system.

How good are the quantitative values obtained for the width and position of the electronic levels? This question shall remain unanswered until suitable experiments are carried out to measure such quantities for the systems which we have dealt with.

Chapter 5

THE CHEMISORPTION OF TRANSITION ATOMS OF THE THIRD SERIES ON TUNGSTEN : REVIEW OF THE THEORY UP TILL NOW

5.1. Introduction

A study of the chemisorption of transition metal atoms of the third series on various single crystal planes of a tungsten substrate has been made by Plummer and Rhodin (1968), using a field ion microscope technique. The general trend they observed was that the binding energy of the atom on the surface varied linearly with the number of electrons in the 5d shell, reaching a triangular maximum at Rhenium and then decreasing linearly. Despite some uncertainty in the numerical values, it is now generally accepted that the trend is correct, these results being corroborated by a similar trend obtained for the activation energies of diffusion (Bassett and Parsley 1970).

These results have stimulated considerable theoretical interest and a number of models have appeared since. These fall into two categories

(i) the band approach, in which the problem is treated as one of self-consistency within the Hartree-Fock approximation

(ii) the surface molecule approach, in which the adatom is assumed to interact strongly with a limited number of atoms on the surface of the metal,

and in which correlation effects are included implicitly.

We shall first discuss the band approach, commencing with a discussion of the tight-binding approximation (Mott and Jones 1936) which has been widely used in describing transition metal d-bands (Friedel 1969).

5.2. The tight-binding approximation

In this approximation, the electrons are assumed to be tightly bound to the atoms. The electron states are thus assumed to be nearly those of the isolated atom. The electron wavefunction may be written in terms of the atomic orbitals $\varphi(\underline{r})$ centred on all the sites $\underline{R}_i$ of the crystal i.e

$$\psi(\underline{r}) = \sum_i c_i \varphi(\underline{r} - \underline{R}_i) \qquad (5.2.1)$$

If H is the Hamiltonian of an electron interacting with a system of atoms situated at $\underline{R}_i$, through a potential $V(\underline{r} - \underline{R}_i)$, the secular equation then reads

$$\sum_j \left[\delta_{ij}(H_{ii} - E) + H_{ij}\right] c_j = 0 \qquad (5.2.2)$$

where $H_{ij} = \int \varphi^*(\underline{r} - \underline{R}_i) H \varphi(\underline{r} - \underline{R}_j) dV$.

Since the orbitals are assumed to be localised, only the integrals H_{ij} with $|\underline{R}_i - \underline{R}_j|$ small will not be negligible. The nearest neighbour approximation consists in taking $H_{ij} = \beta$ for nearest neighbours, $H_{ij} = 0$ otherwise

Several workers (Allan and Longlart 1970, Cyrot-Lackmann 1970, Cyrot-Lackmann and Ducastelle 1971) have used the tight-binding approximation limited to nearest neighbours only, to describe the chemisorption of transition metal adatoms of the third series on tungsten.

Cyrot-Lackmann (1970) has introduced a moment method to describe various properties of transition metal surfaces, including the binding energy of adatoms. If H is the Hamiltonian of an electron interacting with a system of atoms and n(E) the density of states per atom, the moment of order p is then given by the relation

$$\mu_p = \int E^p n(E) dE = \frac{1}{N} \mathrm{Tr}\, H^p \qquad (5.2.3)$$

A knowledge of all the moments μ_p determines the density of states completely

$$n(E) = (2\pi)^{-1} \int_{-\infty}^{\infty} dx e^{ixE} \sum_p \frac{(-ix)^p}{p!} \mu_p \qquad (5.2.4)$$

Keeping only two center, nearest neighbour integrals, and neglecting crystalline integrals $\langle \varphi_i | V_j | \varphi_i \rangle$, compared to the transfer type of integrals $\langle \varphi_i | V_i | \varphi_j \rangle$ (i and j being nearest neighbour, and $V_i = V(\underline{r} - \underline{R}_i)$), it is shown that μ_p can be written in the form

$$\mu_p = P_p \beta^p \qquad (5.2.5)$$

where we have assumed that the integrals are all equal to β , and P_p represents the number of ways one can travel from a given atom, to the same atom by passing through p - 1 atoms, all first neighbours to one another.

Cyrot- Lackmann and Ducastelle (1971) have used the moment method to determine the binding energies of transition metal atoms on transition metals. Starting from a perfect transition metal surface M and a free transition atom A, then A is adsorbed onto M, the coupling between them being established through the hopping integrals. The binding energy of the adatom A is then defined as the difference between the total energy of the substrate M and the atom A, and the energy of the system formed by the substrate and the ad-

sorbed atom. The various energies are computed using for the density of states Gaussians fitted to their respective first moments. The most serious drawback of this method lies in its lack of self-consistency. The charge transfer between adatom and substrate has either been neglected altogether, or included in an arbitrary non-consistent manner.

Their theory predicts that the binding energy varies as a quadratic function of the valence difference between the adatom and substrate atoms.

Allan and Lenglart (1970) use a similar tight-binding description of the d-band, the effect of the surface is represented by a perturbing potential which is determined by use of Friedel's sum rule and by the restriction that the total variation of charge at the Fermi level is zero. The adatom is assumed to bind strongly to a single substrate atom. The extra charge brought to the surface is screened by the substrate d-electrons, the increase of charge at the surface has no effect on the density of states far from the surface, i.e there is no variation of the Fermi level. Self-consistency is then achieved by use of Friedel's sum rule (Friedel 1958), i.e the total charge screened by the W electrons is put equal to the charge brought to the surface. The authors assume that the variations in charge are negligible on all the atoms except for the adatom nearest neighbour.

Their results for the binding energy again show a parabolic trend in contrast to the experiments. Further their values for the binding energies are much smaller than Plummer and Rhodin's experimental values, they attributed this, to the fact that in their model the adatom binds to one substrate atom only, rather than to four substrate atoms in pyramidal form.

The implementation of the Friedel sum rule makes the charge variation ΔN on the adatom go to zero at $N = 0$ and $N = 10$ (N is the number of 5d-electrons on the adsorbate). These results coupled to the chemisorption energy results violate the sum rule

$$\frac{\partial \Delta E(N)}{\partial N} = U \Delta N \qquad (5.2.6)$$

which must be satisfied for a model Hamiltonian description of the problem, as we shall discuss later in the text (also see Newns 1970a,b).

5.3. The virtual level description.

This model (Newns 1970a) is based on the Anderson Hamiltonian which includes electron-electron interactions only within the adsorbed atom, given by

$$H = \sum_{\sigma} \left\{ \epsilon_d \sum_{m} n_{m\sigma} + \sum_{\underline{k}} \epsilon_{\underline{k}} n_{\underline{k}\sigma} + \sum_{\underline{k},m} (V_{m\underline{k}} c^{+}_{m\sigma} c_{\underline{k}\sigma} + h.c) \right\}$$

$$+ \tfrac{1}{2} U \sum_{\sigma,\sigma'} \sum_{m,m'} (1 - \delta_{\sigma\sigma'} \delta_{m,m'}) n_{m\sigma} n_{m'\sigma'} \qquad (5.3.1)$$

This Hamiltonian is similar to that used in chapter 2. The difference being that only one adatom is on the surface, consequently there is no interaction between this and other adatoms, further the adatom now has a variable number of d-electrons in its valence shell, and consequently the orbital degeneracy must be accounted for.

Using the Hamiltonian (5.3.1) Newns (1970a) obtained an expression for the chemisorption energy ΔE in the Hartree-Fock approximation, (ΔE is defined as the energy change on removing the adatom from the surface to infinity), which is dependent on a number of approximations

(i) the m dependence of the adatom-metal hopping integral $V_{m\underline{k}}$ is neglected

(ii) the adatom ionization potential I and the electron affinity A are taken equal to +U/2 and -U/2 respectively, this is not too serious an approximation since it is compatible with the restriction that I must be positive and A negative for the atom to be stable,

(iii) the model is valid for the non-magnetic case only.

In the Hartree approximation, the density of states $\rho(\epsilon)$ for any adatom orbital $|m\sigma\rangle$ is given by the expression (using a simplified version of the argument used in chapter 2)

$$\rho(\epsilon) = (\pi)^{-1} \frac{\Delta(\epsilon)}{(\epsilon - \epsilon_o - \Lambda(\epsilon))^2 + \Delta(\epsilon)^2} \qquad (5.3.2)$$

where the effective d-level ϵ_o is given by

$$\epsilon_o = \epsilon_d + 9UN_d/10 \quad , \quad N_d = \sum_{m\sigma} \langle n_{m\sigma} \rangle = 10 \langle n_{m\sigma} \rangle, \qquad (5.3.3)$$

and Λ and Δ represent the energy shift and the width of the virtual level, defined in the usual way (e.g see chapter 2).

Let us now assume that Λ and Δ are energy independent. The self-consistency conditions (Anderson 1961) are

$$n = \langle n_{m\sigma} \rangle = \int_{-\infty}^{o} \rho(\epsilon) d\epsilon \qquad (5.3.4)$$

together with (5.3.3), and we have taken the Fermi level at zero energy in (5.3.4).

The chemisorption energy ΔE is then given by the relation

$$\Delta E = -E_d^{\,o} + \sum_{r\sigma} \epsilon_{r\sigma} - \frac{9}{10}\frac{U}{2} N_d^{\,2} - \sum_{\underset{\sim}{k}} \epsilon_{\underset{\sim}{k}} \qquad (5.3.5)$$

where $E_d^{\,o}$ is the energy of the free atom, given by

$$E_d^{\,o}(N) = \epsilon_d \sum_i n_i + \tfrac{1}{2}U\Big[\Big(\sum_i n_i\Big)^2 - \sum_i n_i \Big]$$

$$= \epsilon_d N + \tfrac{1}{2}U(N^2 - N) \,, \qquad (5.3.6)$$

and we have used the result $n_i^2 = n_i$. The d-orbital self-energy ϵ_d may be calculated by the use of the simplifying assumption I ==U/2. Indeed, the ionization potential is given by the relation

$$I = E_d^{\circ}(N-1) - E_d^{\circ}(N) = -\epsilon_d - (N-1)U \qquad (5.3.7)$$

the second equality in (5.3.7) follows from (5.3.6). Equating (5.3.7) to U/2 we find immediatly

$$\epsilon_d = -U(N - \tfrac{1}{2}) , \qquad (5.3.8)$$

and substituting back in (5.3.6), we find

$$E_d^{\circ} = -\tfrac{1}{2} U N^2 \qquad (5.3.9)$$

The second term in (5.3.5) represents the Fock eigenvalues of the Hamiltonian, this term may be rewritten in the form (e.g see Newns 1969b)

$$\sum_{r,\sigma} \epsilon_{r\sigma} = -\frac{10}{\pi}\int_{-\infty}^{0} \arctan\left(\frac{\Delta}{\epsilon - \epsilon_o - \Lambda}\right) d\epsilon + \sum_{k} \epsilon_k \qquad (5.3.10)$$

The 3rd term in (5.3.5) has been substracted because it has been counted twice in the sum of the Fock eigenvalues.

$\Delta E(N)$ can be expanded about N = 5, it is easily found that

$$\left.\frac{\partial \Delta E(N)}{\partial N}\right|_{N=5} = 0 \qquad \text{and} \qquad \left.\frac{\partial^2 \Delta E(N)}{\partial N^2}\right|_{N=5} = U\left(\frac{dN_d}{dN} - 1\right) \qquad (5.3.11)$$

now N_d depends on N through its dependence on ϵ_o which itself depends on N_d through equation (5.3.3). The self-consistency is easily determined and we find that

$$\left.\frac{dN_d}{dN}\right|_{N=5} = \frac{10\,U}{2\delta + 9U} \qquad (5.3.12)$$

where δ is given by

$$\delta^{-1} = -\frac{4}{\pi}\int_{-\infty}^{0} \frac{\Delta(\epsilon - \Lambda)}{[(\epsilon - \Lambda)^2 + \Delta^2]^2}\, d\epsilon \qquad (5.3.13)$$

Equations (5.3.11) follow from the sum rule (5.2.6) where here $\Delta N = N_d - N$

Finally we find that to second order in $(N - 5)$, ΔE is given by the relation

$$\Delta E(N) = \Delta E(5) - \tfrac{1}{2} U(N - 5)^2 \left(\frac{2\delta - U}{2\delta + 9U}\right) \qquad (5.3.14)$$

A look at equation (5.3.14) shows how the Hartree-Fock results completely fail to give agreement with experiment in the large U limit; in fact the point $N = 5$ becomes a parabolic minimum for values of U which are greater than 2δ. While if $U < 2\delta$, then $N = 5$ is a parabolic maximum in contrast to the observed triangular maximum.

More complete calculations based on a semi-elliptic form for the width $\Delta(\epsilon)$ give similar results for ΔE (Newns 1970a).

A similar investigation was conducted by Grimley and Thorpe (1971a) (see also Thorpe 1972) with a different form of $\Delta(\epsilon)$ (here $\Delta(\epsilon)$ is still symmetric but it exhibits a minimum at the centre of the band (ϵ_F), with maxima above and below ϵ_F). The results for ΔE obtained in this case do not resemble the experimental curves in any way.

None of the above mentioned models have had any success in reproducing the observed experimental trend. A possible explanation of these discrepancies has been suggested by Newns (1970b) and by Grimley and Thorpe (1971b), who argue that the effects of electron correlation are important, and that they should be greatest in the half-filled case (where theory and experiment

are in greatest disagreement), owing to the greater number of configurations available. In order to investigate this possibility, we must first introduce the concept of the surface molecule.

5.4. Surface molecules

The concept of the surface molecule (Grimley 1971a,b,1973) implies that the adatom-substrate bond is determined by the strong interaction between the adatom orbitals and the localised group orbital formed from the nearest neighbour substrate orbitals.

Assuming that the surface molecule approximation is a good one, then the problem may be described by a two atom Hubbard (1963) Hamiltonian (Newns 1970b, Grimley and Thorpe 1971b). The two treatments differ in many ways.

Grimley and Thorpe (1971b) have chosen to solve their Hamiltonian in the unrestricted Hartree-Fock approximation. The self energies, and intra-atomic Coulomb interactions, of electrons on the adatom were estimated from free atom Hartree-Fock results. The Coulomb repulsion U_d, of electrons on the substrate atom was chosen arbitrarily (they showed that the choice of U_d did not prove critical, as long as they

kept away from the Anderson limit ($U_d = 0$)). Finally the self energy E_d of the electrons on the substrate atom, was fixed by the restriction that $E_d + 9U_d \langle n_d \rangle$ coincides with the Fermi level when $\langle n_d \rangle = 0.5$.

Their results for the binding energy are in good agreement with experiment. The calculated charges indicate that adsorption is predominantly neutral. It should also be noticed that, in this model the sum of charges on the adatom and the substrate is non zero, indicating that the surface molecule does not have a fixed number $5 + N$ of electrons.

Newns (1970b) has used the following two-atom Hubbard Hamiltonian

$$H = \epsilon_a \sum_{i=1}^{10} n_{ai} + \epsilon_b \sum_{i=1}^{10} n_{bi} + \sum_{i=1}^{10} \beta_i \, (a_i^{+} b_i + b_i^{+} a_i)$$

$$+ \tfrac{1}{2} U_a \sum_{i,j} n_{ai} n_{aj} \, (1 - \delta_{ij}) + \tfrac{1}{2} U_b \sum_{i,j} n_{bi} n_{bj} (1 - \delta_{ij}) \qquad (5.4.1)$$

where a_i^{+}, b_i^{+} are creation operators, n_{ai}, n_{bi} are number operators and the atoms a and b represent the adsorbate and substrate respectively, the index $i=1,\ldots.10$ refers to atomic d spin-orbitals. The d-orbital self energies can easily be shown to be equal to

$$\epsilon_a = - U_a (N - \tfrac{1}{2}) \quad , \qquad \epsilon_b = -4.5 U_b \qquad (5.4.2)$$

on the simplifying assumption that $I_\alpha = U_\alpha / 2$ $(\alpha = a,b)$, as discussed in the previous section. The third term in (5.4.1) describes the coupling between the two atoms, the β_i's are the matrix elements $\beta_i = \langle a_i | H | b_i \rangle$. The last terms in the Hamiltonian represent Hubbard-like intra-atomic electron-electron interactions, we remind ourselves that within the Hubbard model only interactions between electrons localised on the same lattice site are retained.

An estimate of the β_i's for the (100) face of W may be made from consideration

of the following bonding configuration (see fig.1), assuming a to be at the origin then b is an effective atom representing the four nearest substrate atoms which are assumed to lie at $(\pm\sqrt{2},0,1)$ and $(0,\mp\sqrt{2},1)$. The symmetry of the d-orbitals is illustrated in fig.2. It is clear from fig.2 that any d-orbital at the origin can only couple to a limited number of orbitals at $(\sqrt{2},0)$. e.g for the $d_{3z^2-r^2}$ orbital at (0,0) the only allowed orbitals at $(\sqrt{2},0)$ are those that have the same parity about the x-axis (i.e the $d_{3z^2-r^2}$, $d_{x^2-y^2}$, d_{xz} orbitals). From the atomic orbitals χ_j of symmetry j, normalised orbitals of symmetry i about the axis (0,0,z) may be constructed. If R denotes a rotation of $\pi/2$ about the z-axis, then the normalised orbitals are given by

$$\varphi_1^{\,j} = \tfrac{1}{2}\sum_{n=0}^{3} R^n \chi_j \qquad j = 1,2b,4 \qquad (5.4.3a)$$

$$\left.\begin{aligned} \varphi_{2a}^{\,j} &= (2)^{-\frac{1}{2}}\,(\chi_j - R^2\chi_j) && j = 2a,3 \\ &= (2)^{-\frac{1}{2}}\,(R\chi_j - R^3\chi_j) && j = 1,2b,4 \end{aligned}\right\} \qquad (5.4.3b)$$

$$\left.\begin{aligned} \varphi_{2b}^{\,j} &= (2)^{-\frac{1}{2}}\,(\chi_j - R^2\chi_j) && j = 1,2b,4 \\ &= (2)^{-\frac{1}{2}}\,(R\chi_j - R^3\chi_j) && j = 2a,3 \end{aligned}\right\} \qquad (5.4.3c)$$

$$\varphi_3^{\,j} = \tfrac{1}{2}\sum_{n=0}^{3} (-1)^n R^n \chi_j \qquad j = 2a,3 \qquad (5.4.3d)$$

$$\varphi_4^{\,j} = \tfrac{1}{2}\sum_{n=0}^{3} (-1)^n R^n \chi_j \qquad j = 1,2b,4 \qquad (5.4.3e)$$

The matrix elements between orbitals at the origin and the linear combinations $\varphi_i^{\,j}$ are now given by $\gamma_1^{\,j} = \langle \psi^1 | H | \varphi_1^{\,j} \rangle$ where ψ^1 is the orbital of symmetry 1, at the origin, e.g when 1 = 1 we have

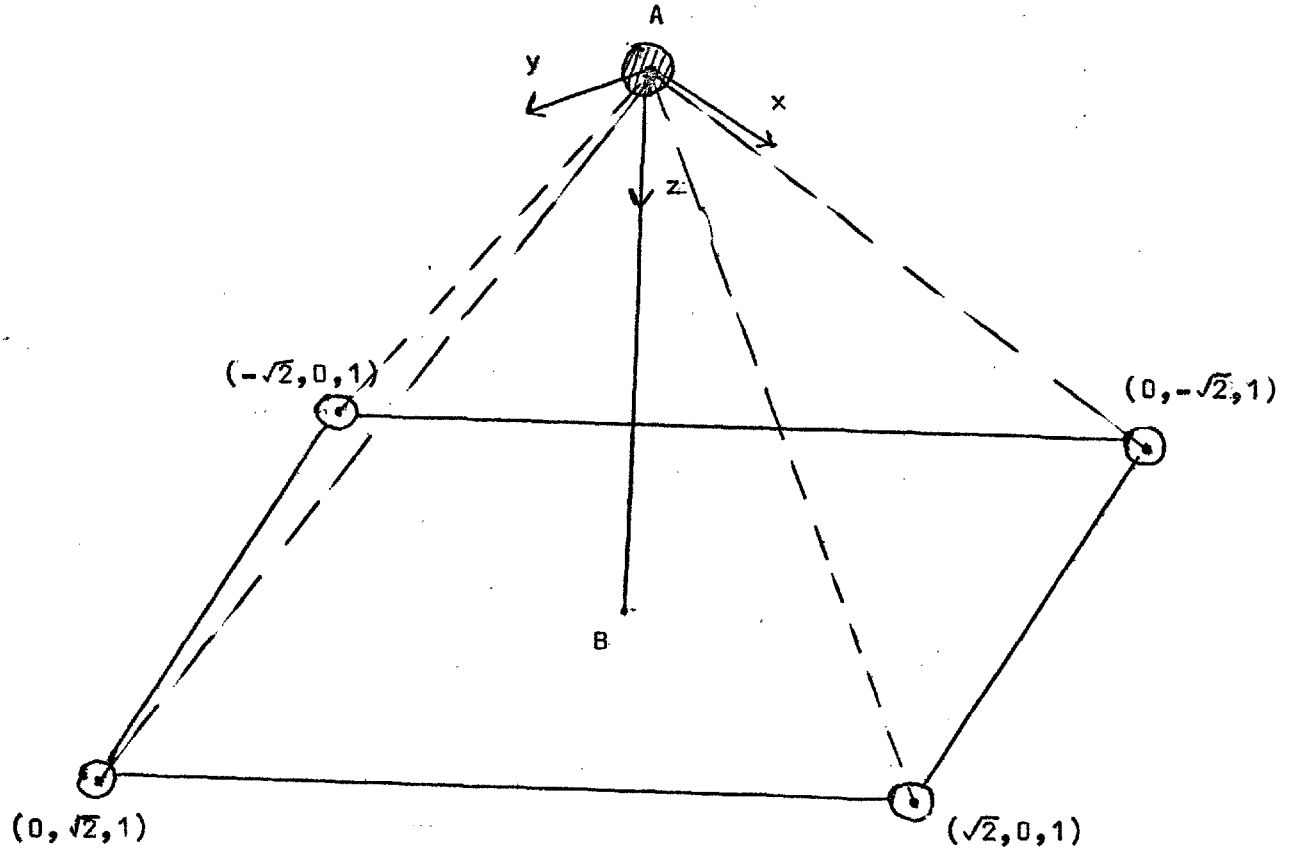
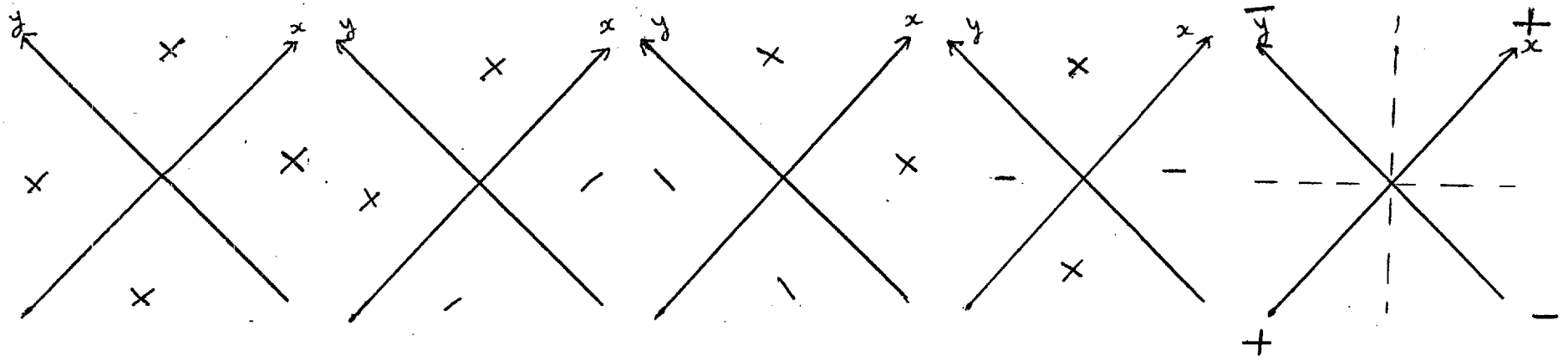


Fig.1 Pyramidal W_4A surface molecule.



1 $3z^2 - r^2$ | 2a yz | 2b xz | 3 xy | 4 $x^2 - y^2$

Fig.2 · Symmetry of various d-orbitals in the x-y plane

$$\gamma_1^{\,j} = \tfrac{1}{2}\sum_{n=0}^{3} \langle \psi^1 | H | R^n \chi^j \rangle = 2\langle \psi^1 | H | \chi_j \rangle \qquad (5.4.4)$$

for the appropriate j's, and we have used the result $\langle \psi^1 R^n | = \langle \psi^1 |$ for all n. These matrix elements can be rewritten in the notation of Slater and Koster (1954), e.g if l = j = 1 we have

$$\gamma_1^{\,1} = 2(3z^2 - r^2 | 3z^2 - r^2) = 2\,\tfrac{2}{3}(dd\pi) + \tfrac{1}{3}(dd\sigma) \qquad (5.4.5)$$

where we have used table 1 of the above reference with the values $l = (2/3)^{\frac{1}{2}}$, m = 0 and $n = (3)^{-\frac{1}{2}}$, of the direction cosines. All the matrix elements may be written in the same notation, they are given in table 1.

Because of the several possible values of j compatible with a given symmetry of the d-orbital at (0,0,z), the Hamiltonian no longer has the simple form (5.4.1) . But for purposes of estimating the β_i's appearing in (5.4.1), we diagonalize the problem at U = 0, which gives linear combinations of the ψ's of a given symmetry. Effective β_i's may then be calculated representing the interaction between a d-orbital at a and the appropriate linear combination.

The secular equation for β_i is easily shown to reduce to the quadratic equation

$$\beta_i^{\,2} - \sum_j |\gamma_i^{\,j}|^2 = 0 \qquad (5.4.6)$$

The results are

$$\left.\begin{aligned} \beta_i &= \tfrac{2}{\sqrt{3}}\left(2(dd\pi)^2 + (dd\delta)^2\right)^{\frac{1}{2}} \simeq .887(dd\sigma) \quad i = xy, 3z^2 - r^2 \\ \beta_i &= \tfrac{2}{3}\left(3(dd\sigma)^2 + 2(dd\pi)^2 + 4(dd\delta)^2\right)^{\frac{1}{2}} \simeq 1.265(dd\sigma), \quad i = xz, yz, x^2 - y^2 \end{aligned}\right\} (5.4.7)$$

where we have expressed $(dd\pi)$ and $(dd\delta)$ in terms of $(dd\sigma)$ using the relative values of Fletcher and Wohlfarth (1951).

The integral $(dd\sigma)$ may be estimated from the band calculations of Mattheiss (1965)

Table 1

Matrix elements γ_1^j in Slater-Koster notation, we have used the abbreviations $\sigma = dd\sigma$, $\pi = dd\pi$, $\delta = dd\delta$.

i \ j	1	2a	2b	3	4
1	$2(3z^2-r^2 \mid 3z^2-r^2)$ $2(\frac{2}{3}\pi + \frac{1}{3}\delta)$		$2(3z^2-r^2 \mid xz)$ $2(\frac{\sqrt{2}}{3\sqrt{3}}\pi - \frac{\sqrt{2}}{3\sqrt{3}}\delta)$		$2(3z^2-r^2 \mid x^2-y^2)$ $2(\frac{-2}{3\sqrt{3}}\pi + \frac{2}{3\sqrt{3}}\delta)$
2a	$\sqrt{2}(xz \mid 3z^2-r^2)$ $\sqrt{2}(\frac{\sqrt{2}}{3\sqrt{3}}\pi - \frac{\sqrt{2}}{3\sqrt{3}}\delta)$	$\sqrt{2}\ (yz \mid yz)$ $\sqrt{2}(\frac{1}{3}\pi + \frac{2}{3}\delta)$	$\sqrt{2}(xz \mid xz)$ $\sqrt{2}(\frac{2}{3}\sigma + \frac{1}{9}\pi + \frac{2}{9}\delta)$	$\sqrt{2}(yz \mid xy)$ $\sqrt{2}(\frac{\sqrt{2}}{3}\pi - \frac{\sqrt{2}}{3}\delta)$	$\sqrt{2}(xz \mid x^2-y^2)$ $\sqrt{2}(\frac{\sqrt{2}}{3}\sigma - \frac{\sqrt{2}}{9}\pi - 2\frac{\sqrt{2}}{9}\delta)$
2b	$\sqrt{2}(xz \mid 3z^2-r^2)$ $\sqrt{2}(\frac{\sqrt{2}}{3\sqrt{3}}\pi - \frac{\sqrt{2}}{3\sqrt{3}}\delta)$	$-\sqrt{2}(yz \mid yz)$ $-\sqrt{2}(\frac{1}{3}\pi + \frac{2}{3}\delta)$	$\sqrt{2}(xz \mid xz)$ $\sqrt{2}(\frac{2}{3}\sigma + \frac{1}{9}\pi + \frac{2}{9}\delta)$	$-\sqrt{2}(yz \mid xy)$ $-\sqrt{2}(\frac{\sqrt{2}}{3}\pi - \frac{\sqrt{2}}{3}\delta)$	$\sqrt{2}(xz \mid x^2-y^2)$ $\sqrt{2}(\frac{\sqrt{2}}{3}\sigma - \frac{\sqrt{2}}{9}\pi - 2\frac{\sqrt{2}}{9}\delta)$
3		$2(xy \mid yz)$ $2(\frac{\sqrt{2}}{\sqrt{3}}\pi - \frac{\sqrt{2}}{\sqrt{3}}\delta)$		$2(xy \mid xy)$ $2(\frac{2}{3}\pi + \frac{1}{3}\delta)$	
4	$2(x^2-y^2 \mid 3z^2-r^2)$ $2(\frac{-2}{3\sqrt{3}}\pi + \frac{2}{3\sqrt{3}}\delta)$		$2(x^2-y^2 \mid xz)$ $2(\frac{\sqrt{2}}{3}\sigma - \frac{\sqrt{2}}{9}\pi - 2\frac{\sqrt{2}}{9}\delta)$		$2(x^2-y^2 \mid x^2-y^2)$ $2(\frac{1}{3}\sigma + \frac{2}{9}\pi + \frac{4}{9}\delta)$

who used two different potentials W_1 and W_2. It is found that (ddσ) varies from 1.33eV for the Σ_3 direction to 1.47eV for the Δ_2, Δ_2', and Δ_5 directions, for the W_1 structure, and from 1.80eV to 1.89eV for the W_2 structure. If we now assume that β_i may be replaced by an average $\beta = \frac{1}{10}\sum_i \beta_i$, we find respectively from W_1 and W_2 β= 1.48eV – 1.63eV and β = 2.0eV - 2.10eV.

U can be estimated from spectral data (Atomic Energy Levels, Circular of the NBS 467, vols II and III) on 4d atoms (U $\simeq$11eV), one can argue that the effective value of U is further reduced by a quantityof the order of the Coulomb integral between nearest neighbours.

The Hamiltonian (5.4.1) was solved exactly by Newns (1970b). The solutions were expressed in terms of the eigenvectors $|n\rangle$ of the Hamiltonian H^o, which is equal to H minus the coupling term between the adsorbate and substrate atoms. The normalised $|n\rangle$ can be written

$$|n\rangle = [h_1!(h_1-n)!n!]^{-\frac{1}{2}} \sum_r (-1)^r \hat{P}_r\, a_1^+ \ldots a_n^+ b_{n+1}^+ \ldots b_{h_1}^+ |0\rangle \qquad (5.4.8)$$

where $|0\rangle$ is the vacuum state, $\hat{P}_r$ are the permutation operators operating on the spin-orbital indices i, and the sum runs over the $\hat{P}_r$.

The set of $\hat{P}_r$'s commute with H, if $|\psi_o\rangle$ is the ground state of H then it is assumed that

$$\hat{P}_r|\psi_o\rangle = (-1)^r|\psi_o\rangle \qquad (5.4.9)$$

where $(-1)^r$ represents the parity of $\hat{P}_r$.

Let us define the operator $N_i = n_{ai} + n_{bi}$, and its eigenvalues ν_i, then we note that N_i also commutes with H, it is also assumed that

$$N_i|\psi_o\rangle \neq 2|\psi_o\rangle \qquad (5.4.10)$$

i.e the possibility of completely full bonds is excluded.

The vectors $|n\rangle$ are also eigenstates of the operator $N_a = \sum_i n_{ai}$ with eigenvalue n ($n = 0,1,.....h_1$) and h_1 represents the number of singly occupied bonds (i.e those for which $\nu_i = 1$).

The matrix elements of H can then be written

$$\langle n | H | n \rangle = \tfrac{1}{2} U_a (N - n)^2 + \tfrac{1}{2} U_b (5 - h_1 + n)^2 \qquad (5.4.11a)$$

$$\langle n | H | n+1 \rangle = \beta [(h_1 - n)(n + 1)]^{\frac{1}{2}} = \langle n+1 | H | n \rangle \qquad (5.4.11b)$$

where the zero of energy is taken at the energy of the separate a and b atoms.

The chemisorption energy which is easily shown to be symmetric about N = 5 is equal to

$$\Delta E = -\langle H \rangle \qquad (5.4.12)$$

The problem is thus reduced to the diagonalisation of the set of matrices (5.4.11) of order $(h_1 + 1)$ for each value of h_1 $(0 \leq h_1 \leq 10)$. The lowest among the resulting set of eigenvalues is then equated to $-\Delta E$. The results which are shown in fig.3 show excellent agreement with the experimental curves for certain values of the parameters. In the Hubbard limit ($U_a = U_b = U$), almost triangular peaks at N = 5 are obtained for $U \geq 4\beta$, whereas in the Anderson limit ($U_a = U$, $U_b = 0$) the curves clearly exhibit parabolic maxima.

If ΔE at N = 5 is fitted to the experimental value of 9.3eV for Re on W(100) (Plummer and Rhodin 1968), it is found that the values of β and U obtained from this extrapollation are consistent with other estimates (e.g in the case $U = 6\beta$, we find a value of $\beta = 1.66$eV and a value of U = 9.95eV which are not far from the values estimated above).

Before going any further it proves of interest to consider two important limits to the exact solution which can be solved analytically.

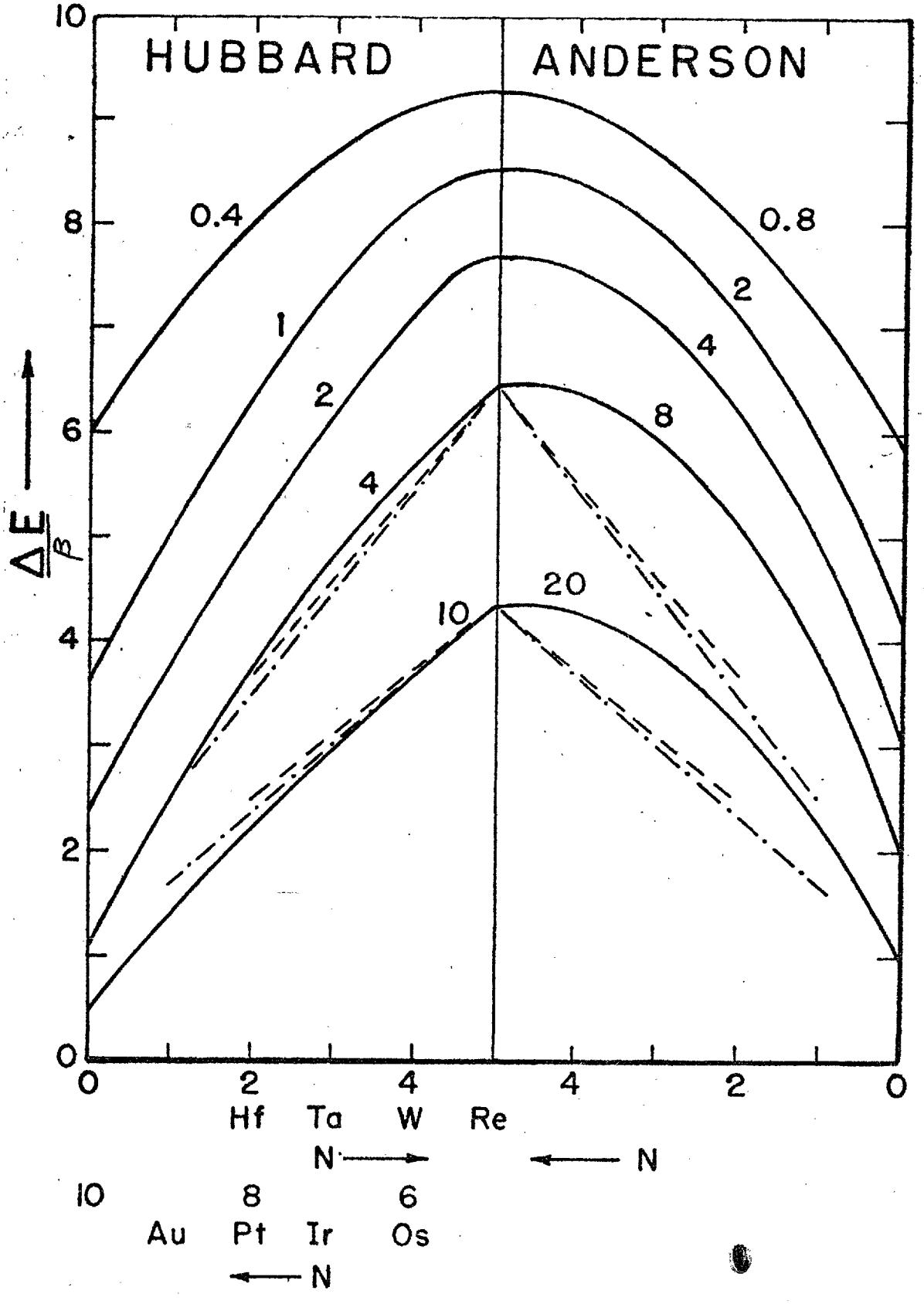


Fig.3 Curves are numbered by values of U/β

(i) The large U limit.

In this limit the basis set $\{|n\rangle\}$ is truncated, so that it consists of only 3 states, which are the neutral state $|N\rangle$, and the two single charge transfer states $|N-1\rangle$ and $|N+1\rangle$. The secular equation then reduces to the 3X3 determinant

$$\begin{vmatrix} -\epsilon + U & \beta\sqrt{6N} & 0 \\ \beta\sqrt{6N} & -\epsilon & \beta\sqrt{5(N+1)} \\ 0 & \beta\sqrt{5(N+1)} & -\epsilon + U \end{vmatrix} = 0 \qquad (5.4.13)$$

which eventually reduces to the quadratic equation

$$\epsilon(\epsilon - U) = \beta^2(11N + 5) \qquad (5.4.14)$$

Grimley and Thorpe have calculated ΔE using this approximation, they estimated that the neglect of multiple charge transfer states contributed at most to 8% of ΔE for large values of U ($U \geq 4\beta$). (Grimley and Thorpe 1972).

The physical interpretation of this approximation is that the Coulomb repulsion on the substrate and adsorbate atoms U_a and U_b, are large enough compared with the coupling β between these two atoms to prevent multiple charge transfer states having any significant amplitude in the ground state.

In the large U limit the smallest root of (5.4.14) may be approximated to $-\beta^2(11N + 5)/U$, so that ΔE is now given by

$$\Delta E = \frac{\beta^2}{U}(11N + 5) \qquad (5.4.15)$$

i.e ΔE varies linearly with N

(ii) The Hartree-Fock limit

The chemisorption problem now resembles that of a diatomic molecule. The wavefunction φ may be written as a linear combination of the orbitals of the adsorbate atom and the nearest neighbour substrate atom.

$$\varphi = a\varphi_a + b\varphi_b \tag{5.4.16}$$

where $|a|^2 = \langle n_a \rangle$, $|b|^2 = \langle n_b \rangle$. The secular equation reduces to the quadratic equation

$$(\epsilon - E_a)(\epsilon - E_b) = \beta^2 \tag{5.4.17}$$

where in the Hartree-Fock approximation, the energy levels are shifted to the positions

$$\left.\begin{aligned} E_a &= U[-(N - \tfrac{1}{2}) + 9\langle n_a \rangle] \\ E_b &= U[-4.5 + 9\langle n_b \rangle] \end{aligned}\right\} \tag{5.4.18}$$

Equation (5.4.17) has two solutions corresponding to the bonding (E_-) and antibonding (E_+) molecular orbitals, given by

$$E_{\pm} = \tfrac{1}{2}\left[E_a + E_b \pm ((E_a - E_b)^2 + 4\beta^2)^{\frac{1}{2}}\right] \tag{5.4.19}$$

We can now find the eigenvectors a and b corresponding to the bonding eigenvalue E_-, and hence deduce the occupancies $\langle n_a \rangle$ and $\langle n_b \rangle$, given by

$$\left.\begin{aligned} \langle n_a \rangle &= \tfrac{1}{2}\left[1 - \frac{E_b - E_a}{((E_b - E_a)^2 + 4\beta^2)^{\frac{1}{2}}}\right] \\ \langle n_b \rangle &= 1 - \langle n_a \rangle \end{aligned}\right\} \tag{5.4.20}$$

The adatom charge $\langle n_a \rangle$ is easily obtained from the self-consistent equations (5.4.18) and (5.4.20). It is found that for $U = 4\beta$, the difference $\Delta N = \langle N_a \rangle - N = 10\langle n_a \rangle - N$, is zero at $N = 5$ as expected, and is a maximum at $N = 0$ equal to 2.4. This value is extremely large (being in fact comparable to the zero correlation result which we shall consider in full detail later in the text).

The adatom charges obtained from the exact eigenvectors corresponding to the smallest eigenvalue of (5.4.11) are substantially smaller (Newns 1974) than the Hartree-Fock results.

The chemisorption energy is given by

$$\Delta E(N) = -E_a^{\,o} - E_b^{\,o} + 10E_{-} - 45U(\langle n_a \rangle^2 + \langle n_b \rangle^2) \qquad (5.4.21)$$

where $E_a^{\,o}$ and $E_b^{\,o}$ are the energies of the free a and b atoms respectively.

Again we expand $\Delta E(N)$ about $N = 5$, using the partial derivatives

$$\left.\frac{\partial \Delta E(N)}{\partial N}\right|_{N=5} = 0 \quad , \qquad \left.\frac{\partial^2 \Delta E(N)}{\partial N^2}\right|_{N=5} = U\left[10\frac{\partial \langle n_a \rangle}{\partial N} - 1\right] \qquad (5.4.22)$$

we find the self-consistent equations

$$\frac{\partial \langle n_a \rangle}{\partial N} = \frac{-2\beta^2}{((E_a - E_b)^2 + 4\beta^2)^{3/2}} \frac{d}{dN}(E_a - E_b) \qquad (5.4.23)$$

$$\frac{\partial (E_a - E_b)}{\partial N} = U\left[-1 + 18\frac{\partial \langle n_a \rangle}{\partial N}\right] \qquad (5.4.24)$$

at $N = 5$ we have $E_a = E_b$ and ΔE reduces to

$$\Delta E(5) = 10(\beta - U/4) \qquad (5.4.25)$$

Finally solving the self-consistent equations (5.4.23) and (5.4.24) at $N = 5$, we find

$$\left.\frac{\partial \langle n_a \rangle}{\partial N}\right|_{N=5} = \frac{1}{2}\,\frac{U}{2\beta + 9U} \qquad (5.4.26)$$

which replaced in (5.4.22) gives immediatly

$$\left.\frac{\partial^2 \Delta E(N)}{\partial N^2}\right|_{N=5} = -U\left(\frac{2\beta + 4U}{2\beta + 9U}\right) \qquad (5.4.27)$$

Hence the expansion for $\Delta E(N)$ about $N = 5$ gives us

$$\Delta E(N) = 10\left(\beta - \frac{U}{4}\right) - U\left(\frac{2U + \beta}{9U + 2\beta}\right)(N - 5)^2 \qquad (5.4.28)$$

which gives us once more the parabolic trend already observed in the virtual level description (eq (5.3.14)) in the small U limit. However unlike equation (5.3.14) it always reproduces a maximum at $N = 5$.

These two models (Newns 1970b, Grimley and Thorpe 1971b) have shown conclusively that the correlation effects play an important role in this problem. Although perhaps, the excellent agreement with experiment is rather fortuitus, depending on the choice of the two-atom Hamiltonian. It would thus prove of interest to consider the situation when we include the possibility of an extra substrate atom situated inside the metal, and this is the subject of the next chapter.

Chapter 6

THE THREE ATOM MODEL

6.1. The model

We showed in the previous chapter the importance of electron correlation effects in the problem of the chemisorption of 5d transition atoms on W. However the inclusion of correlation effects was possible only within the context of a greatly simplified model consisting of two atoms only; it would thus appear of interest to consider these effects within a more complex model taking some account of the band effects.

We do this by introducing the case of three atoms, one adsorbed atom a, taken to have a variable number N of 5d electrons, and two substrate atoms b and c both having M/2 5d electrons (M is the total number of spin-orbitals we take into consideration, in the practical case of the 5d series we have M = 10). (Muscat 1974)

The two atom Hubbard Hamiltonian introduced by Newns (1970b) (eq.(5.4.1)) is conveniently generalised to its present form

$$H = H_0 + H_1 \qquad (6.1.1)$$

where H_0 is the part of the Hamiltonian corresponding to the three free atoms

$$H_o = \sum_{\alpha} \left\{ \sum_{i=1}^{M} \epsilon_{\alpha} n_{\alpha i} + \tfrac{1}{2} U_{\alpha} \sum_{i,j} n_{\alpha i} n_{\alpha j} (1 - \delta_{ij}) \right\} \qquad (6.1.2)$$

where α denotes the atom $\alpha = a,b,c$, the index i refers to the atomic d spin-orbitals $|\alpha i\rangle$.

We showed in the previous chapter how on the basis of the simplifying assumption $I_{\alpha} = U_{\alpha}/2$, we can express the d-orbital self energies in the form

$$\left.\begin{aligned} \epsilon_a &= -U_a(N - \tfrac{1}{2}) \\ \epsilon_{\alpha} &= -\tfrac{1}{2}U_{\alpha}(M - 1) \qquad \alpha = b,c \end{aligned}\right\} \qquad (6.1.3)$$

The remaining term in (6.1.2) describes a Hubbard like intra-atomic electron-electron interaction.

The second term in the Hamiltonian (6.1.1) may be written

$$H_1 = \sum_{i=1}^{M} \beta_i (a_i^{+} b_i + b_i^{+} c_i + h.c) \qquad (6.1.4)$$

This represents the coupling between atoms a and b and atoms b and c, we notice that no hopping between a and c has been included, this is designed to represent the linear chain model we are using, where the adatom a interacts strongly with atom b which effectively represents the four nearest substrate atoms, upon which a is supposed to chemisorb in the pyramidal structure illustrated in fig.1 of chapter 5, and atom b interacts strongly with atom c.

β_i are the transfer integrals

$$\beta_i = \langle ai|H|bi\rangle = \langle bi|H|ci\rangle \qquad (6.1.5)$$

these being assumed equal. An estimate of these integral was given in chapter 5 for the various d-orbitals. We shall assume that the β_i's may be re-

placed by the average $\beta = \frac{1}{M}\sum_{i=1}^{M}\beta_i$.

6.2. Formal solution

The chemisorption energy $\Delta E_3(N)$ which is easily shown to be symmetric about M/2 is given by the expression

$$\Delta E_3(N) = -\langle H\rangle - \tfrac{1}{2}U_a N^2 - \tfrac{1}{4}U_b M^2 - \Delta E_2(M/2) \qquad (6.2.1)$$

where we have assumed that $U_b = U_c$, $\frac{1}{2}U_a N^2 + \frac{1}{4}U_b M^2$ represents the energy of the three separate atoms, and $\Delta E_2(M/2)$ is the binding energy of the two substrate atoms, i.e ΔE_2 is the chemisorption energy as calculated by Newns (1970b) for the two atom problem.

Let us introduce the number operator $N_i = \sum_{\alpha} n_{\alpha i}$, then N_i commutes with H. Now if ν_i are the eigenvalues of N_i and $|\psi_o\rangle$ the ground state of H, we make the following assumptions

$$\text{(i)} \quad N_i|\psi_o\rangle \neq 3|\psi_o\rangle$$
$$\text{(ii)} \quad N_i|\psi_o\rangle \neq 0 \qquad (6.2.2)$$

There are altogether M bonds which must be shared by M + N electrons, where N is an integer not greater than M/2 (we shall limit our discussion to the case $N \leq M/2$ since ΔE_3 is symmetric about M/2). Making the assumptions (6.2.2) implies that we exclude the possibility of completely full or completely empty bonds i. This is not too unreasonable since the singly and doubly occupied bonds are more stable, and thus more likely to occur.

Without loss of generality, we can assume that $\nu_i = 1$ for $0 < i \leq h_1$, $\nu_i = 2$

for $h_1 < i \leq M$, where h_1 and $h_2 = M - h_1$ represent the number of singly and doubly occupied bonds respectively.

The set of permutation operators $\hat{P}$ operating on the spin-orbital indices i also commutes with H. An eigenstate $|\psi\rangle$ of H will therefore be simultaneously an eigenstate of both the N_i and $\hat{P}$.

The Hamiltonian (6.1.1) may be split into two parts

$$H = H_n + H_m \tag{6.2.3}$$

where H_n corresponds to that part of the summation $i \leq h_1$ and H_m to $i > h_1$. An eigenstate $|\psi\rangle$ of H can in general be written in the form

$$\psi = \sum_{i,j} a_{ij} \psi_i^n \psi_j^m \tag{6.2.4}$$

where ψ_i^n, ψ_j^m are eigenstates of H_n and H_m respectively and a_{ij} are coefficients. We shall assume that the ground state of H, ψ_o transforms like the ground state of the two-atom Hamiltonian, i.e that

$$\hat{P}\psi_o = (-1)^p \psi_o \tag{6.2.5}$$

where p is the parity of the permutation $\hat{P}$.

This condition imposes a severe restriction on the allowed a_{ij}; an ansatz which we find to satisfy the condition is the simple form

$$\psi = \psi_o^n \psi_o^m \tag{6.2.6}$$

where

$$\left.\begin{aligned} \hat{P}_m \psi_o^m &= (-1)^{p_m} \psi_o^m \\ \hat{P}_n \psi_o^n &= (-1)^{p_n} \psi_o^n \end{aligned}\right\} \tag{6.2.7}$$

and

$$\hat{P} = \hat{P}_m \hat{P}_n \tag{6.2.8}$$

so that ψ_o^n and ψ_o^m have the same transformation properties as ψ_o with respect to permutations on the variables $i \leq h_1$ and $i > h_1$ respectively.

Let us consider H_n. For $i \leq h_1$ we can express the solution in terms of a complete set of eigenstates of H_n^o (where H_n^o represents the Hamiltonian H_n without the coupling term H_n^1). The states may be specified by the good quantum numbers of H_n^o: n_a and n_b, these represent the number of electrons present on atoms a and b respectively. n_a and n_b must be restricted by the condition $n_a + n_b \leq h_1$.

The normalised vectors can then be written

$$|n_a,n_b\rangle = (h_1!\, n_a!\, n_b!\,(h_1 - n_a - n_b)!)^{-\frac{1}{2}} \sum_{\hat{P}_n} (-1)^{P_n} \hat{P}_n$$

$$a_1^+ \ldots a_{n_a}^+ b_{n_a+1}^+ \ldots b_{n_a+n_b}^+ c_{n_a+n_b+1}^+ \ldots c_{h_1}^+ |0\rangle \tag{6.2.9}$$

where $|0\rangle$ is the vacuum state and the sum runs over the permutations on the variables $i=1,2\ldots.h_1$. The total number of these vectors is equal to the number of arrangements of n_a and n_b as restricted by the condition $n_a+n_b \leq h_1$ this number is equal to $\frac{1}{2}(h_1 + 1)(h_1 + 2)$.

For $i > h_1$, the solution is expressed in terms of the eigenstates of H_m^o, these are specified by two new numbers m_a and m_b, which now determine the number of holes on atoms a and b respectively. From similar considerations, we show that the normalised vectors $|m_a,m_b\rangle$ can be written

$$|m_a,m_b\rangle = (h_2!\, m_a!\, m_b!\,(h_2 - m_a - m_b)!)^{-\frac{1}{2}} \sum_{\hat{P}_m} (-1)^{P_m} \hat{P}_m$$

$$a_{h_1+1} \ldots a_{h_1+m_a} b_{h_1+m_a+1} \ldots b_{h_1+m_a+m_b} c_{h_1+m_a+m_b+1} \ldots c_M |F\rangle \tag{6.2.10}$$

where $|F\rangle$ represents the state with h_2 completely filled bonds. m_a and m_b are restricted in the range $m_a + m_b \leq h_2$, and the total number of these vectors is equal to $\frac{1}{2}(h_2 + 1)(h_2 + 2)$.

The eigenstates of H may now be expressed in terms of all possible products $|n_a,n_b,m_a,m_b\rangle$ of states (6.2.9) and (6.2.10) all these states transforming like (6.2.5).

The total number of these eigenstates in this representation is equal to $\frac{1}{4}(h_1 + 1)(h_1 + 2)(h_2 + 1)(h_2 + 2)$, which is a maximum equal to $\left[\frac{1}{8}(M+2)(M+4)\right]^2$ when $h_1 = h_2 = M/2$. This maximum is a rapidly increasing function of M, being equal to 441 when $M = 10$.

In order to write the matrix elements of $\langle H\rangle$, we must know how H transforms the vectors $|n_a,n_b,m_a,m_b\rangle$. For $i \leq h_1$, the Hamiltonian operates only on the vectors $|n_a,m_b\rangle$ leaving $|m_a,m_b\rangle$ unchanged. We have

$$\sum_{i=1}^{h_1} n_{\alpha i}|n_a,n_b\rangle = n_\alpha|n_a,n_b\rangle \qquad \alpha = a,b,c \qquad (6.2.11)$$

$$\sum_{i=1}^{h_1} (a_i^+ b_i + b_i^+ c_i + h.c)\,|n_a,n_b\rangle = \sqrt{(n_a+1)n_b}\,|n_a+1,n_b-1\rangle$$

$$+ \sqrt{n_a(n_b+1)}\,|n_a-1,n_b+1\rangle + \sqrt{n_c(n_b+1)}\,|n_a,n_b+1\rangle$$

$$+ \sqrt{n_b(n_c+1)}\,|n_a,n_b-1\rangle \qquad (6.2.12)$$

where $n_c = h_1 - n_a - n_b$.

But not all these vectors are defined, for instance if $n_b = 0$ or $n_b = h_1$ then the vectors $|n_a,n_b-1\rangle$ or $|n_a,n_b+1\rangle$ are not defined, if this is the case we put them equal to zero in (6.2.12).

For $i > h_1$, the Hamiltonian now operates on the vectors $|m_a,m_b\rangle$ keeping $|n_a,n_b\rangle$ unchanged. In this case we find

$$\sum_{i=h_1+1}^{M} n_{\alpha i}|m_a,m_b\rangle = (h_2 - m_\alpha)|m_a,m_b\rangle \qquad \alpha = a,b,c \qquad (6.2.13)$$

$$\sum_{i=h_1+1}^{M} (a_i^{+}b_i + b_i^{+}c_i + h.c)|m_a,m_b\rangle = \sqrt{(m_a+1)m_b}\,|m_a+1,m_b-1\rangle$$

$$+ \sqrt{m_a(m_b+1)}\,|m_a-1,m_b+1\rangle + \sqrt{m_c(m_b+1)}\,|m_a,m_b+1\rangle$$

$$+ \sqrt{(m_c+1)m_b}\,|m_a,m_b-1\rangle \qquad (6.2.14)$$

where $m_c = h_2 - m_a - m_b$, and any vector which is not defined is put equal to zero in (6.2.14).

The matrix elements of $\langle H\rangle$ can now be written, the diagonal elements are given by

$$\langle n_a,n_b,m_a,m_b|H|n_a,n_b,m_a,m_b\rangle = \tfrac{1}{2}U_a(n_a + h_2 - m_a - N)^2$$

$$+ \tfrac{1}{2}U_b\,(n_b + h_2 - m_b - M/2)^2 + (h_1-n_a-n_b+m_a+m_b-M/2)^2 \qquad (6.2.15a)$$

where we have taken the energy of the three separate atoms $\sum E_\alpha^{\,o}$ to be zero.

The non-diagonal elements are

$$\langle m_a,n_b|H|n_a+1,n_b-1\rangle = \beta\sqrt{n_b(n_a+1)} = \langle n_a+1,n_b-1|H|n_a,n_b\rangle \qquad (6.2.15b)$$

$$\langle n_a,n_b|H|n_a,n_b-1\rangle = \beta\sqrt{(n_c+1)n_b} = \langle n_a,n_b-1|H|n_a,n_b\rangle \qquad (6.2.15c)$$

$$\langle m_a,m_b|H|m_a+1,m_b-1\rangle = \beta\sqrt{m_b(m_a+1)} = \langle m_a+1,m_b-1|H|m_a,m_b\rangle \qquad (6.2.15d)$$

and

$$\langle m_a,m_b|H|m_a,m_b-1\rangle = \beta\sqrt{(m_c+1)m_b} = \langle m_a,m_b-1|H|m_a,m_b\rangle \qquad (6.2.15e)$$

Equations (6.2.15) define the matrix completely. The diagonalisation of the set of matrices must now be performed, the lowest amongst the set of eigenvalues being equated to $-\Delta E_3(N) - \Delta E_2(M/2)$, a knowledge of $\Delta E_2(M/2)$ now

gives us the chemisorption energy $\Delta E_3(N)$. $\Delta E_2(M/2)$ is obtained by solving the Hamiltonian (5.4.1) for the case of M bonds, this means diagonalising matrices of order M + 1, similar to those defined by equations (5.4.11). The matrices (5.4.11) being in fact for the special case M = 10.

The diagonalisation of the matrices (6.2.15) must now be performed numerically. This proves to be a very time consuming procedure, and in order to give a detailed anlysis of the problem for many values of the parameters, we must confine ourselves to the study of the special case M = 6. We then attempt to generalise the results to the more interesting cases M = 8 and M = 10. For each value of N, the diagonalisation was performed for various values of h_1 and h_2, and the lowest amongst the set of eigenvalues was then selected.

As seen from equations (6.2.15) the matrices are symmetric. We first reduce them to tridiagonal form using the Householder method (Wilkinson 1965). The method states that if A_r is defined as the matrix resulting from r transformations, then A_r is given in terms of A_{r-1} by the relation

$$A_r = P_r A_{r-1} P_r \qquad (6.2.16)$$

$$A_o = A \text{ (the original nxn matrix)}$$

where

$$P_r = I - \underline{u}_r \underline{u}_r^T / 2K_r^2 \qquad (6.2.17)$$

$\underline{u}_r$ is the column vector whose elements are defined by

$$\left.\begin{aligned} \underline{u}_r &= (u_{ir}) \quad , \quad u_{ir} = 0 \quad , \quad i = 1,2,\ldots.r \\ u_{r+1,r} &= a_{r,r+1} \mp S_r \quad , \quad u_{ir} = a_{ri} \quad , \quad i = r+2,\ldots.n \end{aligned}\right\} (6.2.18)$$

S_r is the sum

$$S_r = \left(\sum_{i=r+1}^{n} a_{ri}^2 \right)^{\frac{1}{2}} \qquad (6.2.19)$$

and

$$2K_r^2 = S_r^2 \mp a_{r,r+1} S_r \qquad (6.2.20)$$

The sign associated with S_r in (6.2.18) and (6.2.20) is taken to be that of $a_{r,r+1}$, so that cancellation cannot occur in the summation.

The effect of the r^{th} transformation is to eliminate all the elements of row r except $a_{r,r-1}$, $a_{r,r}$ and $a_{r,r+1}$. After $n - 2$ such reductions, the matrix becomes tridiagonal. Let its elements be denoted by $\alpha_i = a_{ii}^{n-2}$, $\beta_i = a_{i,i+1}^{n-2}$, them in order to obtain the eigenvalues, we need to find the roots of $\det(A^{n-2} - \lambda I) = 0$. This is done by constructing the Sturm sequence

$$\left.\begin{aligned} p_o(\lambda) &= 1 \\ p_1(\lambda) &= \alpha_1 - \lambda \\ p_i(\lambda) &= (\alpha_i - \lambda) p_{i-1}(\lambda) - \beta_i^2 p_{i-2}(\lambda) \quad , \quad i = 2,\ldots.n \end{aligned}\right\} \qquad (6.2.21)$$

The zeroes of $p_n(\lambda)$ are the eigenvalues of A. The determination of the roots is simplified considerably if we make use of the property of the Sturm sequence that the zeroes of $p_r(\lambda)$ must separate those of $p_{r+1}(\lambda)$ (e.g see Wilkinson 1965) at least in the weak sense. We are interested in the smallest eigenvalue here, so that the problem is further simplified. Starting from $\lambda_1 = \alpha_1$, we fimd the root λ_2 of $p_2(\lambda) = 0$ which is smaller than or equal to λ_1, the root λ_3 of $p_3(\lambda) = 0$ which is smaller than or equal to λ_2, and so om until we find the root λ_n of $p_n(\lambda) = 0$ which must satisfy the inequality

$$\lambda_n \leq \lambda_{n-1} \leq \ldots\ldots\ldots\ldots \leq \lambda_1 \qquad (6.2.22)$$

A knowledge of the eigenvector corresponding to the lowest eigenvalue enables us to determine the amounts of charge present on the atoms. These are given by

$$\left.\begin{aligned} \langle N_\alpha \rangle &= \sum_k |X_k|^2 \, (h_2 - m_\alpha + n_\alpha) \qquad \alpha = a,b \\ \langle N_c \rangle &= \sum_k |X_k|^2 \, (m_a + m_b + h_1 - n_a - n_b) \end{aligned}\right\} \qquad (6.2.23)$$

where the summation is over all the combinations on the numbers (n_a, n_b, m_a, m_b) and X_k is the k^{th} component of the eigenvector corresponding to the smallest eigenvalue.

The determination of the eigenvector $\underline{X}$ is straightforward, if λ_n is the smallest eigenvalue of A, then $\underline{X}$ is given by

$$(A - \lambda_n I)\,\underline{X} = 0 \qquad (6.2.24)$$

subject to the normalisation condition

$$\underline{X} \cdot \underline{X}^T = 1 \qquad (6.2.25)$$

The numerical procedure is straightforward, A must be transformed to upper triangular form, and the various X_k can then be simply read off.

6.3. Results and discussion

The Hamiltonian H was solved in the case of six bonds, for many values of

interaction parameters U_a and U_b. The main difference between these results and those obtained in a two atom calculation is the magnitude of ΔE at the maximum, in fact it was found that in general $\Delta E_3(M/2) \lesssim \frac{1}{2}\Delta E_2(M/2)$. This drop in magnitude is not totally unexpected, a simple verification of this phenomenom is provided by the study of the limiting case where no correlation is included ($U_\alpha = 0$). Then the bonds are independent of one another and ΔE is equal to the product of the energy of a single bond times the number of bonds. In the two atom case the energy of a single bond is equal to $-\lambda_2$, where λ_2 is the smallest eigenvalue of the matrix

$$A_2 = \beta \begin{pmatrix} 0 & 1 \\ 1 & 0 \end{pmatrix} , \qquad (6.3.1)$$

so that $\Delta E_2(N) = M\beta$, $N = 0,1,.....M/2$.

In the three atom case, the energy of a single bond is equal to $-\lambda_3 + \lambda_2$, where λ_3 is the smallest eigenvalue of the matrix A_3

$$A_3 = \beta \begin{pmatrix} 0 & 1 & 0 \\ 1 & 0 & 1 \\ 0 & 1 & 0 \end{pmatrix} \qquad (6.3.2)$$

so that $\Delta E_3(N) = M\beta(\sqrt{2} - 1)$, $N = 0,1,....M/2$.

We thus notice that in this case $\Delta E_3 < \frac{1}{2}\Delta E_2$. If the number of atoms taken into consideration in the calculation is increased, it is found that the energy of a single bond is an osscillatory function of the number of atoms (e.g $\Delta E_4(N) \simeq .83M\beta$, $\Delta E_5(N) \simeq .5M\beta$) converging to $2/\pi$ (the result obtained for an infinite number of atoms in a linear chain) (e.g see Newns 1969).

The limit of no correlation is an important one, since the chemisorption energy with $U > 0$ should be smaller than the chemisorption energy with $U = 0$. This means that $\Delta E_3(M/2) < M\beta(\sqrt{2} - 1)$ for all non-zero values of U_a and U_b. If we now take $M = 10$, and equate this maximum value to the experimental value for the chemisorption energy of 9.3eV (Plummer and Rhodin 1968) for Re/W(100), we obtain very large values of the parameter β ($\beta > 2.3$eV)

as compared to the values estimated from band structure above. And as a consequence of this, the values of U as estimated from the extrapolation to the experimental value are much too great.

It would thus seem that the case of three atoms is a rather unfavourable case to consider, just as perhaps the surface molecule results (Newns 1970b, Grimley and Thorpe 1971b) are too favourable.

Apart from the magnitude of ΔE at the maximum, we notice similarities between our results and those obtained from a two atom Hamiltonian.

The qualitative variations observed by Newns (1970b) are still present in our model. For instance, keeping $\frac{1}{2}(U_a + U_b)$ constant, we notice that the triangular peak at M/2 is reproduced for a Hubbard like Hamiltonian ($U_a = U_b = U$) at large values of U, while the maximum is clearly parabolic in the Anderson limit ($U_b = 0$, $U_a = U$), we also notice that the values of ΔE at a given value of $\frac{1}{2}(U_a + U_b)$ are much smaller in the Anderson limit than in the Hubbard limit (see fig.1a).

If we now assume that $U_a = U_b$ (the Hubbard limit), we see that the maximum at M/2 is parabolic for small values of U (e.g $U = .4\beta$), while the peak is triangular in the large U limit (e.g $U = 10\beta$) (see fig 1b).

These results for ΔE are in agreement with the findings of Newns (1970b) that the Hubbard Hamiltonian is more successful in reproducing the qualitative trend in the experiments at large values of U, than the Anderson model, i.e that the correlation effects play an important role in this problem.

These results are corroborated by those obtained in the case M=4. (see fig.2).

This approach was extended to the problem of 8 bonds, we remark the same qualitative behaviour in the results for ΔE as shown in fig.3(the results for the case of four bonds are also plotted). The curves are similar in shape, in fact they look parallel.

If N is kept constant, it is found that ΔE varies linearly with the number of bonds M, at constant U/β. While if N is taken equal to M/2, ΔE is then found to increase parabolically with M (see fig.4). These results are

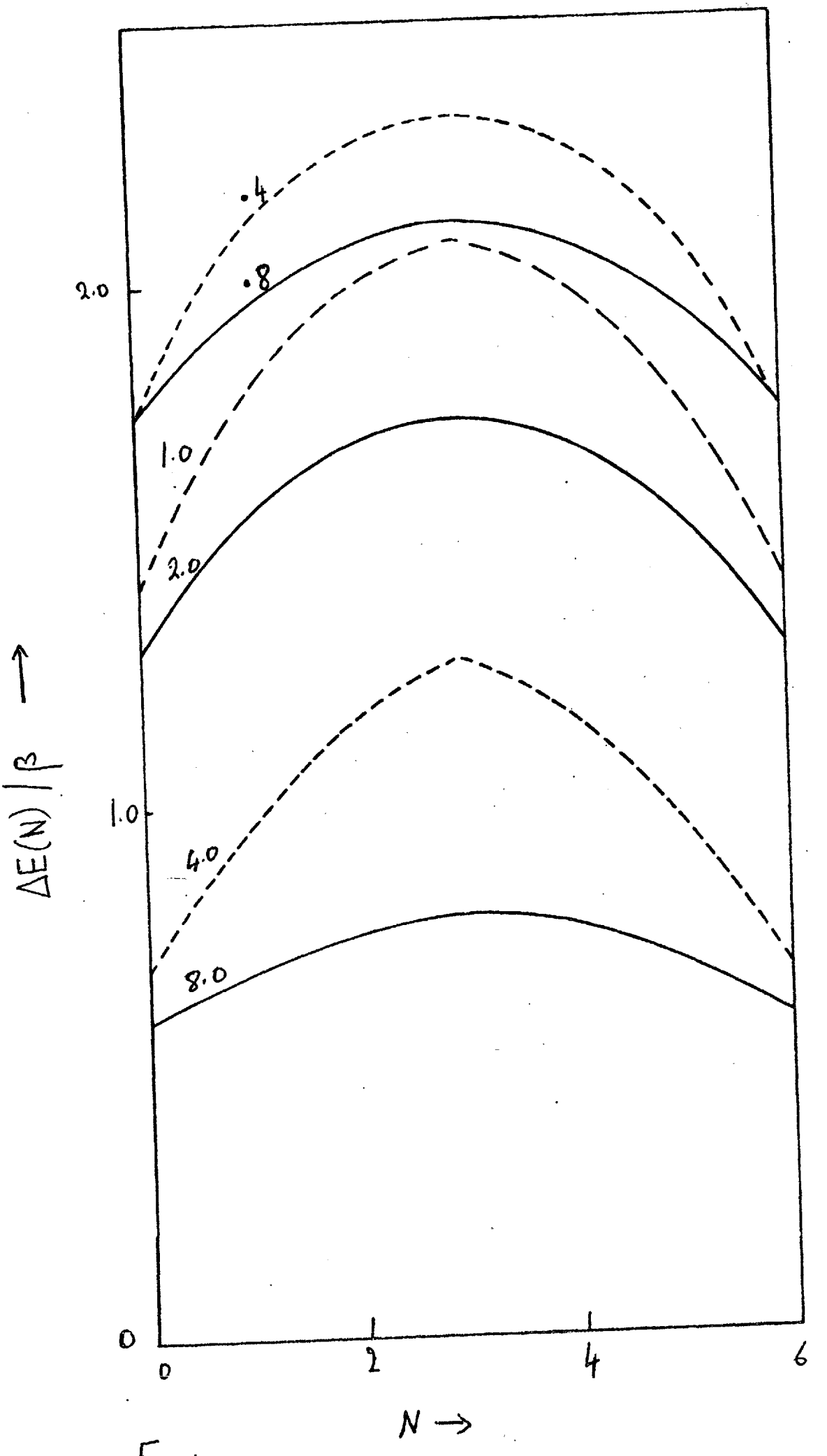


Fig.1a

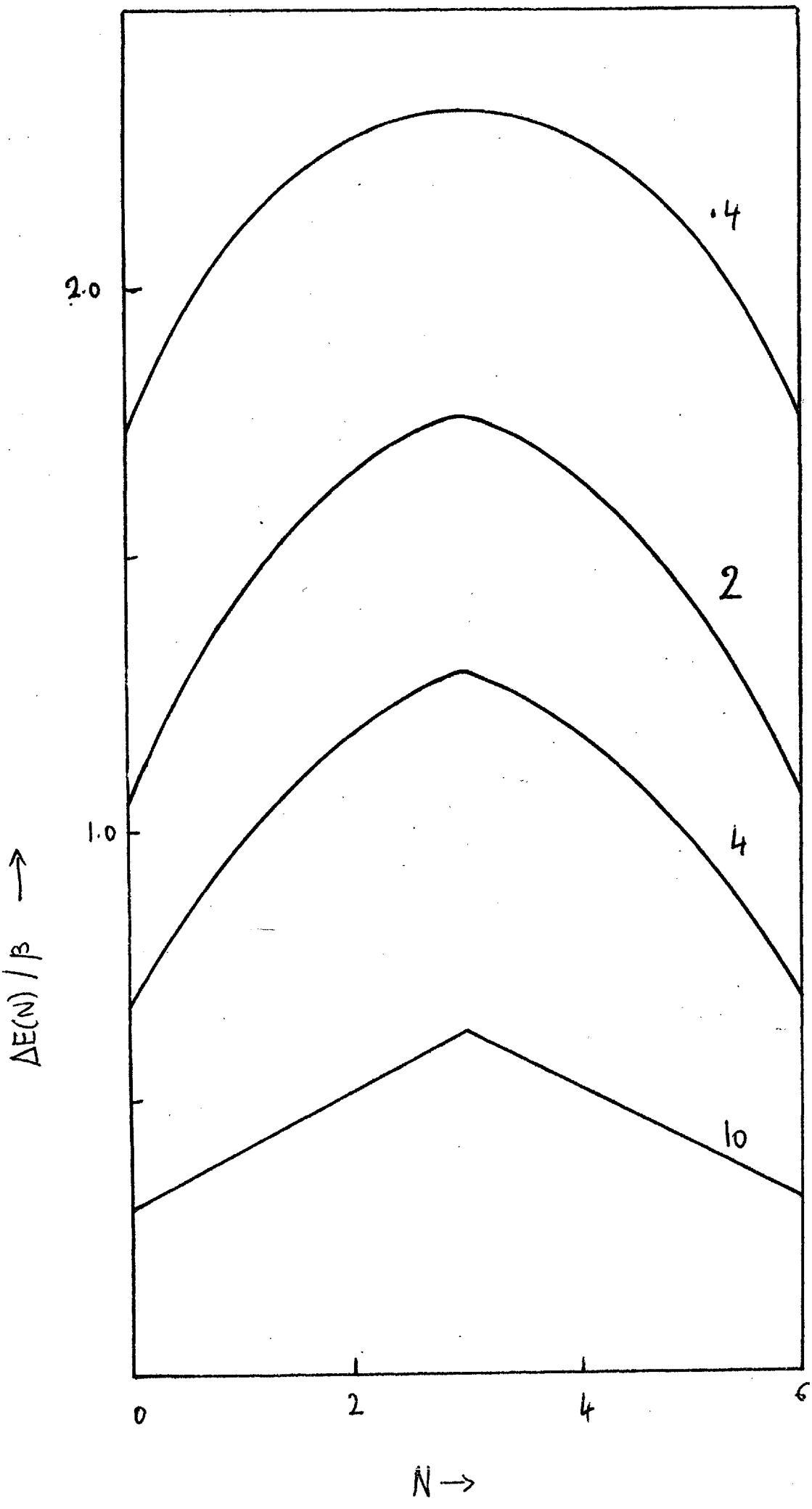


Fig. 1b

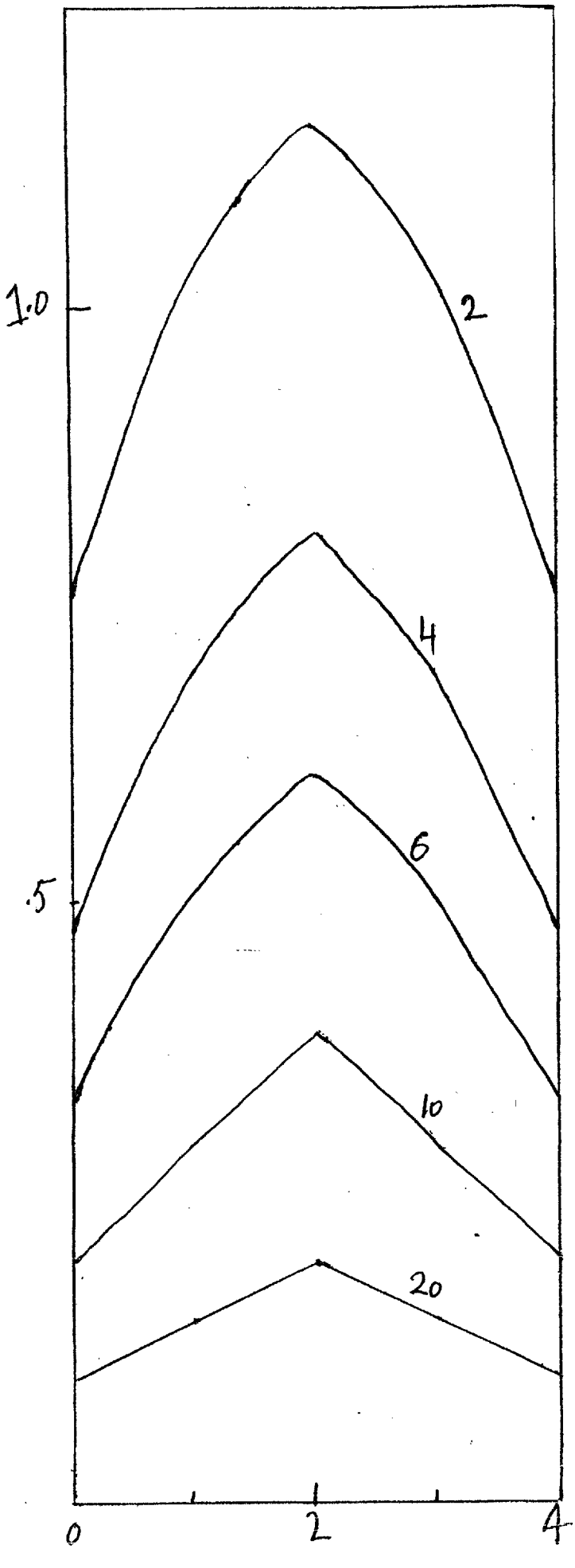


Fig.2

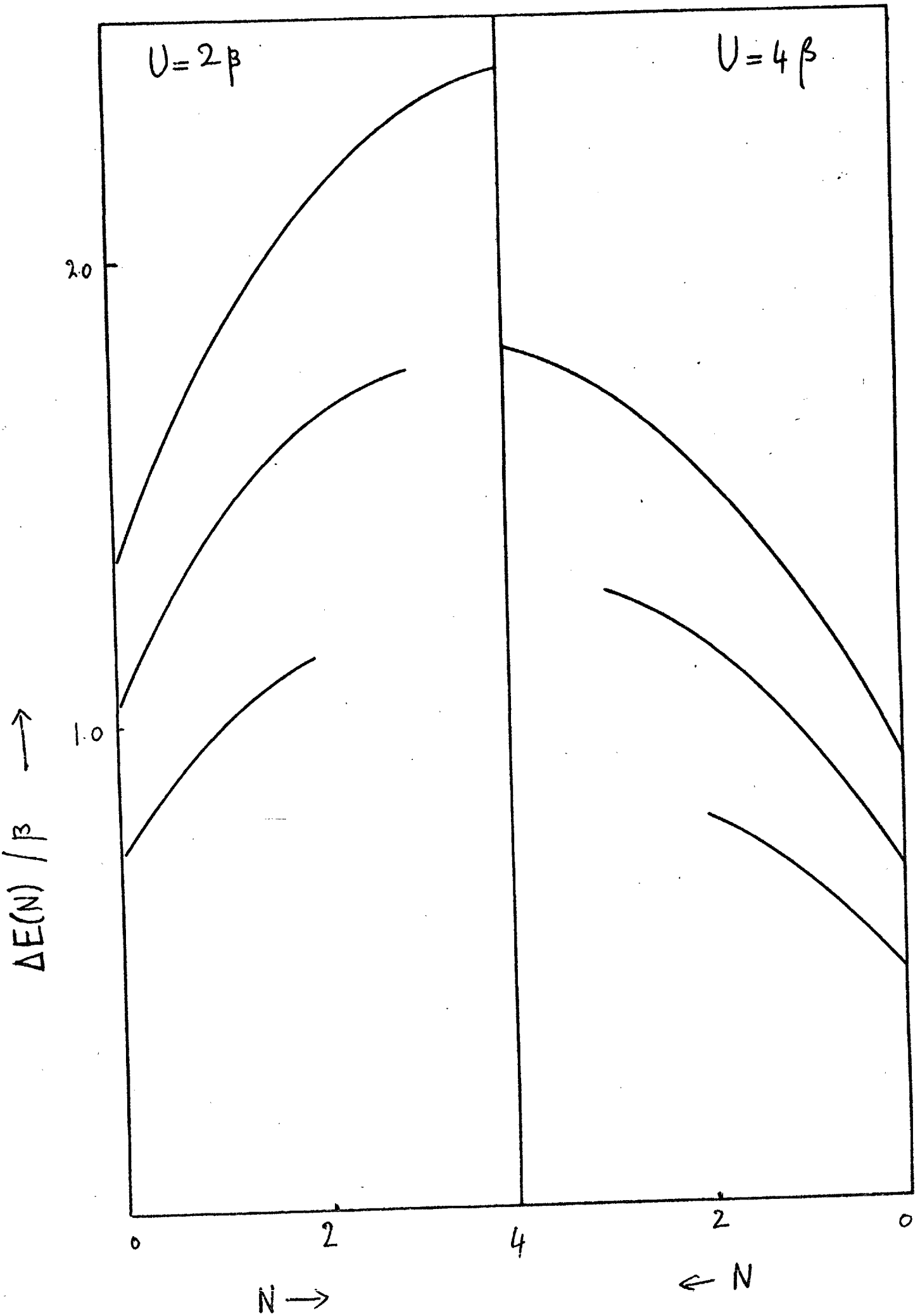


Fig. 3

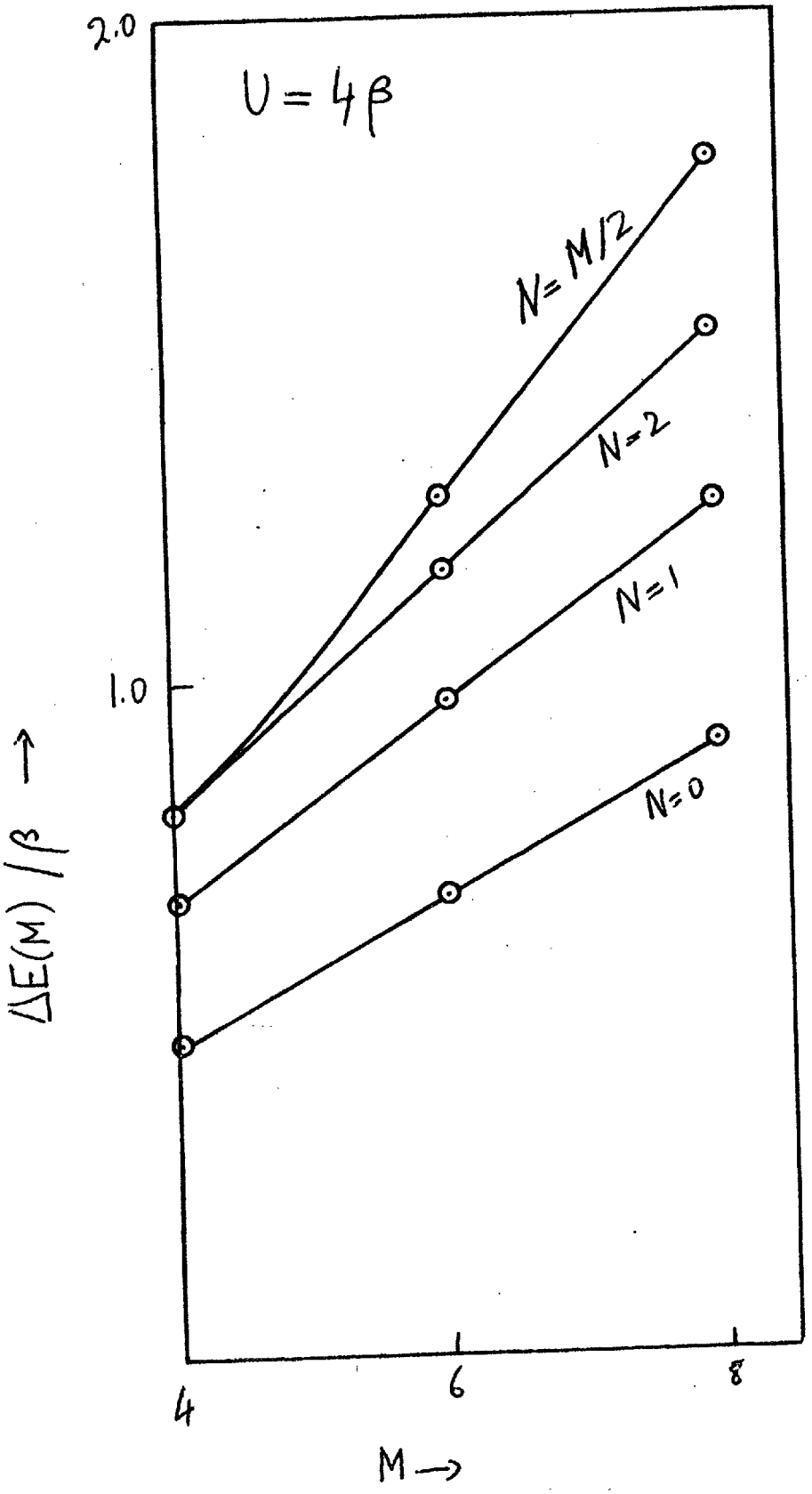


Fig.4

im qualitative agreement with Newns' perturbation theory results, equation (5.4.15) which becomes for a general M

$$\frac{\Delta E}{\beta} = \frac{\beta}{U}\left[(M+1)N + M/2\right] \qquad (6.3.3)$$

The variations of ΔE with M may be used to predict the curves of ΔE vs N for the case M = 10. These predicted curves are similar in shape to those obtained in the cases M = 6 and M = 8.

We now turn to the charges on the atoms. These are given by expressions (6.2.23), the results are plotted for the cases M = 4 (fig.5a) and M = 6 (fig.5b). Again it proves of interest to consider the simple problem of zero correlation.

In the two-atom case, the eigenvector corresponding to the smallest eigenvalue of (6.3.1) is given by the relations

$$\begin{pmatrix} 1 & 1 \\ 1 & 1 \end{pmatrix} \begin{pmatrix} x_1 \\ x_2 \end{pmatrix} = 0 \qquad (6.3.4)$$

together with the normalisation condition

$$x_1^2 + x_2^2 = 1 \qquad (6.3.5)$$

$\underline{x}$ is thus given by $\underline{x} = (1/\sqrt{2}, -1/\sqrt{2})$.

Now in the two atom case there are M bonds to be shared by M/2 + N electroms, and $N \leq M/2$, consequently according to the assumption (5.4.10) we have M/2 + N singly occupied bonds, and M/2 - N empty bonds. The charges on atoms a and b are then easily shown to be equal to

$$\langle N_a \rangle = \langle N_b \rangle = \tfrac{1}{2}(M/2 + N) , \qquad (6.3.6)$$

the charge transfer on the adatom $\Delta N = \langle N \rangle_a - N$, is a linear function of N

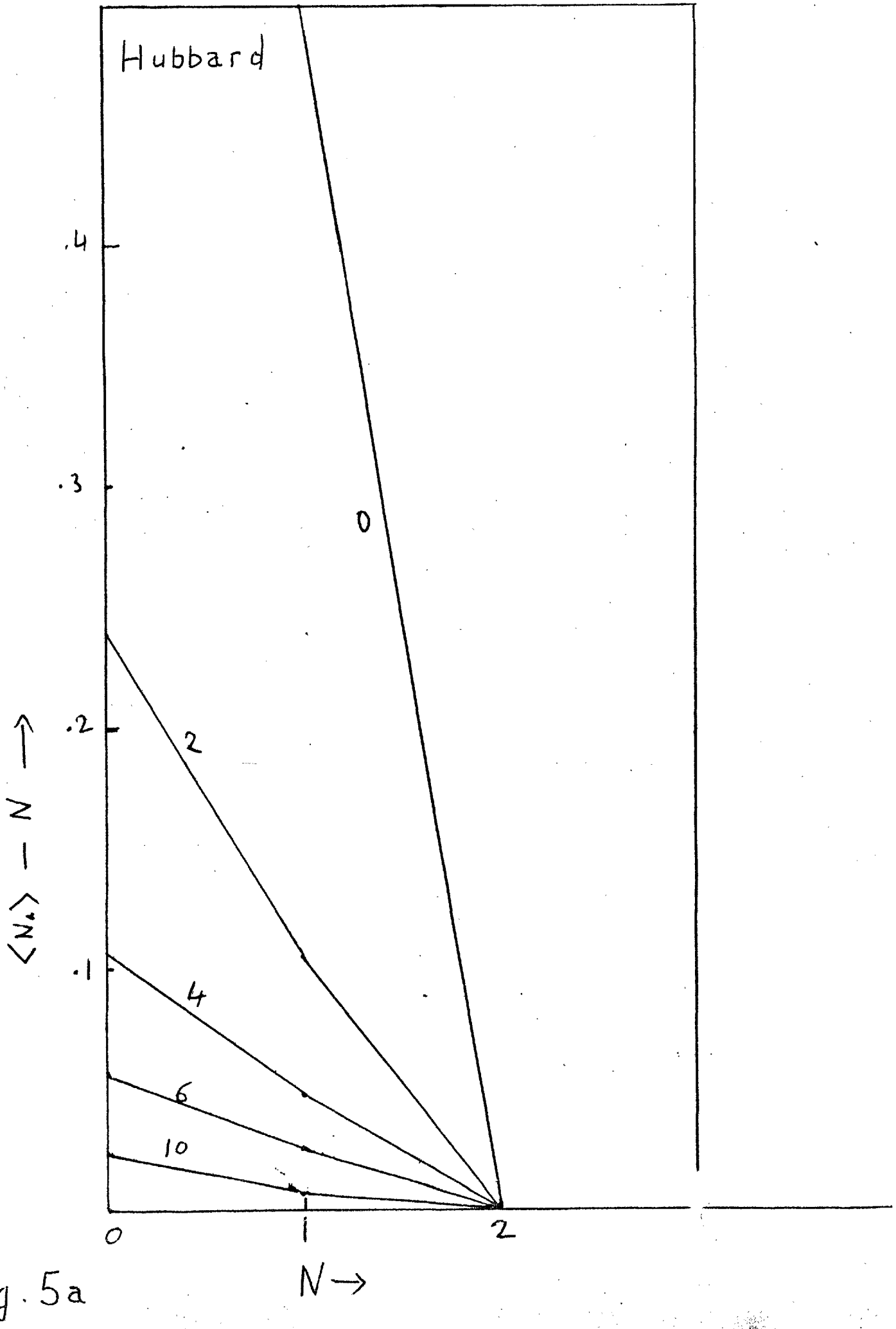

Hubbard
.4
.3
.2
.1
0
2
4
6
10
$\langle N_\downarrow \rangle - N \uparrow$
0
1
2
N→

Fig. 5a

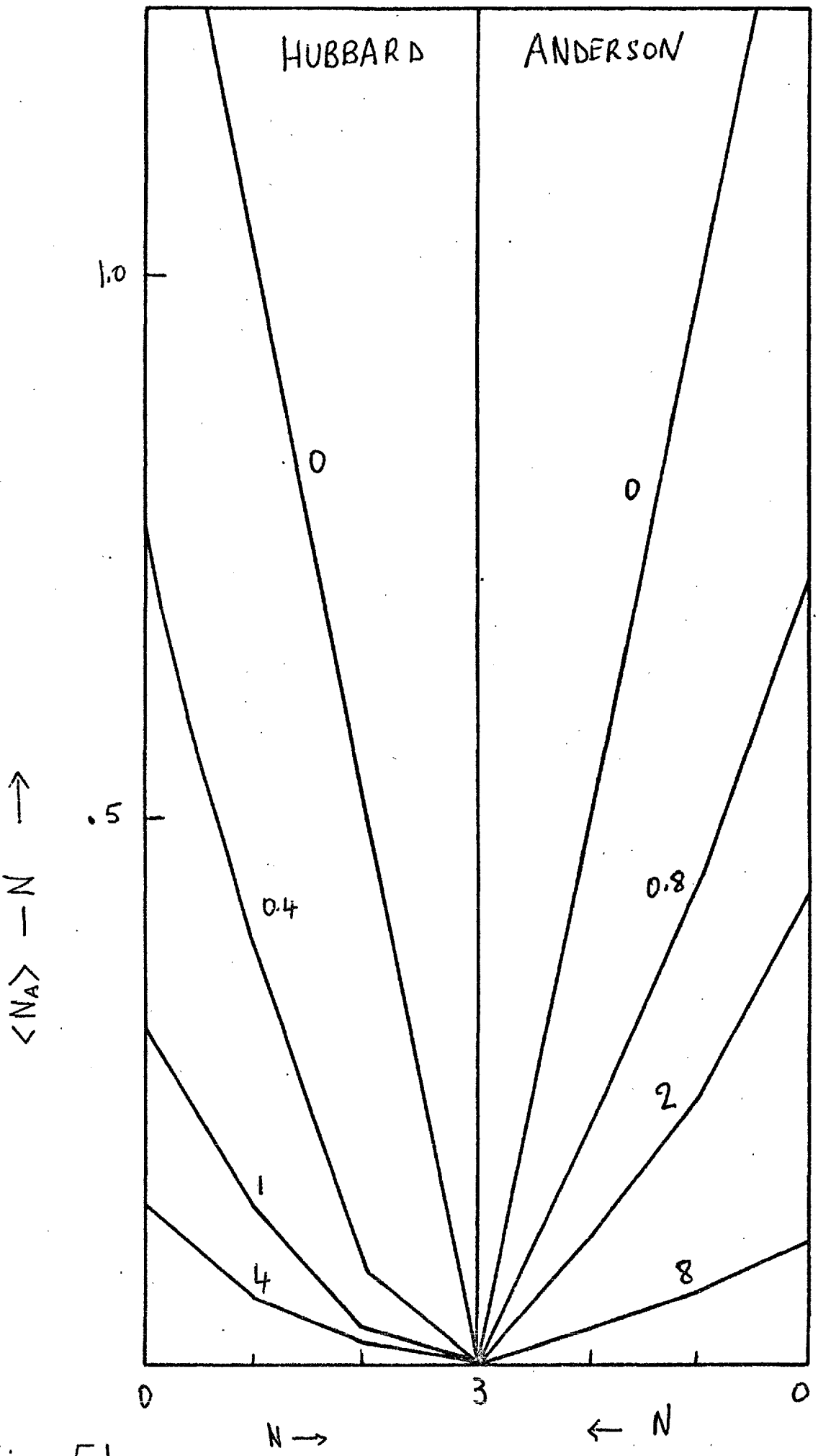


Fig. 5b

Fig 5

decreasing with N. For an increase in N of 1 ΔN decreases by $\frac{1}{2}$.

In the three atom case, the eigenvector corresponding to the smallest eigenvalue of (6.3.2) is given by

$$\underline{x} = (1/2, -1/\sqrt{2}, 1/2) \tag{6.3.7}$$

Now, there are M bonds to be shared by M + N electrons, consequently according to the assumptions (6.2.2), there will be (M - N) singly occupied bonds and N doubly occupied bonds. The charges on atoms a,b and c are then easily shown to be equal to

$$\left.\begin{aligned} \langle N_\alpha \rangle &= (M - N)(\tfrac{1}{2})^2 + N\left[(\tfrac{1}{\sqrt{2}})^2 + (\tfrac{1}{2})^2\right] = \tfrac{1}{4}M + \tfrac{1}{2}N \quad \alpha = a,c \\ N_b &= (M - N)(\tfrac{1}{\sqrt{2}})^2 + N\left[(\tfrac{1}{2})^2 + (\tfrac{1}{2})^2\right] = \tfrac{1}{2}M \end{aligned}\right\} \tag{6.3.8}$$

We notice from (6.3.8) that the charge on atom b remains constant as N is allowed to vary, and that the charge transfer on the adatom varies linearly with N

$$\Delta N = \langle N_a \rangle - N = \tfrac{1}{4}M - \tfrac{1}{2}N \tag{6.3.9}$$

i.e the same linear variation found in the two atom problem.

It is significant that whereas in the case of the chemisorption energy some disparity exists at U = 0 in the values of ΔE between the 2 and 3 atom cases, which is reflected in the results at $U \neq 0$, in the case of the adatom charges, we obtain the same results at U = 0 for the 2 and 3 atom problems which is also reflected in the results at $U \neq 0$. In fact our results are in excellent quantitative agreement with those obtained in a two atom calculation (Newns 1974).

The results for ΔN which are plotted in fig.5 show that ΔN is very small in the large U limit, so that in this limit adsorption is nearly neu-

tral and any violation of the Friedel sum rule does not appear too serious (Grimley 1973).In the small U limit, the adatom charges are larger but still sufficiently small compared to results from other investigations to justify the use of the model.

Let us finish by saying a few words about the results. The results for the chemisorption energy are rather disappointing, however the qualitative trend observed here is similar to that obtained by Newns (1970b) in a two atom calculation, and we thus conclude by again remarking the importance of electron correlation both on the substrate atoms and the adsorbed atom. However we note that the excellent agreement with experiment obtained with the use of the surface molecule approximation should not be taken too seriously, and that the problem is far more complex than it was at first believed to be.

In this thesis we have studied two particular problems in chemisorption theory, and we have shown how the physical nature of the system considered enables us to solve the problem within a given set of approximations, and how these same approximations break down when applied to another problem. The chemisorption systems we have considered here are two of many in this vast field, and the diversity of techniques encountered here shows not only the difficulty but also the great interest that are inherent in theories of chemisorption.

References

Alexander S. and Anderson P.W.1964, Phys.Rev. 133, A1594

Allam G. and Lemglart P. 1970, J.Phys(Paris).Suppl.Fasc. 4, C1.93

Anderson P.W. 1961, Phys.Rev. 124, 41

Baker J.M. and Eastman D.E. 1973, J.Vac.Sci.Technol. 10, 223

Bassett D.W. and Parsley M.J. 1970, J.Phys.D. 3, 707

Beck D.E. and Celli V. 1970, Phys.Rev. B2, 2955

Becker J.A. 1926, Phys.Rev. 28, 241

Becker G.E. and Hagstrum H.D. 1973, J.Vac.Sci.Technol. 10, 31

Bennett A.J. 1968, J.Chem.Phys. 49, 1340

Bennett A.J. and Falicov L.M. 1966, Phys.Rev. 151, 512

Blandin A. 1968, J.Appl.Phys.39, 1285

Brundle C.R. 1974, J.Vac.Sci.Technol. 11, 212

Chang C.C. 1971, Surf.Sci. 25, 53

Chen J.M. and P pageorgopoulos C.A. 1972, Sol.State.Comm. 11, 999

Condon E.U. and Shortley G.H. 1935, "The Theory of Atomic Spectra". C.U.P.

Cyrot-Lackmann F. 1970, J.Phys(Paris) Suppl.Fasc. 4, C1.67

Cyrot-Lackmann F. and Ducastelle F. 1971, Phys.Rev. B4, 2406

Dobson P.J. 1974, private communication

Desplat 1974, Proc.of the Int.Conf.on surf. (Kyoto,Japan)

Duke C.B. 1973, Lecture notes. Varenna Summer School.

Eastman D.E. and Cashion J.K. 1971, Phys.Rev.Lett. 27, 1520

Edwards D.M. and Newns D.M. 1967, Phys.Lett. 24A, 236

Fehrs D.L. and Mackrakis M.S. 1970, Bull.Am.Phys.Soc. 15, 391

Fehrs D.L. and Stickney R.E. 1971, Surf.Sci. 24, 309

Fletcher G.C. and Wohlfarth E.P. 1951, Phil.Mag. 42, 106

Friedel J. 1958, Nuovo Cimento Suppl. 7, 287

Friedel J. 1969, "The Physics of Metals" ed J.M. Ziman C.U.P.

Gadzuk J.W. 1967, Surf.Sci. 6, 133

" " 1974, to be published in "Surface Physics of Crystalline Materials" Academic Press J.M. Blakely ed.

Gadzuk J.W., Hartman J.K. and Rhodin T.N. 1971, Phys.Rev. B4, 241

Gadzuk J.W. and Plummer E.W. 1971, Phys.Rev. B3, 2125

" " " " 1973, Rev.Mod.Phys. 45, 487

Gavrilyuk V.M.,Naumovets A.G. and Fedorus A.G. 1966, Zh.Eksperim.i.Teor.Fiz. 51, 1332 (translation Sov.Phys.JETP, 24, 899, 1967)

Gerlach R.L. and Rhodin T.N. 1969, Surf.Sci. 17, 32

Girvan R.F., Gold A.V. and Phillips R.A. 1968, J.Phys.Chem.Sol. 29, 1485

Gomer R. 1974, Preprint

Gomer R. and Swanson L.W. 1963, J.Chem.Phys. 38, 1613

Grimley T.B. 1967a, Proc.Phys.Soc. 90, 751

" " 1967b, Proc.Phys.Soc. 92, 776

" " 1970a, J.Phys.C 3, 1934

" " 1970b, J.Phys(Paris) Suppl.Fasc. 4, C1.85

" " 1971a, J.Vac.Sci.Technol. 8, 31

" " 1971b, Ber.Bunsenges.Phys.Chem. 75, 1003

" " 1973, Lecture notes Varenna Summer School

Grimley T.B. and Thorpe B.J. 1971a, J.Phys.F.Lett. 1, L4

" " " " 1971b, Phys.Lett. 37A, 459

" " " " 1972, J.Phys.C.Lett, 5, L70

Gurney R.W. 1935, Phys.Rev. 47, 479

Gyftopoulos E.P. and Levine J.D. 1962, J.Appl.Phys. 33, 67

Hagstrum H.D. 1966, Phys.Rev. 150, 495

Hagstrum H.D. and Becker G.E. 1969, Phys.Rev.Lett. 22, 1054

Hayward D.O. and Trapnell B.M.W. 1964, "Chemisorption" Butterworths Scientific Publications Ltd. London

Hewson A.C. 1966, Phys.Rev. 144, 420

Hewson A.C. and Newns D.M. 1974, Proc. of the Int.Conf. on Surf. (Kyoto,Japan)

Hohenberg P. and Kohn W. 1964, Phys.Rev. 136, B864

Hubbard J. 1963, Proc.Roy.Soc.(London), A276, 238

Ives H.E. 1924, Astrophys.J. 60, 209

Kohn W. and Sham L.J. 1965, Phys.Rev.140, A1133

Kubo R. 1957, J.Phys.Soc.(Japan), 12, 570

Lang N.D. 1972, Phys.Rev. B4, 4234

Langmuir I. 1933, J.Chem.Phys. 1,3

Langmuir I. and Kingdon K.H. 1925, Proc.Roy.Soc.(London), A107, 61

McRae A.U., Muller K., Lander J.J. and Morrison J. 1969, Surf.Sci. 15, 483

Mattheiss L.F. 1965, Phys.Rev. 139, A1893

Messiah A. 1965, "Quantum Mechanics" (North Holland-Amsterdam) vol. II, chapter XIX, p 819

Moriya T. 1966, Proc.Int.School.Phys. "Enrico Fermi" couse 37, p 206, Academic Press

Mott N.F. and Jones H. 1936, "The Theory of the Properties of Metals and Alloys" O.U.P

Müller E.W. 1967, Ann.Rev.Phys.Chem. 18, 35

" " 1973, Lecture notes Varenna Summer School

Muscat J.P. 1974, submitted to J.Phys.C

Muscat J.P. and Newns D.M. 1972, Sol.State.Comm. 11, 737

" " " " 1974, J.Phys.C.

Newns D.M. 1969a, J.Chem.Phys. 50, 4572

" " 1969b, Phys.Rev. 178, 1123

" " 1970a, Phys.Lett. 33A, 43

" " 1970b, Phys.Rev.Lett. 25, 1575

" " 1970c, Phys.Rev. B1, 3304

" " 1974, private communication

Palmberg P.W. 1972, in "Electron Spectroscopy" edited by D.A. Shirley

(North Holland Amsterdam) p 835

Papageorgopoulos C.A. and Chen J.M. 1972, J.Vac.Sci.Technol. 9, 570

Plummer E.W., Gadzuk J.W. and Young R.D. 1969, Sol.State.Comm. 7, 487

Plummer E.W. and Rhodin T.N. 1968, J.Chem.Phys. 49, 3479

Plummer E.W. and Young R.D. 1970, Phys.Rev. B1, 2088

Remy M. 1970, J.Chem.Phys. 53, 2487

Schmidt L.D. and Gomer R. 1966, J.Chem.Phys. 45, 1605

Schmidt L.D. 1972, J.Vac.Sci.Technol. 9, 882

Schiff L.I. 1955, "Quantum Mechanics" McGraw-Hill p 265

Schrieffer J.R. 1972, J.Vac.Sci.Technol. 9, 561

" " 1973,Varenna Summer School , Lecture notes

Schrieffer J.R. and Mattis D.C. 1965, Phys.Rev. 140, 1412

Sidorski Z., Pelly I. and Gomer R. 1969, J.Chem.Phys. 50, 2382

Slater J.C. 1930, Phys.Rev. 36, 57

Slater J.C. and Koster G.F. 1954, Phys.Rev. 94, 1498

Steiner D. and Gyftopoulos E.P. 1967, Rept.27th Annual Conf.Phys.Elec.
(Cambridge) p 10

Swanson L.W. and Strayer R.W. 1968, J.Chem.Phys. 48, 2421

Thorpe B.J. 1972, Surf.Sci. 33, 306

Topping A.J. 1927, Proc.Roy.Soc(London) A114, 67

Wilkinson M.A.1965, "The Algebraic Eingenvalue Problem" Clarendon Press
Oxford

Wojciechowski K.F. 1966, Acta.Phys.Polon. 29, 119

" " 1968, Acta.Phys.Polon. 33, 363

" " 1971, Prog. in Surf.Sci. 1, 65

Young D.M. and Crowell A.D. 1962, "Physical Adsorption of Gases"
Butterworths Scientific Publications Ltd. London

Zubarev D.N. 1960, Usp.Fiz.Nauk. 71, 71. Translation: Soviet Physics
Usp. 3, 320

Young P.L and Gomer R. 1973,Phys.Rev.Lett. 30, 955

INTERPRETATION AND CONSEQUENCES OF SURFACE ENHANCED ITINERANT PARAMAGNETISM

J. P. Muscat[+], M. T. Béal-Monod[++], D. M. Newns[+], D. Spanjaard[++]

[+]Department of Mathematics, Imperial College, London SW7, England

[++]Laboratoire de Physique des Solides, associé au C. N. R. S., Université Paris-Sud, Centre d'Orsay, 91405 - Orsay (France)

hys. Sol.
74/59

I - INTRODUCTION -

The magnitude of the surface spin susceptibility of a nearly magnetic metal plays a major role in some approaches to the theory of chemisorption[1] and catalysis[2]. Recently several papers[3 - 7] have appeared concerned with the response in the surface region to a uniform static magnetic field. These papers employ the Hartree-Fock approximation to describe a degenerate electron gas with a strong short range electron-electron interaction. One form of interaction considered in the case of tight-binding models[3][5][7] is the zero-range interaction

$$V(\underset{\sim}{R}_i, \underset{\sim}{R}_j) = I\,\delta(\underset{\sim}{R}_i - \underset{\sim}{R}_j) \quad , \qquad (1)$$

where $\underset{\sim}{R}_i$ denotes the location of the i^{th} site. The variable $\underset{\sim}{R}_i$ becomes continuous in the free-electron limit[4][6]. Finite range interactions have also been considered in Ref. 6. The boundary conditions are that the electron wavefunctions vanish at a plane which defines the surface in the free electron models but which is usually the first atomic plane outside the surface in tight-binding models.

The main point at issue concerns the behaviour of the surface magnetization in the neighbourhood of $\bar{I} = 1$ ($\bar{I}$ is the interaction renormalised to unity at the bulk critical point). Now the Bethe-Salpeter equation for the static surface paramagnetic susceptibility, when expressed in terms of the magnetization, gives a Fredholm equation whose kernel contains a complicated "non-uniform part" due to the surface. It has been found that the calculated surface critical behaviour is in general sensitive to any approximations made either in writing the kernel or in solving the resulting equations.

Numerical solutions of the Fredholm equation exist for the tight binding (with zero range interaction)[7] and free electron models (with zero[4][6] and

finite[6] ranges). It has been found that in the case of zero range interaction the magnetization near the surface is strongly enhanced compared to its bulk value[4][6] ; moreover a surface magnetic phase transition occurs at a value of $\bar{I}$ less than unity, at which the bulk transition takes place, for the free electron model[6] and for some tight binding systems[7]. In the free electron model the surface phase transition occurs at $\bar{I}_s = 0.985$ [6] whereas a value as low as $I_s = 0.9$ has been found in one tight binding model[7]. The surface phase transition is associated with a very large uniform field magnetization as $\bar{I}$ approaches $\bar{I}_s$ from below, which near the surface is much larger than the already enhanced bulk magnetization[4][6][7] . Including a finite range of interaction has been found[6] to suppress the surface magnetic phase transition.

In contrast to these numerical results, the analytical calculation of Ref. 3 is based on the assumption that when $\bar{I}$ is close to unity then long wavelength spatial variations on the scale of the correlation length ξ will be dominant, as is usually the case in critical phenomena. Short wavelength oscillations on the scale of the Fermi wavelength were thus neglected enabling the Fredholm kernel to be approximated by the bulk one which is of Wiener-Hopf form, exactly soluble. This resulted in a magnetization of the form [8]

$$m(z) = \frac{m^\circ(\infty)}{1 - \bar{I}} \left(1 - e^{-z/\xi}\right), \qquad (2)$$

where $m^\circ(z)$ is the magnetization at $\bar{I} = 0$ and z is the distance from the surface. Since $\xi \sim (1 - \bar{I})^{-1/2}$ as $\bar{I} \to 1$, a feature of this Fermi-Thomas type of result is that the magnetization close to the surface diverges only as $(1 - \bar{I})^{-1/2}$; this result was shown to be retrieved in ref. 6 when the non uniform part of the kernel was neglected. Analytical results can also be obtained[9] by replacing the

nonuniform part of the kernel with a separable function chosen so as to include Friedel oscillations in an apparently realistic way but, in that case the uniform field magnetization either agreed with the conclusions of the last mentionned approximations, i. e. is depressed near the surface, or is, at most, unchanged compared to its bulk value ; in particular no surface phase transition could be found that way ; this point will be settled in section III. Another type of analytically soluble form of the kernel has been discussed in ref. 5, which however leads to results depending strongly on the parameters chosen ; this model will be mentioned again below.

At this stage it is of interest to compare the above results on itinerant magnetism with numerous studies[10][11] devoted to localised magnetism for Heisenberg or Ising models. In particular the results of ref. (3)(9) and (6) discussed in the preceding paragraph are quite analogous to those found in ref. (10) for the Heisenberg model in mean field theory. A useful review of the results obtainable using the phenomenological Ginzburg-Landau equation has been given in recent papers[11] which go on to discuss the exact critical exponents for the Ising model. In these papers, two measures of surface paramagnetic susceptibility are emphasised. The susceptibility χ_1 describes the magnetization in the surface region due to a uniform magnetic field, as calculated in ref (3) - (7). An additional susceptibility χ_{11} describes the magnetization in the surface region due to a magnetic field itself localised near the surface but translationally invariant in the surface plane. In the phenomenological approach, results similar to those of ref. (3), (6) and (9) for χ_1, and to those of ref. (9) for χ_{11} (allowing for the reasonable transposition of temperature T_c/T to the interaction $\bar{I}$) are obtained when the logarithmic derivative of the magnetization is positive at the surface.

However a surface phase transition in the region $\bar{I} < 1$ is predicted for a negative logarithmic derivative.

In conclusion to the above, the numerical solutions for the exact kernels of the integral equation tend to show, in the case of zero range interaction, enhanced uniform field magnetization at the surface and a surface phase transition at $\bar{I}_s < 1$. The analytical models employing simplified kernels of ref. (3)(6) (9) show on the contrary a reduced or unchanged magnetization at the surface when $\bar{I} \to 1$ compared to the bulk value. The model of ref. 5 and the phenomenological theory[11] show parameter dependent behaviour.

A need for some explanation of the superficially anomalous surface phase transition emerging from the numerical calculations, together with a description of the singularities in χ_1 and χ_{11} associated with it seems to exist. This we attempt in the following using the zero range interaction and free-electron model. We preface the following with a discussion of the structure of the kernel in real and reciprocal space. The homogeneous Fredholm equation for the magnetization is then inspected for a solution $\bar{I} = \bar{I}_s$ corresponding to a surface magnetic phase transition by a variational technique, yielding the result $\bar{I}_s < 0.992$. The interpretation of this result is discussed. The susceptibility χ_{11}, which seems to be more directly related to the surface phase transition than χ_1, is then discussed in terms of the solutions to the homogeneous equation. This relationship enables interpretation of numerical calculations of χ_{11}, which we found to present less difficulty than χ_1. Finally an exact relationship between χ_{11} and the uniform field magnetization (i.e. χ_1) is given, with results which confirm the numerical calculations of ref. (6).

II - GENERAL FORMALISM AND QUALITATIVE DISCUSSION -

We begin by recapitulating the main points of the basic formalism, discussed in detail in ref. (3). The unperturbed (I = 0) wavefunctions and energy eigenvalues for one electron in the model of ref. 12 are given by

$$\phi_{K_{//}, k}(X, z) = e^{i K \cdot X} \sin kz \qquad (3)$$

$$\varepsilon(K_{//}, k) = \frac{1}{2} (K^2_{//} + k^2) ,$$

(in atomic units), where z is the axis normal to the surface, given by the plane z = 0, $X = (y, x)$ is a two dimensional vector in the surface plane, and k and $K_{//}$ are the corresponding components in reciprocal space. Using translational invariance parallel to the surface a susceptibility $\chi(K_{//}\ z\ z'\ \omega)$ may be introduced through the equation

$$m(K_{//}\ z\ \omega) = \int_0^\infty \chi(K_{//}\ z\ z'\ \omega)\ H(K_{//}\ z'\ \omega)\ dz' \qquad (4)$$

where m and H are the magnetization and applied magnetic field respectively (the Bohr magneton is taken as unity). These quantities appear in the form of their Fourier transforms with respect to parallel wavevector $K_{//}$ and frequency ω. Within the R. P. A. as shown in ref. (3), the susceptibility obeys the Bethe-Salpeter equation

$$\chi(K_{//}\ z\ z'\ \omega) = \chi^\circ(K_{//}\ z\ z'\ \omega) + I \int_0^\infty \chi^\circ(K_{//}\ z\ z''\ \omega)\ \chi(K_{//}\ z''\ z'\omega)dz'' \qquad (5)$$

in the presence of the interaction (1). Note that we suppose here that the interaction is the same everywhere whereas in ref. 3 it was allowed to be different in the surface plane. Here χ° is the susceptibility when I = 0, and may be calculated starting from (3). The solution of (5) is in general difficult ; we shall confine ourselves to the case of static fields, non-varying parallel to the surface

($K_{//} = 0$, $\omega = 0$). We therefore drop the suffixes $K_{//}$ and ω in the following.

It is convenient to introduce the dimensionless quantities $Z = 2k_F z$, $\bar{I} = IN(E_F)$, and to write $h = HN(E_F)$ where $N(E_F)$ is the density of states at the Fermi level. A one-sided cosine transform f(b) of any function f(Z) is then introduced by

$$f(b) = \sqrt{\frac{2}{\pi}} \int_0^\infty f(Z) \cos bZ \, dZ \qquad (6)$$

(b obviously stands for $k/(2k_F)$).

This transform is its own inverse. Equations (4) and (5) may now be rewritten

$$m(b) = \int_0^\infty \chi(b\ b')\ h(b')\ d\ b' \qquad (7\ a)$$

$$m(Z) = \int_0^\infty \chi(Z\ Z')\ h(Z')\ dZ' \qquad (7\ b)$$

$$\chi(b\ b') = \chi^\circ(b\ b') + \bar{I} \int_0^\infty \chi^\circ(b\ b'')\ \chi(b''\ b')\ db'' \qquad (8\ a)$$

$$\chi(Z\ Z') = \chi^\circ(Z\ Z') + \bar{I} \int_0^\infty \chi^\circ(Z\ Z'')\ \chi(Z''\ Z')\ dZ'' \qquad (8\ b)$$

Note that a factor $2k_F/N(E_F)$ has been absorbed into χ to make this quantity dimensionless.

Equations (8) may be expressed in terms of the magnetization by using (7)

$$m(b) = m^\circ(b) + \bar{I} \int_0^\infty \chi(b\ b')\ m(b')\ db' \qquad (9\ a)$$

and alternatively :

$$m(Z) = m^\circ(Z) + \bar{I} \int_0^\infty \chi^\circ(Z\ Z')\ m(Z')\ dZ' \qquad (9\ b)$$

where m° is the magnetization when $\bar{I} = 0$.

χ° has been shown[13] to be given by

$$\chi^\circ(b\ b') \equiv D(b)\ \delta(b - b') - A(b\ b') \qquad (10)$$

where

$$D(b) = \frac{1}{2} + \frac{1 - b^2}{4b} \ln \left| \frac{1 + b}{1 - b} \right| \tag{11}$$

$$A(b\ b') = \theta\left(1 - (b + b')\right) + \theta(b + b' - 1)\ \theta(1 - |b - b'|)\ \frac{1 - (b - b')^2}{4bb'}$$

and

$$\theta(x) = 1,\ x > 0 \quad ; \quad \theta(x) = 0,\ x < 0.$$

The functions D and A are plotted in Figs. 1 a and 1 b. D(b), which appears in the static Lindhard dielectric function, possesses a well-known but weak singularity at b = 1. The non-uniform part A is important only in giving a correct description for perturbations in the surface region. The behaviour of A(bb') is seen from (11) and Fig. 1 b to be highly singular near the points (0, 1) and (1, 0), and this behaviour gives a dominant contribution to Friedel oscillations in the surface response[12].

The functions D and A are related by the sum rule

$$D(b) = \int_0^\infty A(b\ b')\ d\ b' \tag{12}$$

Using (7), (9) and (12) it is easy to derive the consequences

$$\begin{aligned} &m(b) = 0 \quad ; \quad h(b) = h \\ &\int_0^\infty m(b)\ d\ b = 0 \quad ; \quad \text{all } h(b) \end{aligned} \tag{13}$$

Returning to real space via (6), the implication of (13) is that there is no magnetization for a field consisting of a delta function at the surface and no magnetization at the surface for any field. These results must follow for wave-functions (3) having a node at the surface.

It is also useful to consider the real space form of the equation (9 b)

where $\chi^\circ(Z, Z')$ is given by the cosine Fourier transform of (10) :

$$\chi^\circ(Z\ Z') = \frac{2}{\pi} \int_o^\infty \int_o^\infty \chi^\circ(b\ b') \cos bZ \cos b'Z'\ db\ db' \qquad (14)$$

This calculation is straightforward though lengthy, and we give only the result

$$\chi^\circ(Z\ Z') = \frac{1}{4}\left\{g(Z + Z') + g(\ |Z - Z'|\ ) - 2\ g(Z)\ \theta(Z-Z') - 2g(Z')\ \theta(Z'-Z)\right\} \qquad (15)$$

where

$$g(u) = -\frac{d}{du}\left(\frac{\sin u}{u}\right) - si\ (u) \qquad (16\ a)$$

$$si(u) = -\int_u^\infty \frac{\sin t}{t}\ dt \qquad (16\ b)$$

$$\int_o^\infty g(u)\ du = 2 \qquad (16\ c)$$

The first two terms in (15) are due to the uniform part of $\chi^\circ(b, b')$ (i. e. the D part) whereas the last two are due to the nonuniform contribution (i. e. the A part connected with interference effects at the surface). The function g(u) is illustrated in Fig. 2 a ; note that although g is predominantly positive a small negative region exists at $u \sim 4 - 5$ whose importance is emphasised below. The full kernel $\chi^\circ(Z, Z')$ is plotted in Fig. 2 b as a function of Z' for various Z.

We note that the magnetization for the uniform field

$$h(Z) = h$$
$$h(b) = h\sqrt{\frac{\pi}{2}}\,\delta(b) \qquad (17)$$

in the unperturbed ($\bar{I} = 0$) case is found from (7) to be

$$m^\circ_{uf}(Z) = h\left(1 - \frac{\sin Z}{Z}\right) \qquad (18)$$

Furthermore, Eq. 7 b written for the non interacting case, would be identically verified if one could approximate the kernel $\chi^\circ(Z, Z')$ by the form

$$\overline{\chi}^\circ(Z, Z') = \frac{m^\circ(Z)}{h(Z)}\ \delta(Z - Z') \qquad (19)$$

Such an approximated kernel would put the main emphasis on the maxima of the real $\chi^\circ(Z, Z')$ of fig. 2 b if one takes into account that those maxima $\chi^\circ(Z, Z)$ follow approximately the curve $m^\circ(Z)$. Therefore one expects that the approximation (19) would overestimate reality. If (19) is used in (9 b) in the uniform field case $(h(Z') = h)$ one finds at once :

$$\bar{m}(Z) = \frac{m^\circ(Z)}{1 - \bar{I}\, m^\circ(Z)} \qquad (20)$$

Such a form qualitatively agrees with the previously cited numerical results ; in particular it means that $\bar{m}(Z)$ could diverge for values of $\bar{I}$ such that :

$$\frac{1}{\max m^\circ(Z)} \lesssim \bar{I} \lesssim 1 \quad , \text{ i. e. } \quad 0.83 \lesssim \bar{I} \lesssim 1 \qquad (21)$$

therefore for values of $\bar{I}$ for which the bulk is paramagnetic. This result indeed exagerates what really happens since it was noted in ref. 4 that some singularity appears for $\bar{I} \sim 0.97 - 0.99$ and the value corresponding to a surface phase transition was found to occur at $\bar{I} = 0.985$ in ref. 6. However the approximation (20) appears useful in the sense that it allows for a reasonable physical explanation for the occurence of surface phase transition. Indeed, in the bulk the magnetization for a uniform field is :

$$m_B = \frac{m_B^\circ}{1 - I N_B(E_F)} \frac{h}{1 - \bar{I}} \qquad (22)$$

if one naively transpose this R. P. A. result as to apply near the surface, one could think of the following form for $m(Z)$:

$$m(Z) \simeq \frac{m^\circ(Z)}{1 - I\, N(E_F, Z)} \qquad (23)$$

where $N(E_F, Z)$ would be the density of states at the Fermi level submitted to the

Friedel type oscillations due to the presence of the surface ; this would lead to :

$$m(Z) \simeq \frac{m^{\circ}(Z)}{1 - \bar{I}\,(1 - \frac{\sin Z}{Z})} \qquad (24)$$

for free electrons[12] as is the case here. Similar oscillations are found in tight binding models too [13]. Therefore this hand waving type of argument allows to predict a magnetic transition near the surface simply because the surface induces oscillations in the behavior of the density of states (among other properties), so that $N(E_F, Z)$ can be larger than its bulk value and therefore (23) predicts then a divergence in m(Z) near the surface. As we shall see the real Z dependence of m(Z) is not that simple and it even appears impossible to be calculated explicitly. However we believe that the above argument renders understandable the magnetic surface phase transition found numerically. We also believe that any feature which would smooth out the surface oscillations (a finite range for I[6] as well as surface roughness or mean free path effects) would tend to suppress the divergence in m(Z) so that one would recover the results of ref 3, 9, 10 and 11, i. e. a depression of magnetism near the surface rather than an enhancement. Indeed a finite range for I was shown[6] to lead back to the results of ref. 3. For practical purposes, we expects that experimental data measuring surface quantities will strongly depend on the precise characteristics of the sample used much more than bulk experiments.

III - EXISTENCE OF SURFACE PHASE TRANSITION.

A surface phase transition will correspond to the existence of a solution to the homogeneous equation

$$m(b) = \bar{I} \int_0^{\infty} \chi^{\circ}(b, b')\, m(b')\, db' \qquad (25)$$

when $\bar{I} = \bar{I}_S < 1$.

One model which enables (25) to be solved exactly is obtained on replacing A by the separable function[9]

$$A(b, b') = \frac{1}{\alpha} D(b) D(b') \qquad (26)$$

where

$$\alpha = \int_0^\infty D(b)\, db$$

The choice (26) is the only possible symmetric separable function satisfying the sum rule (12). It is in fact possible to find an approximate function D(b) which on substitution into (26) and (8a) reproduces quite well the unperturbed susceptibilities χ_1° and χ_{11}° [9]. Now on substitution of (26) and (10) into (25) we have

$$\int_0^\infty \frac{D(b)\, db}{1 - \bar{I} D(b)} = 0 \qquad (27)$$

For any reasonable D(b) we should have $0 < D(b) \leq 1$, as is the case for the exact function (11). With this condition the left hand side of (27) is always positive so that (27) can not be satisfied. We conclude that no surface phase transition exists in the separable model (26) with any reasonable D(b). Hence the separable approximation is unreliable, and we turn to methods based on the exact kernel (11).

An analytical approach which retains the exact kernel may be founded on a variational solution of the homogeneous equation (25). Using a Dirac-like notation, we rewrite (25) as

$$\bar{I}\, \chi^\circ \mid m > = \mid m > \qquad (28)$$

or

$$(1 - \chi^\circ) \mid m > = E \mid m > \qquad (29)$$

where $$E = \left(1 - \frac{I}{\bar{I}}\right). \qquad (30)$$

We shall assume that the eigenvalue $\bar{I}_S$ belonging to eigenfunction $\mid S >$ which we

are seeking is the lowest eigenvalue of (25). Hence we are looking for an eigenvalue E_S which is lthe lowest eigenvalue of (29). It follows that if $| m >$ is a trial function, then there exists the variational equality

$$E_S < \frac{< m | (1 - \chi^\circ) | m >}{< m | m >} \equiv F \tag{31}$$

Since (30) implies that $E_S < 0$ if $0 < I_S < 1$, than a demonstration that $F < 0$ is equivalent to proving that a surface phase transition exists.

This can be done by employing the trial function

$$m(Z) = e^{-\lambda Z} - \frac{\sin Z}{Z} \tag{32}$$

For $\lambda = 0$, this is proportional to the unperturbed uniform field magnetization (18). The function (32) was used by one of the present authors in deriving a correction to the Fermi Thomas static dielectric response[12].

We wish to calculate $F(\lambda)$, obtained by inserting (32) into (31) and eventually to minimize this with respect to λ. We first note that in reciprocal space

$$m(b) = \left(\frac{2\lambda}{\pi(\lambda^2 + b^2)} - \theta(1 - b) \right) \sqrt{\frac{\pi}{2}} \tag{33}$$

from which it is easily shown that the denominator of (31) is

$$\int_o^\infty m(b)^2 \, db = \left(\frac{1}{\pi\lambda} - \frac{4}{\pi} \tan^{-1} \left(\frac{1}{\lambda}\right) + 1 \right) \frac{\pi}{2} \tag{34}$$

Unfortunately the evaluation of the numerator of (31) is difficult except in the limit $\lambda \to 0$. In this limit the leading term of (34) is $\frac{\pi}{2} (\pi \cdot \lambda)^{-1}$. Hence in order to evaluate (31) to order λ, it is in fact sufficient to evaluate the numerator of (31) only to zeroth order in λ. We first evaluate

$$\int_o^\infty \left(1 - D(b)\right) m(b)^2 \, db$$

$$= \frac{\pi}{2} \int_o^1 (1 - D(b)) \, db + O(\lambda) \tag{35}$$

$$= \frac{\pi}{2} \sum_{n=1}^{\infty} \frac{1}{(2n-1)(2n+1)^2} + O(\lambda)$$

$$= \frac{\pi}{2} \, 0.134 + O(\lambda) \tag{36}$$

Similarly we find

$$\int_0^\infty \int_0^\infty A(b, b')\, m(b)\, m(b')\, db'\, db$$

$$= -\frac{\pi}{2} + \frac{\pi}{2} \int_0^1 db \int_0^1 db'\, A(b, b') + O(\lambda) \tag{37}$$

$$= \frac{\pi}{2}\left[-\frac{1}{8} - \frac{1}{2} \sum_{n=2}^{\infty} \frac{1}{(n+2)^2\,(n-1)} \right] + O(\lambda) \tag{38}$$

$$\simeq -0.21\, \frac{\pi}{2} + O(\lambda) \tag{39}$$

hence we have

$$F(\lambda) = -.22\, \lambda + O(\lambda^2). \tag{40}$$

Eq. (40) demonstrates that even when $\lambda \to 0$, the variational function (32) is good enough to give $F < 0$, i. e. to show that a surface phase transition exists.

It is evident from (40) that E may be lowered by increasing λ. At finite λ the integral on the left hand side of (35) may be performed as a numerical quadrature, and this is also true of the left hand side of (37) which may be analytically reduced to a single variable integration. Performing these quadratures $F(\lambda)$ is found as a function of λ, giving a minimum at $\lambda \simeq 0.08$ at $F(\lambda) = -0.008$. Using (30) we thus have

$$\bar{I}_S \leq 0.992 \tag{41}$$

This result should be compared with that of ref. 6, $\bar{I}_S = 0.985$, obtained from a numerical solution of the inhomogeneous problem with a uniform field and a zero range interaction.

We attempt to interpret these results physically by rewriting the non-uniform part of the kernel in real space using (15) and (16), when (31) can be written

$$F = \frac{1}{< m \mid m >} \{ \int \left(1 - D(b)\right) \; m^2(b) + \int_0^\infty m(Z) \int_Z^\infty g(Z') \, m(Z') \, dZ' \; \} \tag{42}$$

We note that for small b

$$1 - D(b) \simeq b^2/3 \tag{43}$$

so that we are tempted by analogy with the one-particle Schrödinger equation to interpret the first and second terms of (42) as kinetic and potential "energies" and $F < 0$ as the condition for a "bound state". For λ small (and $\lambda \simeq 0.08$ is quite small) the main term in the "kinetic energy" comes from the second term in the magnetization (33) which using (43) is approximately $\frac{1}{3} \int_0^1 b^2 \, db = \frac{1}{9}$. This is a slight underestimate compared with (10) but it is clear that the "kinetic energy" comes essentially from the small b region, and the logarithmic singularity in D(b) does not play any very important role in determining its value.

The "potential energy" term in (42), though not simply related to a potential function, nevertheless has the form of a double integral containing the product g(Z) m(Z). The function m(Z) (32) at $\lambda = 0.08$ is plotted in Fig. 3, and is seen to be dominated by a peak at $Z \simeq 4.5$ which coincides with the minimum in g(Z) (see Fig. 2 a) so that m(Z) g(Z) possesses negative values near $Z = 4.5$. Now the second integral in the double integral is weighted by the factor m(Z) so we can see how the integral might lead to a significant negative value overall despite the fact that g(Z) is a mostly positive function.

Our interpretation is thus that by peaking near $Z = 4.5$ where $g(Z) < 0$ m(Z) is enabled to derive a negative "potential energy" from the "potential" g(Z), but the m(Z) function is not too sharply peaked to build up significant "kinetic energy" enabling a "bound state"

to be formed. A useful comparison is afforded with the work of Ref. 5, in which an approximate kernel was employed which nevertheless possessed the structure (15) when the parameter $\bar{\sigma}$ was allowed to become infinite. The function g(Z) then took the form

$$g(Z) \propto e^{-2|Z|/\sigma} \qquad (\sigma = \text{const.}) \qquad (44)$$

This form is always positive, though otherwise not unlike the correct g(Z), and it is significant that an exact calculation of the uniform field susceptibility using (44) showed no sign of a surface magnetic phase transition.

The exact kernel with finite range interaction has been considered in ref. 6. We shall not consider this in detail here, but we note that in this model the "potential energy" term now contains m(Z') g(Z), where (Z' - Z) is finite due to the finite range of the kernel. Hence even a magnetization highly localised near the minimum of g(Z) will be affected by the strongly repulsive "core" of g(Z) to an extent increasing with interaction range. In this way the negative contribution to the "potential energy" can be easily counterbalanced, giving a qualitative understanding of the disappearance of the surface phase transition[6].

IV - THE SUSCEPTIBILITIES $\chi_{\perp}$ AND $\chi_{\parallel}$

The kernel χ° may be expanded in terms of the complete set of normalised eigenfunctions $|\, n >$ with corresponding eigenvalues $\bar{I}_n^{-1}$ belonging to the homogeneous equation (28)[4] :

$$\chi^{\circ} = \sum_n \frac{|\, n > < n\,|}{\bar{I}_n} \qquad (45)$$

Using (45),(7) and (9), the solution $| m >$ of the inhomogeneous equation for magnetic field $| h>$ can be written

$$| m > = \sum_n \frac{|n > < n | h >}{\bar{I}_n - \bar{I}} \qquad (46)$$

If $\bar{I}$ is very close to $\bar{I}_S$, and if h is a magnetic field localised near the surface, then the term in $(\bar{I}_S - \bar{I})^{-1}$ should dominate (46), so we have

$$| m > \simeq \frac{| S > < S | h >}{\bar{I}_S - \bar{I}} \quad ; \qquad \bar{I} \to \bar{I}_S \qquad (47)$$

or

$$m(Z) = \frac{m_S(Z)}{\bar{I}_S - \bar{I}} \int m_S(Z) \; h(Z) \; dZ \qquad (48)$$

where $m_S(Z) = < S \mid Z >$.

The susceptibility χ_{11} is loosely defined as the response in the surface region to a magnetic field localized near the surface. This susceptibility is seen from (48) to diverge as $(\bar{I}_S - \bar{I})^{-1}$ near the surface phase transition;.

A convenient form for h(Z) proves to be

$$h(Z) = \frac{h \sin Z}{Z} \quad , \qquad (49)$$

and we shall here define χ_{11} as the response to (49) at h = 1. We have performed a numerical calculation of the magnetization which is appropriate for a film of thickness ℓ with the applied field $h(Z) - h(\ell - Z)$. In this case the equations resemble those given by one of the present authors for the film dielectric response[12]

$$\sum_b (1 - \bar{I} \chi^\circ_{bb'}) \, m_b = m^\circ_{b'} \qquad (50)$$

$$m^\circ_b = \sum_{b'} \chi^\circ_{bb'} \, h_{b'} \, ,$$

where

$b = (2n + 1)\,\pi/\ell$. Here χ° is given by

$$\chi^{\circ}_{bb'} = -A_{bb'} \qquad b \neq b'$$

$$\chi^{\circ}_{bb} = \sum_{b' \neq b} A_{bb'} \tag{51}$$

It is necessary to truncate the infinite matrix $\chi^{\circ}_{bb'}$ at $b = b' = b_o$ after which (50) is soluble by a standard routine. The choice $b_o = 3$, leads to negligible error for $\bar{I} \leq 0.95$ but b_o needs to be increased in the region $0.95 < \bar{I} < \bar{I}_S$. Furthermore the computed magnetization will only correspond to the single surface problem studied in this paper if ℓ greatly exceeds the range of the magnetization $m_S(Z)$. With these limitations reasonable accuracy has been achieved except for the largest value $\bar{I} = 0.983$ employed, where our results may underestimate m(Z) by 20 %.

Equation (48) suggested plotting 1/m(Z) versus $\bar{I}$ at fixed Z, a value Z = 4.5 close to the maximum in m(Z) being chosen. The plot proved to be accurately linear in the range $0.95 \leq \bar{I} < \bar{I}_S$, with intercept at $\bar{I}_S = 0.985$. This is in agreement with the $\bar{I}_S$ obtained in ref. 6 from a similar plot in the case of a uniform field, which actually presents a more complicated problem (see below)

According to Eq. (48), the quantity $(\bar{I} - \bar{I}_S)\, m(Z)$ should be proportional to $m_S(Z)$, and thus be independent of $\bar{I}$. This function is illustrated in Fig. 3 for various $\bar{I}$, verifying that this prediction is fairly reasonable and also giving us a plot of the function $m_S(Z)$ which is the exact solution of the homogeneous equation. Fig. 3 also shows a plot of $(\bar{I}_S - \bar{I})\, m(Z)$ calculated by substituting the normalised variational function (32) into (48) for $m_s(Z)$. We see that the exact

$m_S(Z)$ is even more sharply peaked at $Z \simeq 4.5$ than the variational function ; in the context of the discussion of the previous section, this presumably gives an even more dominant contribution to the "potential energy" from the $g(Z) < 0$ region than in the case of the variational function.

We now turn to the uniform field susceptibility χ_1, which has been the subject of most previous studies[3][7]. It is easily shown that a relationship exists between the magnetization $m_{uf}(Z)$ in the presence of the uniform field (17) a and $m(Z)$ corresponding to the local field (49), which is exact within the context of the present model. This relationship is straightforward :

$$m_{uf}(Z) = \frac{m^\circ_{uf}(Z) - \bar{I}\, m(Z)}{1 - \bar{I}} \qquad (52)$$

(Here $m^\circ_{uf}(Z)$ is given by (18)) and can be obtained as follows :
We define the function $m(Z)$ as :

$$m(Z) = m_{uf}(Z) - \int \chi^\circ(Z, Z')\ m_{uf}(Z')\, dZ' \qquad (53)$$

We replace in ref. (53) $m_{uf}(Z)$ by its expression (9 b) in terms of the Bethe Salpeter equation. It thus appears that $m(Z)$ obeys the same Bethe Salpeter equation (9 b) with a source term $m^\circ(Z)$ given by :

$$\begin{aligned} m^\circ(Z) &= m^\circ_{uf}(Z) - \int \chi^\circ(Z\, Z')\, m^\circ_{uf}(Z')\, dZ' \\ &= \int \chi^\circ(Z, Z') \left[h - m^\circ_{uf}(Z') \right] dZ' \qquad (54) \\ &= \int \chi^\circ(Z\, Z') \frac{h \sin Z'}{Z'}\, dZ' \end{aligned}$$

hence $m(Z)$ and $m^\circ(Z)$ are the magnetizations (in presence and absence of interaction respectively) for the local field $h(Z) = \frac{h \sin Z}{Z}$. On the other hand, if one eliminates $\int \chi^\circ(Z\, Z')\, m_{uf}(Z')\, dZ'$ between (9b) and (53), one obtains at once the relationship (52)

Eq. (52) may be regarded as a relationship between χ_l on the left hand side and $m_{uf}(Z)$ ($= \chi_{ll}$). Substituting (48) into ((52) we have for $\bar{I}$ near $\bar{I}_S$:

$$m_{uf}(Z) = \frac{m^{\circ}_{uf}(Z)}{1 - \bar{I}} - \frac{\bar{I}\, m_S(Z) < S \mid h >}{(1 - \bar{I})\,(\bar{I}_S - \bar{I})} \qquad (55)$$

For small Z, the second term of (55) will be dominant. This has a double divergence at $I = 1$ as well as $I \simeq I_S$, so that an enormously large uniform field magnetization may occur at $\bar{I}$ near $\bar{I}_S$, which has the form of $m_S(Z)$. At large Z, $m_S(Z)$ will be small and the first term of (55), representing the bulk enhancement alone, will be dominant. Thus if $\bar{I} \to \bar{I}_S$ we can say that χ_l diverges as $(1 - \bar{I})^{-1}(\bar{I}_S - \bar{I})^{-1}$ but $m_{uf}(Z)$ itself displays a complicated Z-dependent behaviour as a function of $\bar{I}$ and Z.

We have inserted the computed localised field magnetization m(Z) into (52) and obtained results in excellent agreement with those of ref. 6.

At this point it is appropriate to compare the numerical calculations of this paper and ref. 6 with those of ref. 4 since all refer to the same kernel. The most notable point is that a numerical solution of the homogeneous equation (28) was carried out in ref. 4 but no eigenvalue $\bar{I}_S < 1$ corresponding to a surface phase transition was found although the approach of a singularity around $\bar{I} \sim 0.97 - 0.99$ was noticed as already recalled in section II. Nevertheless insertion of the eigenvalues and eigenfunctions of (28) into (46) predicted results for the uniform field magnetization in reasonable agreement with this work and ref. 6 up to $\bar{I} = 0.95$. Presumably, though insufficiently accurate to separate a "bound state" from the "band" $I \gtrsim 1$, the technique of ref. 4 replaced this bound state by a virtual bound state which gave nearly correct results in (46) for the region $0 < \bar{I} \lesssim 0.95$.

Finally we wish to point out that the relationship (52) is not confined to the precise kernel χ° which has been employed above. The result is appropriate for any reasonable χ° ; if the definition (49) of the local field causing the magnetization m(Z) is replaced by

$$h(Z) = h - m^\circ_{uf}(Z) \tag{56}$$

Since $m^\circ_{uf}(Z) \to h$ as $Z \to \infty$, (56) is indeed seen to be a local field.

V - CONCLUSION -

The point of departure for this paper has been the finding of a large surface-uniform field susceptibility χ_1 [4], followed by the identification of surface magnetic phase transitions [6][7], in numerical H. F. calculations on enhanced paramagnets. In view of the fact that some approximate analytical calculations [3][5][9] have shown small uniform field magnetizations near the surface under analogous conditions, with no surface phase transition, our aim has been to gain some further insight into the former results especially since, as was shown in section II, we had the feeling that the surface magnetic instability could be simply interpreted in terms of the oscillations in the density of states caused by the presence of the surface in its neighbourhood. We have worked with the free electron model, with an infinite square surface barrier, and a zero-range electron-electron interaction I.

The existence of a surface magnetic phase transition implies a solution of the homogeneous equation (25) for the magnetization at $\bar{I} = \bar{I}_S < 1$. Using a simple variational function, we demonstrate essentially analytically that $\bar{I}_S < 1$ and we find an upper bound $\bar{I}_S < 0.992$. The "non-uniform part" of the kernel of the equation (25) plays an important role, and its structure is revealed when the kernel is written in real space in terms of the function g(Z). An analogy is noted between the existence of a surface magnetic phase transition and the separa-

tion of a bound state in the one-particle Schrödingen equation, in which the non-uniform part of the kernel plays the role of an attractive potential energy. The solution $m_s(Z)$ to the homogeneous equation at $\bar{I} = \bar{I}_s$ posesses a large peak at $Z = 4.5$ where the function $g(Z)$ is negative, enabling a negative"potential energy" to be achieved despite the strongly repulsive nature of the "core" of $g(Z)$. The function $m_s(Z)$ at $Z > 4.5$ shows slow exponential decay with oscillations ; we have noted that, by adopting this form, the variational function retains a relatively low "kinetic energy". A model calculation[5] with a kernel of the correct form but with non-negative $g(Z)$ showed no evidence of a surface transition, consistent with the above argument. Other analytical calculations[3][9] did not retain the correct complete form of the kernel and again found no evidence of the surface phase transition. If however the interaction $\bar{I}$ has sufficiently long range, then even a function $m_s(Z)$ sharply peaked at $Z = 4.5$ will be brought into interaction with the repulsive part of $g(Z)$, and a surface phase transition should be inhibited, as found in ref. 6.

The susceptibility in the paramagnetic region $\bar{I} < \bar{I}_s$ may be investigated via an expansion in eigenfunctions of the homogeneous equation[4]. The magnetization for a field localised at the surface is proportional to $(\bar{I}_s - \bar{I})^{-1} m_s(Z)$ when $\bar{I} \to \bar{I}_s$, so that if χ_{11} is the surface-surface susceptibility then $\chi_{11} \alpha (\bar{I}_s - \bar{I})^{-1}$ In fact choosing the local field $h(Z) = h \sin Z/Z$ we have calculated the magnetization numerically, and used the latter result to estimate $\bar{I}_s = 0.985$ (in agreement with ref. 6, 7) and also to illustrate the function $m_s(Z)$ (Fig. 3). We have found an exact relationship between the uniform field magnetization and the magnetization corresponding to the above local field $h(Z)$. The magnetization for a uniform field then takes the form (55) when $\bar{I} \to \bar{I}_s$. In the latter limit the surface-uniform field susceptibility χ_1 is then seen to posess the strong divergenc

$\chi_\perp \propto (\bar{I}_S - \bar{I})^{-1}$ $(1 - \bar{I})^{-1}$. On the other hand if $Z \to \infty$ at fixed $\bar{I}$, the bulk magnetization $m = (1 - \bar{I})^{-1}$ is retrieved. It may be coincidental, but should be noted that the figure given in Weiner's paper[7][8] for the f.c.c. (100) surface at $\bar{I} = 0.9$ shows comparables enhancements for the uniform field magnetization and the "local" susceptibility $\chi(Z, Z)$, in contrast to the above.

In chemisorption applications[1][2], the spin of an atom on the surface is assumed to be coupled to the spin fluctuations of the solid via a short range exchange interaction. In this problem the perturbing field is thus localised near the surface, but also localised about a point in the surface plane, and the appropriate susceptibility is only approximately χ_{11}, though evidently $\chi_\perp$ is inappropriate. In the absence of a surface phase transition Ginzburg-Landau equation[11] predicts that χ_{11} is enhanced, with only a cusp at $\bar{I} = 1$. In terms of the HF itinerant model, we can rewrite Eq. (52) as

$$m(Z) = I^{-1} \left(m^{\circ}_{uf}(Z) - (1 - \bar{I})\, m_{uf}(Z) \right). \qquad (57)$$

Thus the magnetization $m(Z)$ due to the local field (56), which enters χ_{11}, will in general be unenhanced unless $m_{uf}(Z)$ diverges at $\bar{I} = 1$ more strongly than $(1 - \bar{I})^{-1}$ or posesses a singularity at $\bar{I} = \bar{I}_S < 1$. Hence calculations with zero-range interaction[3][6][9] showing $m_{uf}(Z)$ to be enhanced less (or as) strongly near the surface than (as) in the bulk should tend to show an unenhanced χ_{11}. On the other hand, in the presence of a surface phase transition, $m(Z)$ and χ_{11} diverge like $(\bar{I} - \bar{I}_S)^{-1}$ as shown above. Nevertheless, we have found, for the model studied in this paper, that at a practical enhancement such as $\bar{I} = 0.95$, $m(Z)$ has the unspectacular maximum value of $m(4.5) = 0.66$ h, for the local field (49). A more significant χ_{11} could however result if

(a) $\bar{I}_s$ were closer to the actual $\bar{I}$ of the solid (we recall Weiner's finding of $\bar{I}_S = 0.9$); (b) the overlap $< S \mid h >$ of the applied local field $h(Z)$ with the solution $m_S(Z)$ at $\bar{I} = \bar{I}_S$ of the homogeneous equation were larger than is the case for (49). On the other hand, since the surface phase transition is a phenomenon of long wavelength in the surface plane, the divergence associated with it may enter in diminished form into the susceptibility seen by an adsorbed atom. It is difficult to make a general statement, but the possibility that this susceptibility be large seems likely to depend on (i) the existence of a surface phase transition with $\bar{I}_S$ close to the $\bar{I}$ of the material (ii) a fairly long range atom-metal exchange interaction. Strongly enhanced paramagnetism in the bulk does not appear to be a sufficient condition.

It is necessary to take into account a number of factors before a prediction of the occurrence of a surface magnetic phase transition in a real material can be made. Weiner[7] found that the occurrence of the transition was sensitive to the parameters of the model, and the sensibility to interaction range found by Zaremba and Griffin[6] has already been noted. The effect of taking into account the finiteness of the potential barrier presented by the surface is still unknown. The possibility that $\bar{I}$ be different in the surface layer from its bulk value was considered in Ref. 3, and a larger surface value of $\bar{I}$ was found to facilitate a surface phase transition. Such a variation of $\bar{I}$ is probable because both the Herring screening of I [14] and the Kanamori t-matrix effect[15] should be sensitive to the surface environment, but the total sign of the effect is difficult to predict. At a real transition metal surface effects such as band degeneracy and the transfer of electrons between s and d bands need to be considered. The cumulative complexity of these phenomena, given the apparent sensitivity of the

surface phase transition to parameters of the model, evidently renders prediction somewhat hazardous at this stage.

Our discussion in this paper has been on the basis of the molecular field approximation, which may be poorer for surface than for bulk problems since the former present a situation somewhere between two and three dimensions. Furthermore it appears[16] that, while R P A is correct, at 0°K, for uniform bulk systems, when translational invariance is broken up in the case of a local impurity perturbation, R. P. A. is not sufficient, and beyond that, the effect of the fluctuations is to prevent the approach of the instability. If we extrapolate this statement to the present problem, which is another example of breaking down of translational invariance, it might be that the fluctuation effects suppress the surface instability. Taking over a result from exact studies of the Ising model[11], χ_{11} may in fact posess a very weak divergence at $\bar{I} = 1$ even in the absence of a surface phase transition, rather than the simple cusp found in molecular field theory. This may render our comments on the possibility of finding a large susceptibility seen by an adsorbed atom a little too restrictive.

Acknowledgement.

One of us (D. M. N.) wishes to acknowledge the hospitality of the Laboratoire de Physique des Solides, Orsay, where this work was initiated, J. P. M. wishes to acknowledge the support of the Science Research Council.

REFERENCES

(1) J. R. Schrieffer and R. Gomer, Surf. Sci. 25, 315 (1971)

(2) H Suhl, J. M. Smith and P. Kumar, Phys. Rev. Lett. 25, 1442 (1970)

(3) D. L. Mills, M. T. Béal-Monod and R. A. Weiner, Phys. Rev. B 5, 4637 (1972)

(4) M. T. Béal-Monod, P. Kumar and H. Suhl, Sol. State Comm., 11, 855 (1972) ; M. T. Béal-Monod, P. Kumar, D. L. Mills, H. Suhl and R. A. Weiner, Proceedings of the International Conference on Low Temp., Phys. Boulder, Colorado (1972), to be published.

(5) R. A. Weiner, M. T. Béal-Monod, D. L. Mills, Phys. Rev. B 7, 3399 (1973)

(6) E. Zaremba and A. Griffin, Sol. State Comm., 13, 169 (1973) ; E. Zaremba, Thesis, Toronto (1974), unpublished.

(7) R. A. Weiner, to be published in the Proceedings of the 19th Conference on Magnetism and Magnetic Materials, see also for the Heisenberg model : R. A. Weiner, Phys. Rev. Letters, 31, 1588, (1973) and P. Kumar, "Magnetic phase transition at the surface : mean field theory" preprint (1974)

(8) In Ref. 3 a typographic error appears in Eq.(42) and the following line where the ratio $(1 - \bar{I})^{1/2} / \sigma$ should appear instead of its inverse. Furthermore, the plane $\ell = 0$ actually refers to the first neighbour plane on the vacuum side of the surface plane ; this minor confusion arose from earlier replacement of a sum starting at $\ell' = 1$ by an integral from $\ell' = 0$ to ∞.

(9) M. T. Béal-Monod and D. M. Newns, unpublished. (1973)

(10) D. L. Mills, Phys. Rev., B 3, 3887 (1971)

(11) K. Binder and P. C. Hohenberg, Phys. Rev. B 6, 3461 (1972) ; K. Binder and P. C. Hohenberg, preprint (1973) ; T. C. Lubensky and M. H. Rubin, preprint.

(12) D. M. Newns, Phys. Rev., B 1, 3304 (1970) ; D. E. Beck and V. Celli, Phys. Rev. B 2, 2955 (1970) ; D. E. Beck, Phys. Rev. B4, 1555 (1971)

(13) See for instance F. Cyrot-Lackman and M. C. Desjonqueres, Surface Science 40, 423 (1973)

(14) C. Herring, Exchange Interactions among Itinerant Electrons, Magnetism IV (New York) (1966)

(15) J. Kanamori, Progr. Theor. Phys. 30, 275 (1963)

(16) See for instance in M. T. Béal-Monod, Sol. State Comm., 14, 677, (1974) and to be published.

FIGURE CAPTIONS

Fig. 1 (a) : The uniform part D(b) of $\chi^{\circ}(b, b')$ versus b, formula (12).

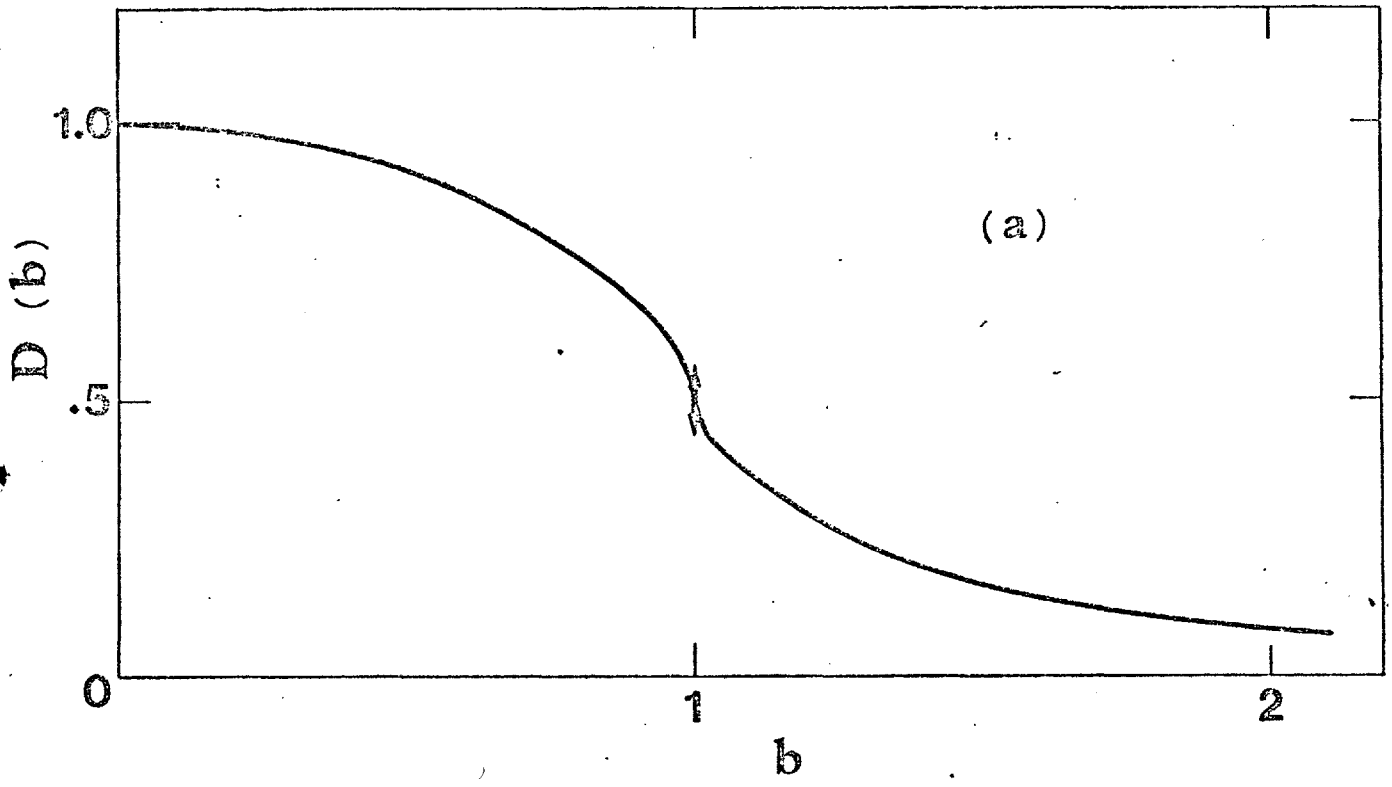
Fig. 1 (b) : The non uniform part A(b, b') of $\chi^{\circ}(b, b')$ versus b for several fixed b', formula (12).

Fig. 2 (a) : The function g(u)/g(o) versus u, formula (21)

Fig. 2 (b) : The function $\chi^{\circ}(Z, Z')$ versus Z' for several fixed Z, formula (20) ---, the charge neutrality boundary.

Fig. 3 : Broken and dot-dash curves ; $(\overline{I}_S - \overline{I})$ m(Z), where m(Z) is magnetization for local field (49). Full curve ; normalised trial function $m_S(Z)$ (see Eq. (32)) for $\lambda = 0.08$, multiplied by $< S \mid h >$.

Fig 1



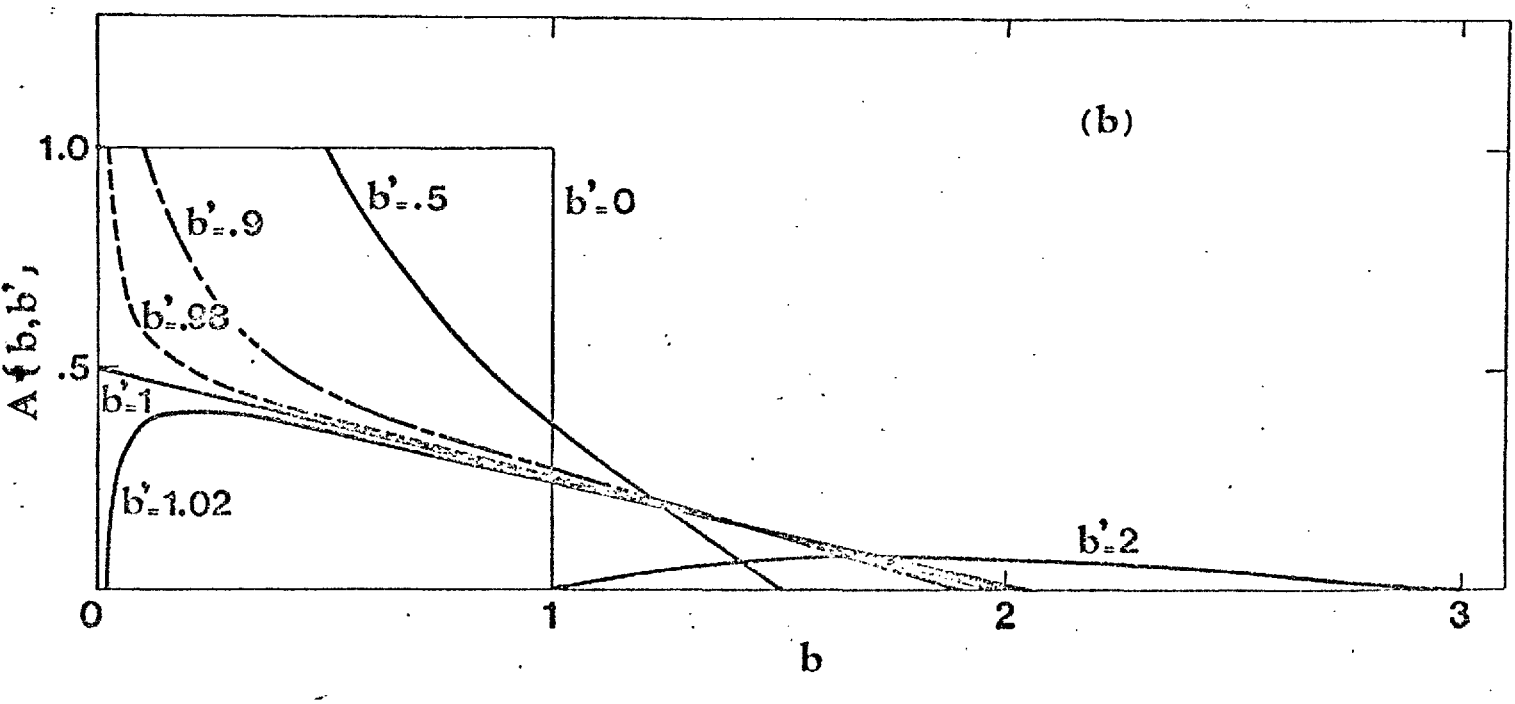


Fig 2 (a)

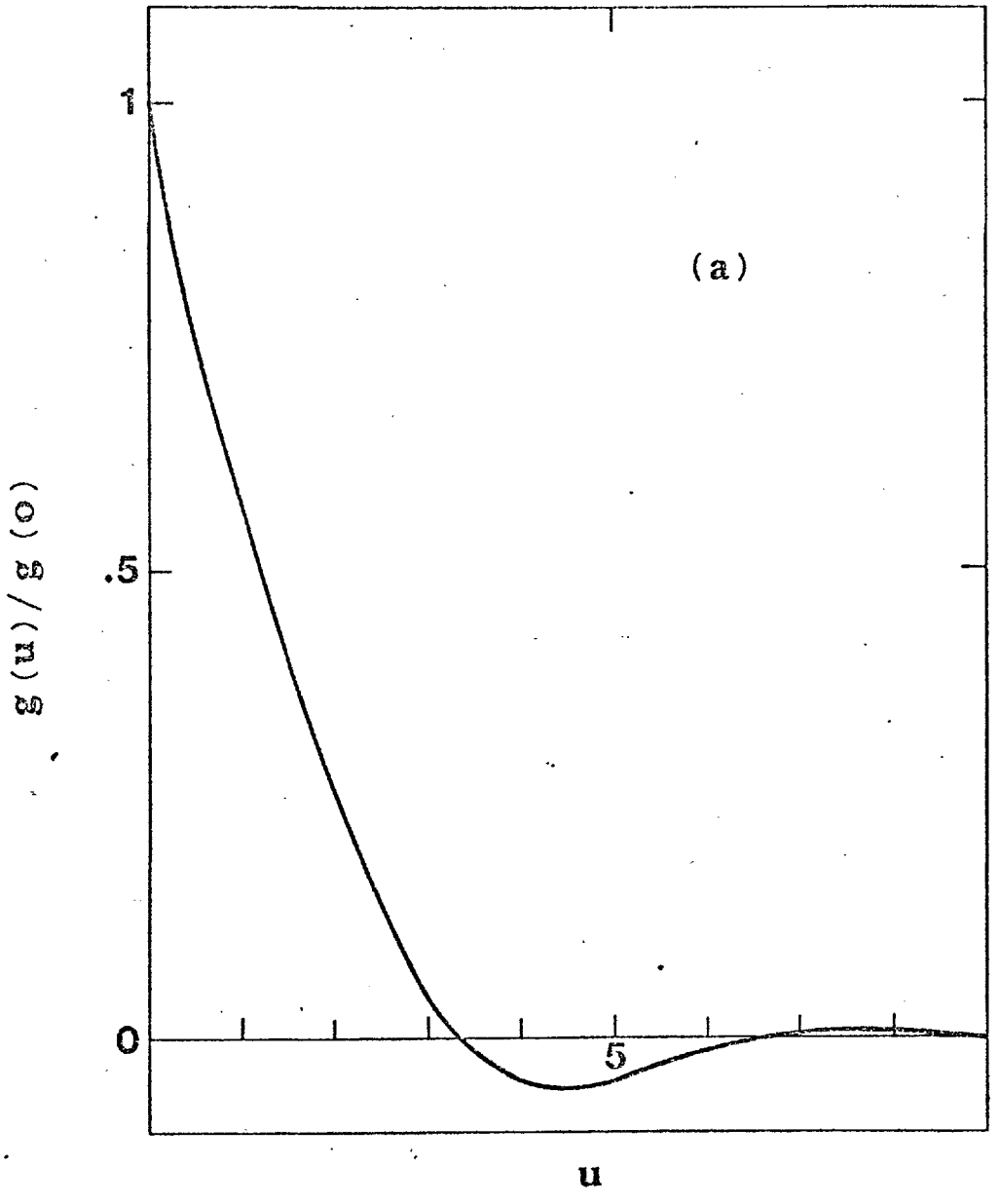


Fig 2 (b)

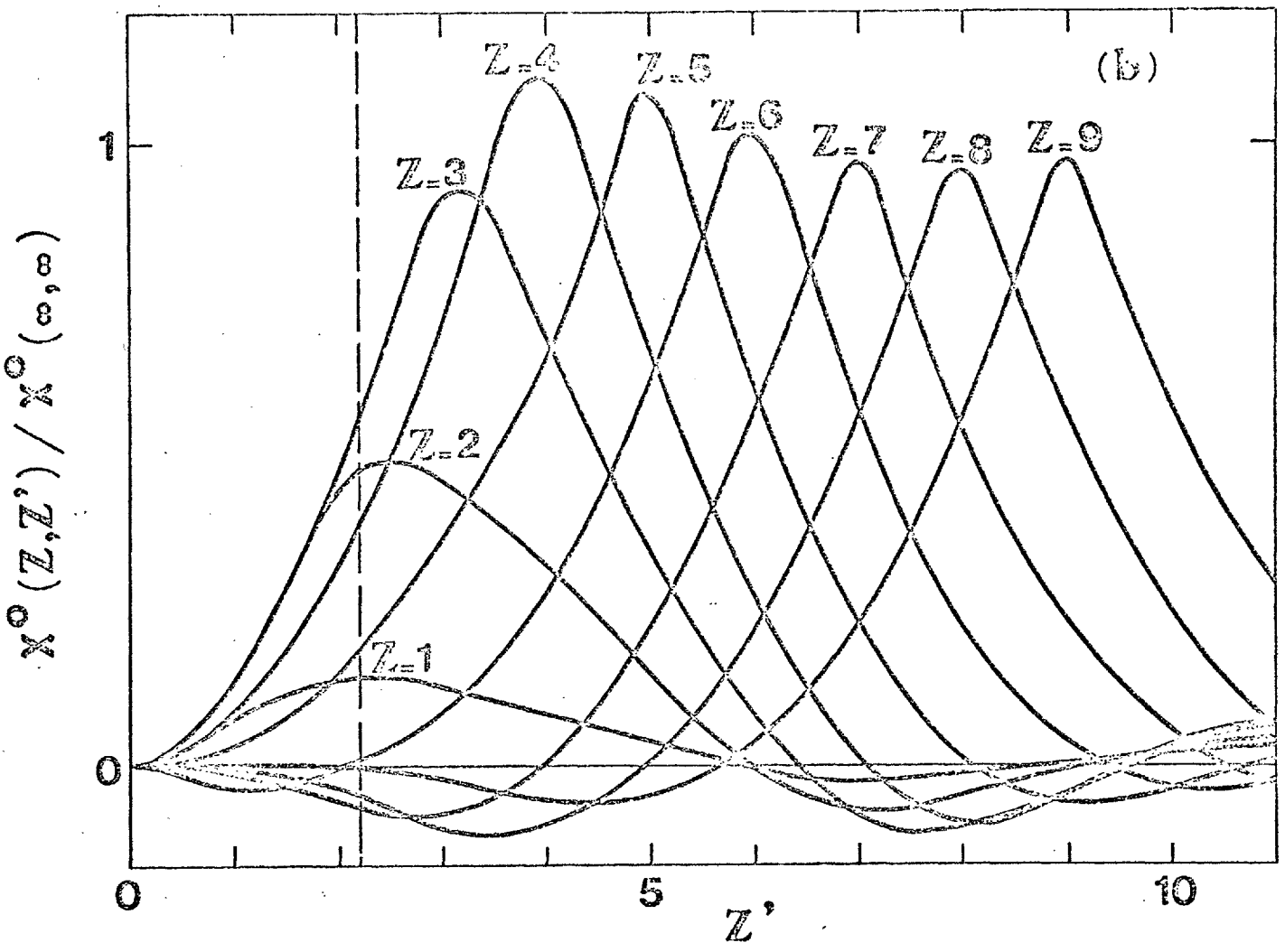
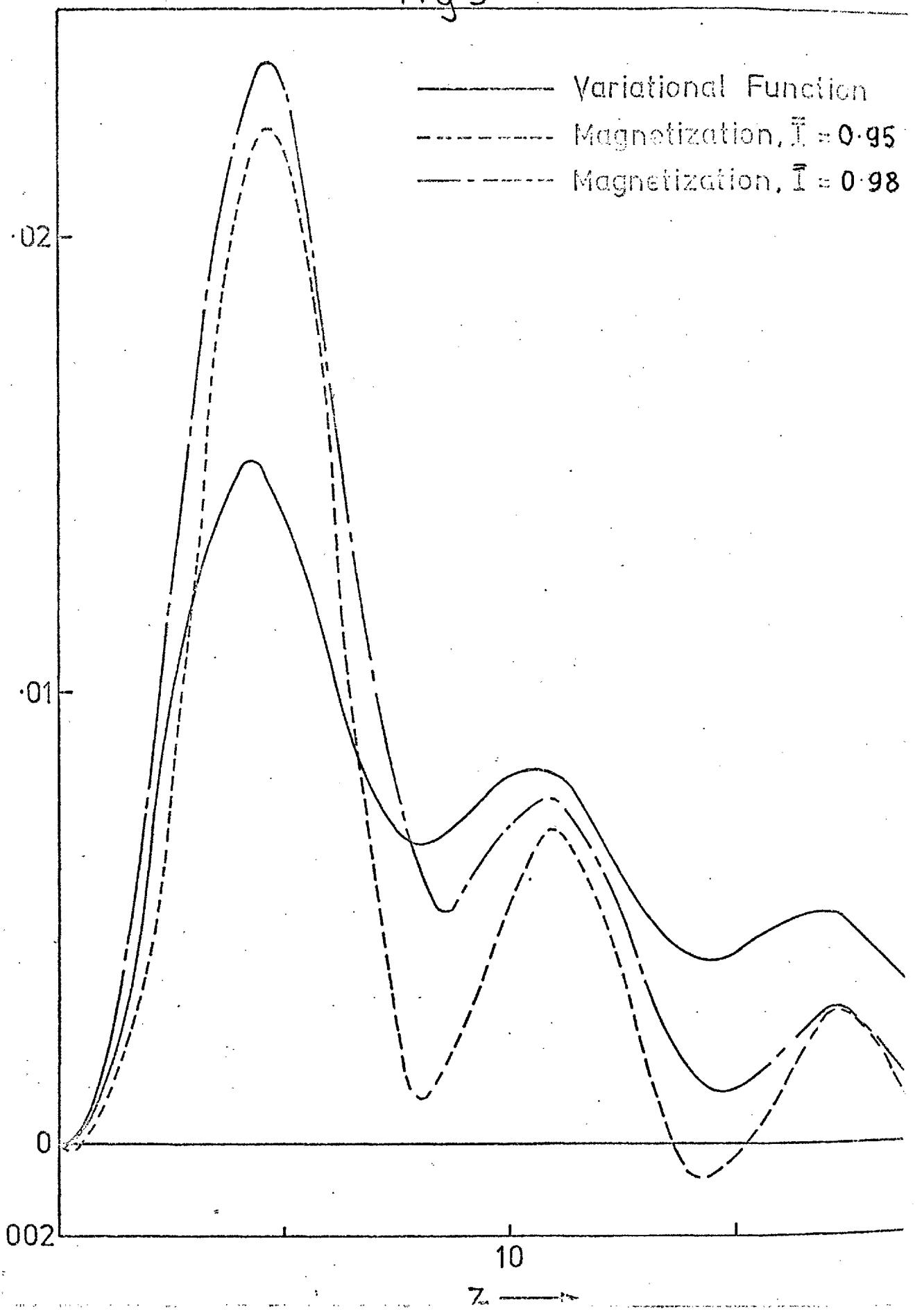


Fig 3


Variational Function
Magnetization, $\bar{I} = 0.95$
Magnetization, $\bar{I} = 0.98$
·02
·01
0
002
10
z